SOME PHYSICO-CHEMICAL PROPERTIES OF HOMO- AND CO-POLYMERS FROM MONO- AND DI-ALKYL ESTERS OF ITACONIC ACID

A thesis submitted to the
University of Stirling
for the degree of
Doctor of Philosophy

Zia-ul Haq

Department of Chemistry
June 1976

Ph.D. conferred ~~awarded~~ March 1977
(awarded December 1976)

To my parents

without whose encouragement this

thesis would not have been written

ACKNOWLEDGEMENTS

I wish to express my sincere thanks to Professor JMG Cowie for his active encouragement and supervision of this work. I am also extremely grateful to both Professor Cowie and to Dr. I. J. McEwen for the many stimulating and rewarding discussions which have helped to further my knowledge of, and increase my interest in, polymer science.

I wish to thank all those members of the academic and technical staff who have contributed to this work by their advice and assistance. Most especially I am indebted to J. Jason and W. Grant of the engineering workshop, to W. Stirling for his help with electrical problems, to T. Forrest for his assistance with the electron microscope and to J. Weber for typing the manuscript of this thesis.

I am also grateful to the members of the polymer group at Glasgow University, not only for providing the facilities for degradation studies, but also for their useful advice during these studies.

Last, but by no means least, I express my sincere gratitude to my family and especially my brother, Dr. R. Haq, for their patience and encouragement throughout the period of my studies.

ABSTRACT

Polymers and copolymers of mono- and di-n-alkyl esters of itaconic acid, with side chain lengths from one to twelve carbons have been prepared. The reactivity ratios of selected copolymer systems have been established. The thermo-mechanical behaviour of both homopolymers and copolymers has been studied. Torsional braid analysis and differential scanning calorimetry were employed to locate glass transition temperatures and sub-transition temperatures. As the length of the ester side chains in the poly(di-n-alkyl itaconates) changes from methyl through to decyl, the glass transitions were found to decrease to a minimum at heptyl and increase slightly thereafter. A second major transition was observed in poly(di-esters) when the side chains contain seven or more carbon atoms. This has been assigned to relaxation of the side chain prior to the onset of main chain relaxation.

The thermal stability of the polymers was studied by both thermal volatalisation analysis and thermogravimetric analysis. The thermal behaviour of the di-ester polymers was found to be comparable with the corresponding polyacrylates while mono ester polymers were observed to undergo thermal modification, involving the formation of anhydride structures, at ∿430K. Except for poly(monononyl itaconate) and poly(monodecyl itaconate), glass transitions were not observable for the latter series.

Ionomers, based on copolymers of a mono- and a di-ester were prepared by neutralising the free carboxyl groups with sodium and caesium hydroxides. The mechanical behaviour of these was studied using linear viscoelastometry. This showed the ionomers to possess both increased mechanical and thermal stability when compared with parent copolymers. The morphology of the ionomers was investigated using electron microscopy. The results indicate the absence of ionic aggregation at low ion concentration, but the possible presence of aggregation at high ion concentration.

CONTENTS

continued:

CHAPTER 1

INTRODUCTION

1.1 ITACONIC ACID

Itaconic acid (methylene succinic acid) is a dicarboxylic acid with an external methylene group and can be regarded as a structural variant of acrylic and methacrylic acids.

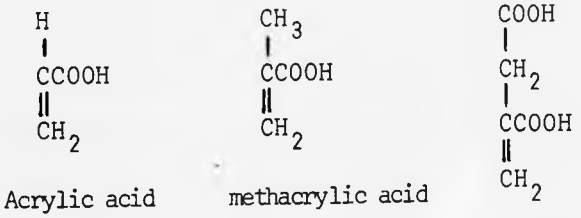

Acrylic acid — methacrylic acid — itaconic acid

It presents attractive possibilities in the plastics and coatings industries as a comonomer for incorporating carboxyl functionality and as a precursor of a range of polymerisable mono- and diesters.

Itaconic acid was originally isolated in 1836 from the pyrolysis products of citric acid by Baup[1], who characterised it by solubility and melting point. The name "itaconic acid" came a few years later. Interest in the acid then seems to have lapsed until the 1880's, when several investigations[2] were undertaken, both on itaconic acid itself and on a number of its esters. By the outbreak of the first world war the chemical and physical properties of itaconic acid, and many of its derivatives, had been well established[2]; in particular, the nature of the isomerisation which occurs above the melting point of the acid.

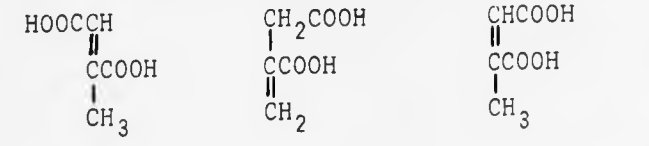

mesaconic acid — itaconic acid — citraconic acid

The preparation of itaconic acid by fermentation was first reported by Kinashita[3] in 1931. He isolated, from dried and salted plums, a fungus (Aspergillus Itaconicus) which was capable of fermenting sugars to itaconic acid in yields of up to 24% (based on sugars consumed). However, this process was never developed on a commercial scale. Other investigators[4] later reported that the fermentation of carbohydrates by certain strains of Aspergillus Terreus could produce the acid under surface culture conditions. The subsequent development of submerged culture (agitated and aereated) techniques[5,6] using Aspergillus Terreus raised the yield to between 40% and 50%.

The production of itaconic acid by decarboxylation of alkaline earth aconitates, separated from molasses, has also been studied[7]. Partial acidification converts most of the aconitate to aconitic acid and, during autoclaving at 413K, the residual alkaline earth aconitate promotes the decomposition of the aconitic acid to itaconic acid and carbon dioxide.

Until recently itaconic acid was relatively expensive and consequently very little applied research had been undertaken. The recent development of a large scale fermentation process (using Aspergillus Terreus with molasses as the source of carbohydrate) by Pfizer Chemicals in U.K. has considerably reduced the price of this potentionally useful chemical.

1.2 POLYMERISATION AND COPOLYMERISATION OF ITACONIC ACID

Although it was originally reported[8] that itaconic acid did not homopolymerise, later studies[9,10] established that slow oligomerisation does occur. The rate of the reaction is enhanced in solutions of low pH[11]. Bulk polymerisation is restricted by the high melting point of itaconic acid (441K) and by isomerisation above the melting point. However, both solution (using α,α'-Azo-bis-iso-butyronitrile (AIBN) as initiator) and emulsion (using persulphate as initiator) techniques, can be effectively used.

Copolymerisation of itaconic acid, especially with unsaturated monomers which produce resonance stabilised radicals during propagation, is much more easily realised and is of greater importance. Although in some cases the poor solubility of itaconic acid in normal organic solvents somewhat restricts the amounts which can be incorporated, high molecular weight copolymers have been obtained with acrylic and methacrylic esters, styrene, butadiene, vinylidene chloride and acrylonitrile[12,13]. More recently it has been reported that acid incorporation of up to 30% is possible in selected copolymer systems[14]. The use of itaconic acid as a comonomer is now fairly widespread in the fibre, coatings and adhesives industries[15].

1.3 ESTERS OF ITACONIC ACID

Esterification of itaconic acid was first reported in 1873[16]. Resin formation by itaconic acid esters was noted early in this century and initiated considerable efforts in this field[15]. Numerous patents[15] relating to itaconic

acid based esters have been issued since that time. These describe their use in such applications, as oil additives, plasticizers, coatings and synthetic fibres.

Apart from the patent literature, very little detailed information was available on the polymerisation of itaconic acid and its esters until a review article was published by Tate in 1967[10,17]. Since then, interest in polymers based on itaconic acid esters has gradually increased. The next section is essentially a review of the literature reports relating to their polymerisation, and also to the solution and physical properties of the resulting polymers.

1.4 THE POLYMERISATION OF ITACONIC ACID ESTERS

In 1958 Marvel and Shepherd[9] published the first detailed study of the homopolymerisation of dimethyl-, diethyl- and dibutyl itaconates. Later, in 1960, Nagai and his co-workers[18] undertook a dilatometric study of the kinetics of the bulk polymerisation of dimethyl-, diethyl-, di-n-propyl-, di-n-butyl- and di-n-octyl itaconates at 323K using AIBN as initiator. They suggested the following rate equation,

$$R_p = k[M][I]^{\frac{1}{2}} \qquad (1)$$

where R_p is the rate of polymerisation, k the apparent rate constant, [M] and [I] the concentrations of monomer and initiator respectively. As the alkyl group was changed from methyl through to octyl the value of k was found to increase. The proposed explanation for such behaviour is that there is chain transfer to monomer yielding relatively stable free radicals which delay propagation, but, as the alkyl group

becomes larger such transfer reactions become less likely due to increasing steric hindrance.

The same workers also studied[19,20] the bulk copolymerisation of 2-chloroethyl itaconate with styrene and methyl methacrylate, and of dimethyl-, diethyl-, diisopropyl- and di-n-octyl itaconates with vinyl chloride. They determined reactivity ratios and proposed that the presence of even a small amount of dialkyl itaconate in a copolymerisation feed lowers the polymerisation rate and reduces the bulk viscosity of the copolymer formed. Changing the ester from methyl to octyl did not affect significantly the reactivity of the itaconate double bond.

In 1967 Tate[10,17] published reviews on the polymerisation and copolymerisation of itaconic acid and its esters. He suggested that dimethyl and dibutyl itaconate (DMI and DBI) polymerise to give relatively low molecular weight products. On the assumption that the viscosity-molecular weight relation for poly(methyl methacrylate) (PMMA) applies to poly(dimethyl itaconate) (PDMI), he calculated that the degree of polymerisation of PDMI was ten to twenty times less than that of PMMA polymerised under the same conditions. Tate also noted that, under controlled conditions, it is possible to obtain good yields of monoalkyl esters of itaconic acid which can then be polymerised to poly(monoalkyl itaconates).[21]

In a comparison of the rate of the bulk polymerisation of DMI with that of monobutyl itaconate (MBI) under various conditions, he concluded that MBI polymerises approximately six times faster than DMI.[18,22,23] From the results of previous workers

Tate concluded that lower dialkyl itaconates can undergo ideal copolymerisation. The greatest tendency towards alternation occurs with itaconic acid, monobutyl itaconate, or with lower dialkyl itaconates and styrene. The alternation tendency is apparently less with vinyl chloride and lower dialkyl itaconates. It was also suggested that itaconate esters copolymerise more slowly than the corresponding methacrylic or methacrylonitrile comonomers, but more rapidly when used in systems where the comonomers themselves are acrylates or acrylonitriles. The reactivity ratios of the copolymer system monomethyl itaconate (MMI) and (MBI) have also been established[24].

While Tate paid very little attention to the physico-chemical properties of itaconate polymers, he did study the decarboxylation[25] of polyitaconic acid itself but no conclusive data was presented. He also suggested that polymers of dialkyl itaconates are similar in hardness to the polymers of corresponding alkyl methacrylates and quoted the softening point of PDMI to be about 335K and that of poly(dibutyl itaconate) (PDBI) to be about 285K.

Valickovic and co-workers[26-28] have published a series of papers on the hydrodynamic properties of itaconic acid based polymers. They measured the refractive index increments of a comprehensive series of di-n-alkyl itaconate polymers and copolymers and have established Kuhn-Mark Houwink-Sakurada (KMHS) relations and unperturbed dimensions for these systems. The same workers[28] have also polymerised dicyclohexyl itaconate, using AIBN as initiator, and have

established the solubility parameters and KMHS relationship for the product. The hydrodynamic properties of random copolymers of MBI and DBI have also been studied[29].

Nagai and Fujiwara[30] have elucidated the structures of poly(itaconic acid) derivatives by using thermal degradative gas chromatography techniques and concluded that itaconic acid and MMI normally polymerise to yield head-to-tail linear polymer, but that under certain conditions they can subsequently change their structure with evolution of carbon dioxide.

In 1975 Yokata et al.[31] prepared PDMI by esterification of poly(itaconic acid) (PIA). The PIA sample used for the esterification was prepared by two methods, (i) by polymerisation of the acid itself and (ii) by polymerising itaconic anhydride and subsequent hydrolysis. Using differential scanning calorimetry (DSC) and thermogravimetry (TG) these workers established that PIA loses water rapidly between 343K and 373K and undergoes an additional, abrupt weight loss at 443K. They propose that, at 373K, PIA has dehydrated to form poly(itaconic anhydride) which subsequently decomposes at 443K.

Overall, polymers based on esters of itaconic acid have received relatively little attention and, apart from two recent studies by Cowie and his co-workers[32,33], very little has been published on their thermomechanical properties.[34] The main object of this present study is to establish the solid state thermomechanical, and other related properties, of polymers based on esters of itaconic acid.

CHAPTER 2

THE THERMOMECHANICAL BEHAVIOUR OF POLYMERS

2.1 AMORPHOUS POLYMERS

The majority of high polymers form transparent glasses when they are cooled from the liquid or rubber-like state. It is usually assumed that, in the amorphous state (glass, liquid or rubber), the polymer chains are arranged in a completely random manner, with none of the restrictions imposed by the ordering which occurs in partly crystalline polymers. There is, however, no unambiguous evidence for such a hypothesis, and it has been proposed[35] that amorphous polymers do contain elements of order in the form of globules or bundles of polymer chains. Happily, the major transition of an amorphous polymer (to be discussed shortly), the glass transition, can be qualitatively explained by considering either picture[36].

2.2 VISCOELASTIC BEHAVIOUR

The mechanical properties of elastic solids can be described in classical terms by Hooke's law; the corresponding description for liquids is embodied in Newton's law[37]. In many cases, polymeric materials exhibit the characteristics of both solids and liquids, they are said to be in a viscoelastic state.

The physical nature of an amorphous polymer is related to the extent of molecular motion in the sample. In the glassy state, cooperative motion along the chain is frozen and the material has most of the characteristics of an elastic solid. When the elastic modulus is measured it is normally found to be of the order 10^{10}-10^{9} Nm^{-2}. The

polymer chains behave as stiff springs which, if deformed, will store the available energy as potential energy.

If now thermal energy is supplied so that cooperative movement of the polymer chains is generated by rotation about the single bonds connecting the atoms of the chain, a transition from the glass to the rubber-like state begins to take place. At this temperature, the glass transition temperature (Tg), dramatic changes in the physical properties, such as hardness and elasticity, are observed. As the temperature is further raised an increasing number of polymer chains begin to move with greater freedom. Finally, when molecular motion has increased to a sufficient level, the polymer chains can be considered as behaving as weak springs, able to store only a fraction of the potential energy. The elastic modulus of the polymer is now several orders of magnitude lower than that in the glassy state.

There are five distinguishable viscoelastic states in which a linear amorphous polymer can exist; these are most readily illustrated by a study of a parameter such as the elastic modulus as a function of temperature which is shown in figure 2.1.

(i) The glassy state (A-B). Here cooperative motion is frozen and the polymer responds to strain like an elastic solid. The modulus is high ($\sim 10^{10}$ Nm^{-2}) and mechanical damping is low.

(ii) The leathery region (B-C). The modulus is rapidly falling and the mechanical damping rises through a maximum value. Molecular motion is increasing rapidly in this region.

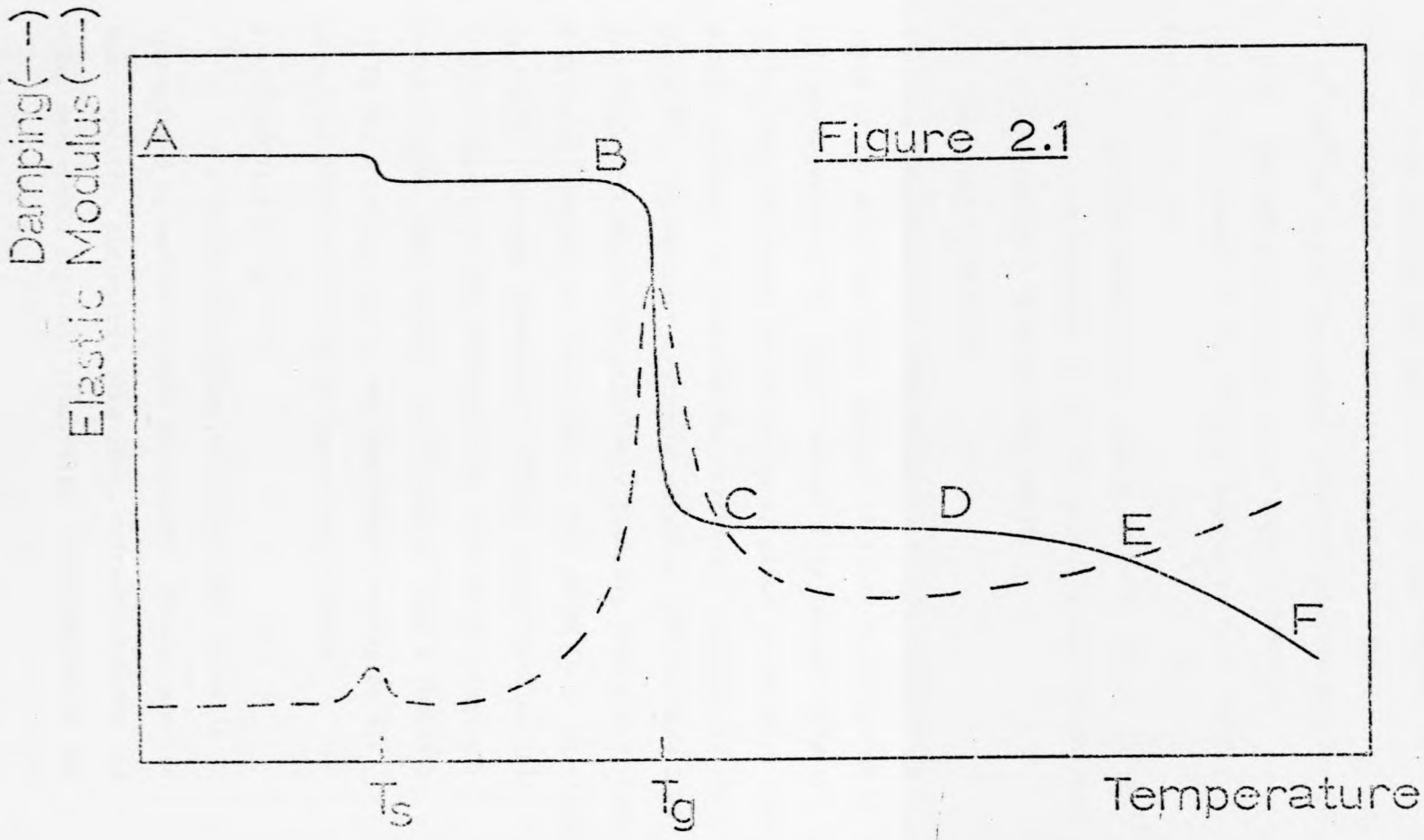

Figure 2.1

(iii) The rubbery plateau (C-D). In this region the modulus maintains an approximately constant value ($\sim 10^6$-10^5 Nm^{-2}) and the polymer exhibits elastic recovery.

(iv) Rubbery flow region (D-E). Elastic recovery begins to decrease and the modulus begins to fall rapidly again.

(v) Viscous state (E-F). The modulus is low ($\sim 10^4$ Nm^{-2}), there is little evidence of elastic recovery and the polymer behaves essentially as a viscous liquid.

2.3 THE GLASS TRANSITION

The transition from the glass to the rubber-like state is the most important feature of solid state amorphous polymer behaviour. The actual value of Tg depends largely on the chemical nature of the polymer, since it reflects the energy necessary to overcome the rotational barriers in the chain[38]. Tg for most synthetic polymers lies between 170K and 500K. Polymers with relatively flexible chains will have a Tg value towards the lower end of this range (e.g. polyisoprene, Tg = 200K), whereas those with stiffer chains will exhibit higher transition temperatures (e.g. atactic poly(methyl-methacrylate), Tg = 378K). It is obvious that a knowledge of Tg for a polymer has a very important bearing on its potential applications as an engineering material.

2.4 DETECTION OF Tg

The change from glass to rubber-like state is accompanied by marked changes in specific volume, modulus, heat capacity, dielectric behaviour, refractive index and other measurable physical properties. Observation of the

change in such a property can thus be used to detect Tg. Since the transition also possesses, to some extent, the characteristics of a relaxation process[38]; the precise value found can depend on the method used and on the rate of the measurement.

The methods used for locating Tg can be divided into two categories, dynamic and static. In a static technique, the temperature dependence of a property (such as density or heat capacity) is followed, allowing the sample to equilibrate and relax at each observation temperature. The three techniques employed in this study (differential scanning calorimetry, the torsional braid pendulum and linear visco-elastometry, see sections 3.10, 3.9 and 3.11 respectively) are essentially dynamic techniques.

Differential scanning calorimetry involves the measurement of specific heat (Cp) while the temperature of the sample is continuously changed at some chosen rate. The glass transition is evidenced by a sharp change in the value of Cp, the actual temperature of the change is a function of the temperature scan rate.

The torsional braid pendulum and linear visco-elastometry are dynamic mechanical techniques in which a large change in modulus or a maximum in mechanical damping is indicative of the glass transition (see figure 2.1). Here, however, the precise location of Tg is dependent on the frequency of the applied force[38]; at low frequencies this is often within a few Kelvins of that obtained by static methods.

2.5 FACTORS AFFECTING Tg

As already noted, the location of the Tg depends largely on the amount of thermal energy required to maintain the polymer chains in motion. Several factors affect the ease of rotation about chain links.

(i) Chain flexibility. This is probably the single most important factor, for a symmetric polymer the chemical nature of the chain backbone is all important. Polymers containing sequencies which can rotate easily, such as $\{CH_2\text{-}CH_2\}$, $\{CH_2\text{-}O\}$ or $\{Si\text{-}O\}$, have inherently low values of Tg.

(ii) Steric effects. When polymer chains are substituted, giving repeat units of the type $\{CH_2\text{-}CHX\}$ an additional restriction to rotation is introduced. As the bulk of group X increases, so then does the value of Tg, for example, in the series polythene (X = H, Tg = 188K), polypropylene (X = CH_3, Tg = 253K), polystyrene (X = C_6H_5, Tg = 373K).

(iii) Microstructure. Cis-trans isomerism in polybutadienes and tacticity[37] variations in α-methyl substituted polymers alter chain flexibility and affect Tg.

(iv) Cross links. When cross links are introduced between polymer chains their motion is impeded and Tg consequently rises. If the number of cross links is large, the transition will become broad and ill-defined. Cross linking has the additional effect of increasing the extent of the rubbery plateau (see figure 2.1) and of increasing the elastic modulus in this region.

(v) Effect of molecular weight. At high molecular weights Tg is essentially constant, but is found to decrease when the molecular weight of the sample decreases. The precise molecular weight at which this occurs varies from polymer to polymer[39].

2.6 SECONDARY TRANSITIONS

The glass transition results from the onset of cooperative motion of the polymer chains when sufficient thermal energy has been supplied to overcome the rotational barriers about the linking atoms of the chains. Motion of smaller sections of the polymer chain architecture, requiring considerably less energy, can occur in the glassy state. One such transition, generally termed a sub-transition, is indicated by T_s in figure 2.1. T_s is accompanied by a small increase in damping and a minor drop in the modulus.

Although sub-transitions can be fairly easily detected, especially using low-frequency dynamic mechanical methods, their molecular origin is generally much less obvious. Probably only in one instance can the origin of a sub-transition be unambiguously defined - when a cyclohexyl ring is present in a polymer side-chain. Low temperature ($\sim$ 190K) transitions in cyclohexyl methacrylate[40] and dicyclohexyl itaconate[33] polymers has been assigned to ring conformational changes; when the cyclohexyl ring is replaced by the rigid phenyl ring the transition is absent.

General agreement also exists as to the cause of the broad sub-transition which is present ($\sim$ 283K) in alkyl methacrylate polymers. This is thought to arise from hindered rotation of the -COOR group about the C-C link to the main chain, although it is not clear whether or not the main chain itself is locally involved in the movement. Another, widely postulated, molecular movement which is often assigned to a sub-transition is the so-called crankshaft motion[38]. This is thought to occur with polymethylene chains of at least four

carbons long and may be visualised as follows:-

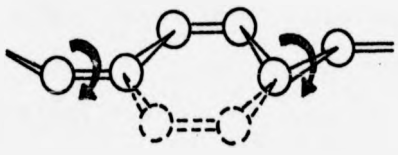

Other, postulated causes of sub-transitions include group rotations, e.g. methyl or phenyl rotation[38], and relaxations due to absorbed species, e.g. water in poly(methylmethacrylate)[38].

Polymers, therefore, do not form perfect elastic solids, limited amounts of bond rotation in the glassy state allow slight plastic deformation; this makes them somewhat tougher than inorganic glasses.

2.7 COPOLYMERS

Only for a very few random copolymers composed of compatible monomer pairs, e.g. styrene and butadiene, is a simple linear relationship between Tg and copolymer composition found. More commonly, non-linear behaviour is observed and several equations relating Tg and copolymer composition have been proposed, all of which can be derived from a general expression first presented by Wood[41]

$$A_1 w_1 (Tg - Tg_1) + A_2 w_2 (Tg - Tg_2) = 0 \qquad (2.1)$$

where Tg_1 and Tg_2 are the glass transition temperatures for the homopolymers 1 and 2, A_1 and A_2 are constants and w_1 and w_2 are the weight fractions of comonomer 1 and comonomer 2 in

the copolymer. If certain relationships exist between the constants, according to Fox[42] (2.1) becomes

$$\frac{1}{Tg} = \frac{w_1}{Tg_1} + \frac{w_2}{Tg_2} \qquad (2.2)$$

where $A_2Tg_2/A_1Tg_1 = 1$.

If $\frac{A_2}{A_1} = 1$ then equation (2.1) reduces to

$$Tg = (Tg_2 - Tg_1)w_2 + Tg_1 \qquad (2.3)$$

with a linear relation between Tg and w_2.

From theoretical considerations different authors have given the constants A_1 and A_2 a physical significance allowing them to be calculated from other quantities. Gordon and Taylor[43] give

$$A_i = \beta_{i\ell} - \beta_{ig} \qquad (2.4)$$

where β_i is the volume-temperature coefficient for homopolymer i in the liquid (ℓ) and glassy (g) states respectively. Gibbs and DiMarzio[44] interpret the constants in a different manner

$$A_i = \alpha_i/M_i \qquad (2.5)$$

where α_i is the number of single bonds per monomer unit of molecular weight M_i.

The glass transition behaviour of block copolymers is less predictable and certain pairs of comonomers will form a block copolymer possessing two glass transitions. This is usually explained in terms of the "domain concept". Blocks

of one comonomer tend to aggregate in domains and are surrounded by areas composed almost exclusively of the other comonomer. These two different regions within the polymer then display glass transition behaviour corresponding to the equivalent homopolymers. Such behaviour has lead to the construction of very useful plastics such as SB rubber which is composed of glassy styrene blocks and elastomeric butadiene blocks.

2.8 IONOMERS

The word "ionomer" was coined to describe thermoplastic ionic polymers consisting of a hydrocarbon backbone with pendant carboxylic acid groups which have been neutralised (partially or completely) with some suitable metal cation. This increases the association forces between carboxyl groups and creates what may be termed ionic crosslinks between polymer chains. Most work has been done on ethylene-methacrylic acid copolymers[45] and X-ray analysis of these compounds suggests that the ions aggregate into spherical clusters embedded in an amorphous network.

At low ion concentrations (up to ~6%) ionisation has a marked effect on the modulus, especially above Tg. The resulting polymers are generally tougher, and are more resistant to plastic flow. If the ion concentration is too large however, the product will be a rather intractible brittle solid.

2.9 CRYSTALLINITY IN AMORPHOUS POLYMERS

The presence of significant crystalline order in an amorphous polymer will have a considerable effect on its general mechanical properties[37]. Regions D-E and E-F in figure 2.1 are not realised until sufficient thermal energy

has been supplied to melt out crystallinity, after which viscous flow can occur. The presence of crystalline regions, therefore, has the effect of extending the temperatures over which leathery or rubber-like response occurs and can lead to a more useful material in many practical applications.

Crystallinity can occur when a polymer possesses a symmetrical chain structure allowing close-packing and/or polar groups which encourage strong inter-molecular forces. Polymers with the structural repeat unit $\leftarrow CH_2\text{-}CX_1X_2\rightarrow$ do not readily crystalline unless $X_1 = X_2 = H$ (polythene) or are arranged in a non-random tactic configuration. If one of the side groups (X_1 or X_2) itself contains a crystallisable structure then this also can have a significant effect on the properties of the polymer.

CHAPTER 3

EXPERIMENTAL

TABLE 3.1

Abbreviated Names of Poly(di-n-alkyl itaconates) and Poly(mono-n-alkyl itaconates) used in this thesis.

Name of Sample	Abbreviated Name
Poly(di-methyl itaconate)	PDMI
Poly(di-ethyl itaconate)	PDEI
Poly(di-n-propyl itaconate)	PDPrI
Poly(di-n-butyl itaconate)	PDBI
Poly(di-n-pentyl itaconate)	PDPI
Poly(di-n-hexyl itaconate)	PDHI
Poly(di-n-heptyl itaconate)	PDHpI
Poly(di-n-octyl itaconate)	PDOI
Poly(di-n-nonyl itaconate)	PDNI
Poly(di-n-decyl itaconate)	PDDI
Poly(di-n-undecyl itaconate)	PDUI
Poly(di-n-dodecyl itaconate)	PDDoI
Poly(mono-methyl itaconate)	PMMI
Poly(mono-ethyl itaconate)	PMEI
Poly(mono-n-propyl itaconate)	PMPrI
Poly(mono-n-butyl itaconate)	PMBI
Poly(mono-n-pentyl itaconate)	PMPI
Poly(mono-n-hexyl itaconate)	PMHI
Poly(mono-n-heptyl itaconate)	PMHpI
Poly(mono-n-octyl itaconate)	PMOI
Poly(mono-n-nonyl itaconate)	PMNI
Poly(mono-n-decyl itaconate)	PMDI

3.1 SYNTHESIS OF MONOMERS

3.1.1 Di-n-Alkyl Itaconates

Di-n-alkyl itaconate esters were prepared by sulphuric acid catalysed esterification of itaconic acid in benzene as solvent[46]

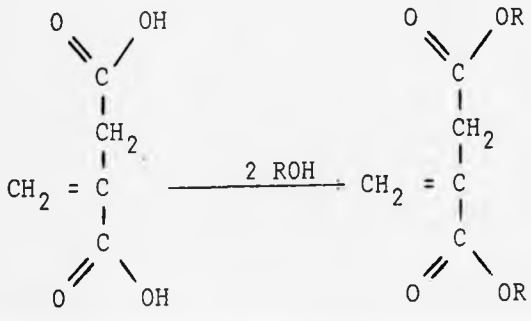

Itaconic acid (pure) was obtained from either Pfizer Chemicals or Koch Light Laboratories and was used without further purification. Methanol (BDH, A.R. Grade), Butan-1-ol (BDH, A.R. Grade) and Heptan-1-ol (Koch Light, puriss grade) were fractionally distilled prior to use. Decan-1-ol (BDH, "specially pure") was used without further purification. Benzene (BDH, A.R. Grade) was distilled and dried over molecular sieves before use.

The quantities of reagents used in each preparation are shown in table 3.2. The mixtures were refluxed with constant stirring for six hours, during which time the esters formed and passed into the benzene layer. After cooling, distilled water was added to the reaction flask. The benzene layer was then separated and washed repeatedly with water until the washings were neutral to litmus. The benzene/ester solution was dried overnight with anhydrous potassium or sodium sulphate,

TABLE 3.2

Amounts of reagents used in the preparation of diesters of itaconic acid.

Ester	Acid moles	Alcohol moles	Benzene cm^3	H_2SO_4 cm^3
DMI	1	3-4	375	33
DBI	1	3-4	400	35
DHpI	1	3	500	35
DDI	1	3	1000	35

TABLE 3.3

Details of reaction products from the preparations of diesters of itaconic acid.

Ester	Boiling Range		Yield/%	Refractive Index	Melting point*/K
	Temp/K	Pressure/torr			
DMI	363-368	1 - 1.2	68	1.4412	309
DBI	395-403	0.3 - 0.1	72	1.4419	-
DHpI	461-463	0.3 - 0.2	70	1.4497	-
DDI	488-498	0.4 - 0.2	50	1.4561	279

* Melting point detected by DSC, see section 3.10.

filtered and vacuum distilled to yield a crude product. This was redistilled twice, again under vacuum, to yield the pure diester.

Complete esterification was verified by NMR analysis (see section 3.17) and in no case were residual acid groups detectable in the final products. These were stored in the dark at 298K until required. The boiling ranges and pressures of the pure products are shown in table 3.3, along with percentage yields, melting points and refractive indices.

A slight variation of the technique described above proved necessary during the preparation of the didecyl ester which formed a thick, stable, emulsion during the washing of benzene layer. This was overcome by separating the benzene layer directly from the reaction flask and washing with 5% sodium bicarbonate solution. The resulting white emulsion was washed twice with large quantities of water and left at 313K overnight. A considerable amount of water could be separated off the next day. The remainder was removed by adding a large amount of anhydrous sodium sulphate to yield, after filtration, a clear benzene solution of didecyl itaconate, which was treated as before.

3.1.2 Mono-n-Alkyl Itaconates

The preparation of mono methyl- and mono-n-butyl itaconate has been reported by Baker et al.[47] The method outlined by these authors proved suitable for the preparation of the series of mono-n-alkyl itaconates used in this study.

Methanol, ethanol, propan-1-ol, butan-1-ol, pentan-1-ol and hexan-1-ol were all A.R. grade supplied by BDH and were fractionally distilled prior to use. Heptan-1-ol (Koch-Light, puriss), octan-1-ol (Koch-Light, puriss) and nonan-1-ol (Koch-Light, pure) were used without further purification. Mono esterification of itaconic acid, according to the equation,

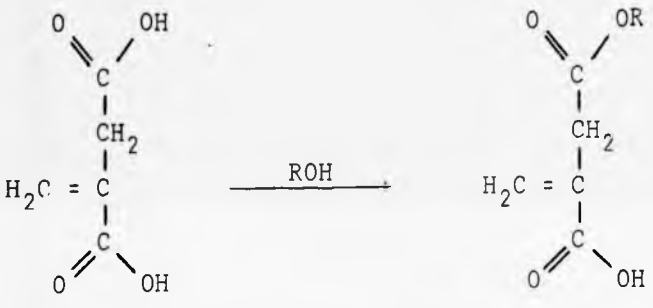

was carried out by refluxing (for 10-15 minutes) a mixture of itaconic acid and excess alcohol in the presence of acetyl chloride as catalyst. This was followed by rapid removal of unreacted alcohol under reduced pressure. The monoester was then isolated by fractional distillation under reduced pressure. The product was further purified by a minimum of three recrystallisations at 278K from benzene-petroleum ether solutions until a sharp melting point was obtained. The pure products were stored in the dark at 278K until required.

The amounts of reagents used in the preparations, and yield of each monoester are shown in table 3.4. This table also shows the boiling ranges and pressures used to isolate the crude products and the melting points of the recrystallised products.

TABLE 3.4

Ester	Acid/Moles	Alcohol/Moles	Acetychloride/cm^3	Boiling Range Temp./K	Pressure/torr	Yield %	Melting point/K
MMI	1	3 - 4	2	395-440	25 - 20	60	341-342
MEI	1	3 - 4	3	323-348	5 - 4	60	329-330
MPrI	1	3 - 4	3	413-423	6 - 5	50	308-309
MBI	1	3 - 4	3	442-448	8 - 10	65	314-315
MPI	1	3 - 4	4	423-428	0.6 - 0.5	60	313-314
MHI	1	3 - 4	4	423-433	0.5 - 0.4	50	317-318
MHpI	1	3 - 4	4	453-457	0.6 - 0.5	60	323-324
MOI	1	3	4	443-448	0.3 - 0.5	60	330-331
MNI	1	3	5	443-455	0.05 - 0.01	50	334-335
MDI	1	3	5	503-523	0.05 - 0.01	50	342-343

During the preparation of this series of mono esters, the following points of technique were found to improve yields and reduce contamination of products.

(a) Acetyl chloride catalyst should be dried, freshly distilled and added dropwise with stirring to the warm reaction mixture prior to refluxing.

(b) Efficient and continuous stirring from the start of the reaction helps to increase yields and suppress contamination by impurities.

(c) The main impurities encountered in the product monoesters were unreacted itaconic acid, itaconic acid anhydride and di ester. During the preparation of MMI, MEI and MPI, recrystallisation steps must be undertaken to ensure complete removal of these impurities.

During the recrystallisation of monomethyl to monopropyl itaconates, a benzene/petroleum ether mixture (1:1) was used; for remaining higher monoesters petroleum ether alone was used.

After purification, each monoester was characterised by its melting point measured using DSC techniques (section 3.10), infrared analysis (section 3.16), NMR analysis (section 3.17) and by titration of the carboxyl groups (section 3.5). Representative infrared spectra and NMR spectra are shown in figures 3.1 and 3.2 respectively.

3.2 SOLUTION AND BULK POLYMERISATION OF MONO-n-ALKYL ITACONATES

Several monoesters of itaconic acid were polymerised using conventional solution and bulk techniques. AIBN (BDH) which was used as initiator, was recrystallised from methanol

Fig.3.1

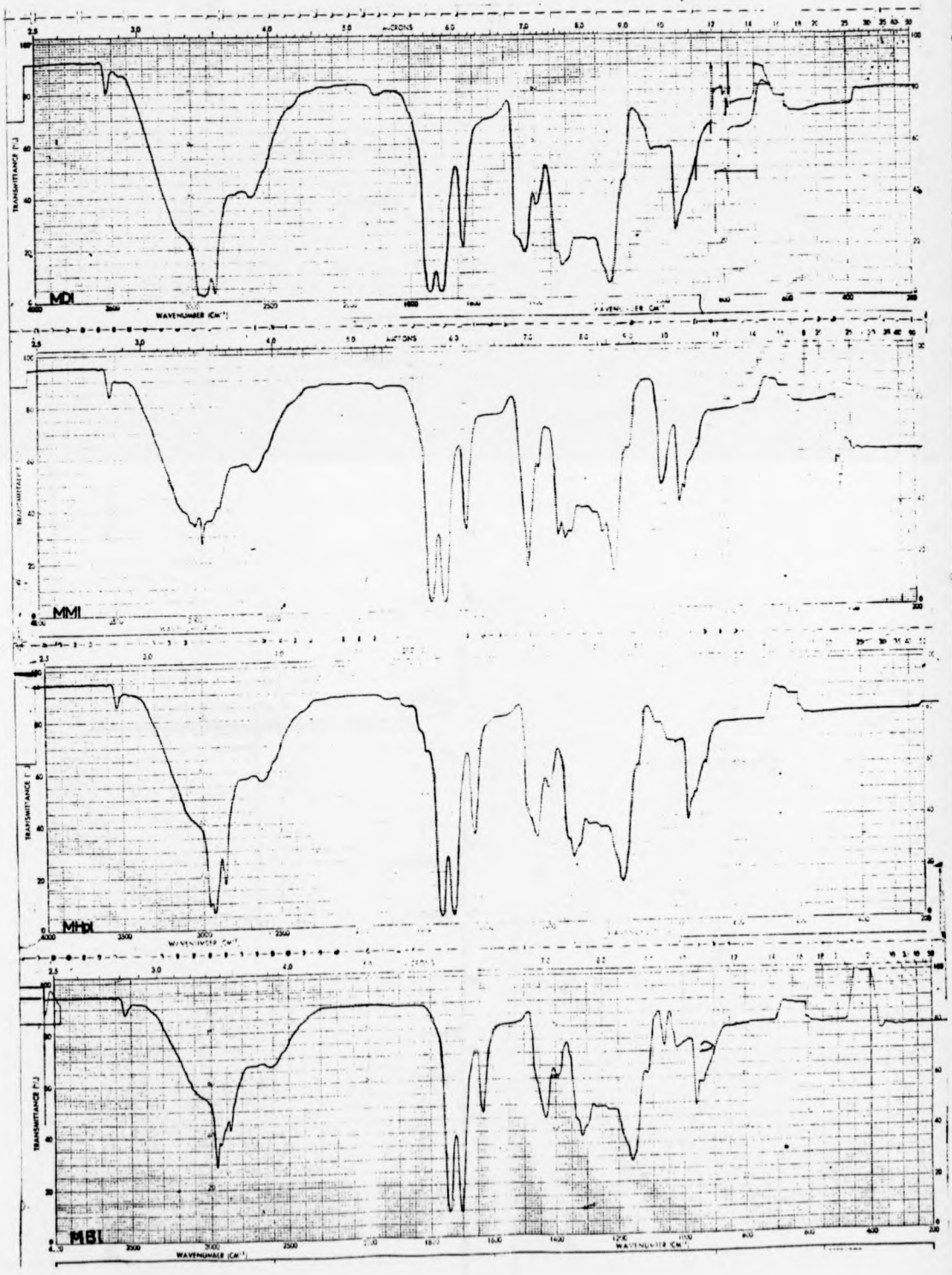

Fig.3.2

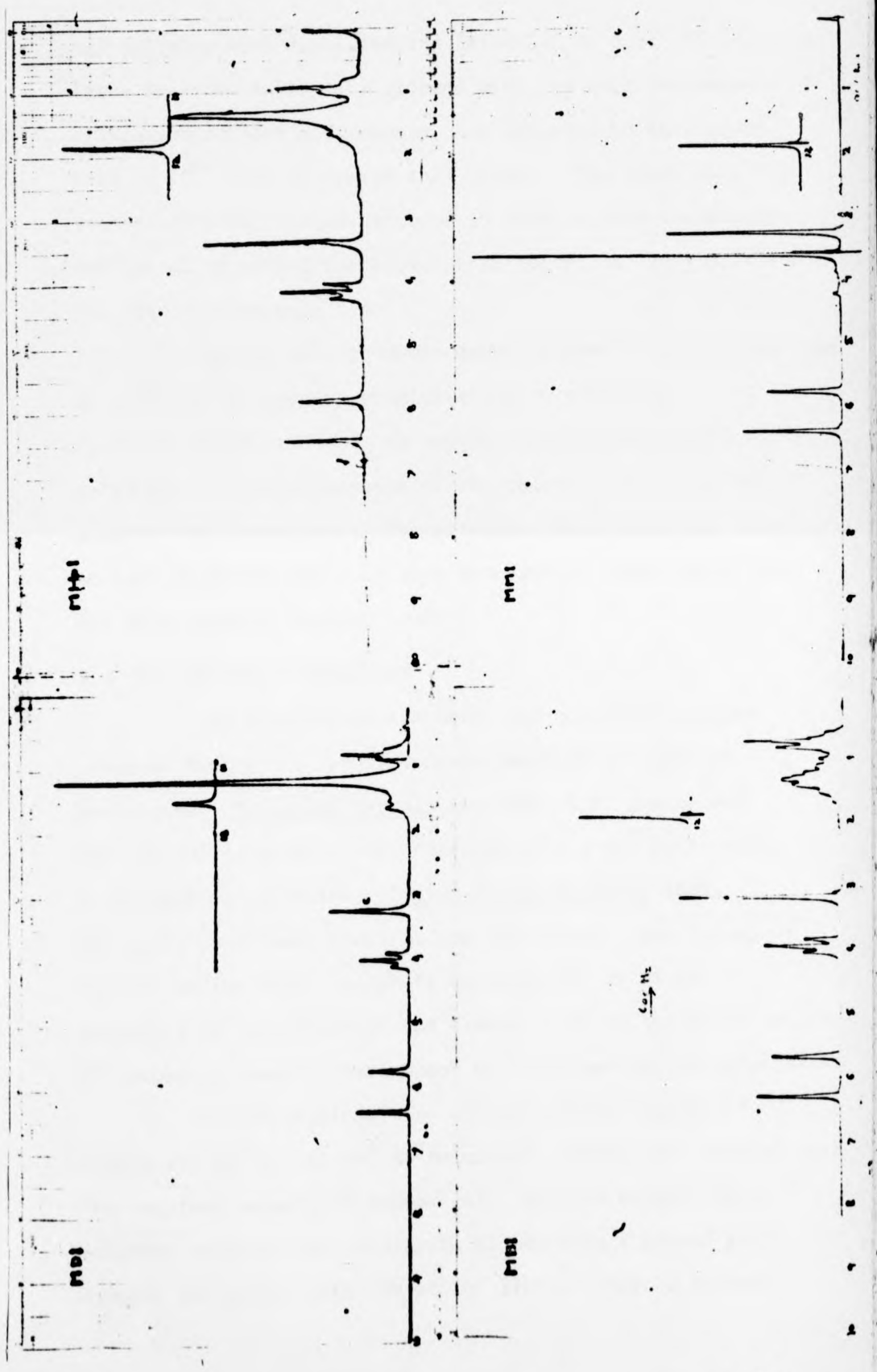

and solvents were distilled and dried before use. Heavy-walled Pyrex reaction tubes were charged with the required amounts of initiator, solvent and monomer, and degassed on the vacuum line at 10^{-5} torr by freeze-thaw cycles. The tubes were then sealed-off under vacuum, allowed to warm to room temperature and placed in an oil thermostat bath controlled to $\pm$ 0.1K for the required reaction time.

The reaction products were isolated by dissolving them in methanol followed by precipitation in n-butanol. Purification was effected by several further reprecipitations, until the infra-red spectrum of the polymer was free from monomer C=C absorptions. The polymers, which were all white solids, were then dried at room temperature under vacuum for two days prior to further study.

3.3 EMULSION POLYMERISATION

The majority of the homo- and copolymer samples prepared during this study were polymerised by emulsion techniques. Potassium persulphate (BDH, A.R. grade) was used as initiator at a concentration of 0.5 wt % with respect to monomer in all cases. Sodium lauryl sulphate (BDH, specially pure) was chosen as the emulsifier. The volume of aqueous sodium lauryl sulphate solution (2% to 5% w/v according to requirements) was always equal to the total volume of monomer(s) used in each homo- or copolymerisation undertaken.

Polymerisations were carried out in "Quickfit" flasks (25 cm^3 to 250 cm^3 as required). These were charged with the required amounts of monomer(s), aqueous sodium lauryl sulphate solution and initiator, closed with a ground glass stopper and sealed with "Parafilm" strip. Where a monomer

was a solid at room temperature this was first melted in the reaction flask and mixed with emulsifier solution before adding initiator.

Agitation was effected by attaching the reaction flasks to a specially constructed extension arm fitted to a Griffith flask shaker and immersing them about three quarters in a bath filled with shell "Nonadet" detergent, thermostatted within $\pm$ 0.5K. Gentle shaking provided stable emulsions for all the preparations carried out here.

After the required reaction time, crude polymer was coagulated from the emulsion by the addition of a small amount of water miscible non-solvent. The product was washed several times with warm distilled water (to remove emulsifier) and finally left overnight in water. Unreacted monomer was removed by several washings with a suitable non-solvent for the polymer which was then finally purified by reprecipitation until the infrared spectrum of the product was free from C=C absorbance. If, after the first reprecipitation, a clear solution was not obtained, the solution was centrifuged to remove any traces of emulsifier. The purified polymer was dried under vacuum at room temperature for at least two days prior to any further study.

Table 3.5 contains the details of the polymerisations of the mono esters of itaconic acid and table 3.6 the details of the polymerisation of the diesters. Additionally, the polymers listed in table 3.7 were kindly supplied by J. Velickovic[25] of the Faculty of Technology and Metallurgy, Belgrade.

TABLE 3.5

EMULSION POLYMERISATION DETAILS FOR MONO-n-ALKYL ITACONATES

Monomer	Emulsifier Solution % w/v	Temp. K	Reaction Time h	Coagulant used	Precipitant System		Yield %
					Solvent	Precipitant	
MBI	2	328	24	Diethyl ether	Ethanol	Cyclohexane+ Diethyl ether	90
MPI	2.5	323	28	"	"	"	42
MHI	2.5	324	40	"	"	"	60
MHpI	2.5	333	24	Methanol	Ethanol	Cold methanol	50
MOI	5.0	338	20	"	THF	"	38
MNI	5.0	338	30	"	"	"	25
MDI	5.0	348	28	"	Warm Dioxan or Dioxan + Diethyl ether	"	27

TABLE 3.6

EMULSION POLYMERISATION DETAILS OF DI-n-ALKYL ITACONATES

No.	Monomer	Emulsifier Solution % w/v	Temp. K	Reaction Time h	Coagulant used	Precipitant System		Yield %
						Solvent	Precipitant	
1	DMI	2.0	328	22	Diethyl ether	Acetone	Diethyl ether	18
2	DBI	2.0	328	23	"	Acetone	Cold (283K) methanol	65
3	DHpI	2.5	328	23	Methanol	Methyl-ethyl ketone	Cold (228K) methanol	52
4	DDI	5	328	40	"	Diethyl ether	"	65

TABLE 3.7

POLYMER SAMPLES SUPPLIED BY J. VELICKOVIC

Polymer	Mol.wt.($\bar{M}_w$) x 10^{-5}
DDEI	2.0
PDPrI	4.89
PDHI	2.77
PDOI	4.00
PDNI	3.00
PDUI	18.40
PDDoI	2.00

3.4 COPOLYMERISATION OF ITACONIC ACID MONO- AND DI-ESTERS

Six series of copolymers were prepared by the emulsion technique described in the section 3.3, again using 0.5 wt % of potassium persulphate as initiater in all cases. The following convenient nomenclature for the description of a copolymer has been adopted, for example -

Poly(MBI + DBI): copolymer of mono butyl itaconate and di butyl itaconate.

Conversion to copolymer was limited to less than 13% in all cases. Crude copolymers were isolated and purified essentially as described in the previous section; solvent and non-solvents were selected according to which homo-polymer the copolymer feed was nearer.

(i) Poly(MBI + DBI)

A series of copolymers was prepared at 328K with different monomer feed ratios, using 2.5% w/v emulsifier solutions. The following conversions were obtained.

TABLE 3.8

Monomer feed ratio		Polymerisation time/h	Conversion %
MBI/g	DBI/g		
1	9	5	10.5
3	7	4	11.0
4	6	4	9.2
6	4	3	10.2
8	2	2	13

(ii) Poly(MBI + DMI)

This series of copolymers was prepared using 2% emulsifier solutions at 328K. The following conversions were obtained for the different feed ratios.

TABLE 3.9

Monomer feed ratio		Time/h	Conversion %
MBI/g	DMI/g		
2	8	11	12
4	6	7	7.2
5	5	5.5	8.5
6	4	5	6
7	3	6.5	8

(iii) Poly(MHpI + DHpI)

Copolymers were prepared with different monomer feed ratio at 331K, using 2.5% emulsifier solutions. Conversions are shown in the table below.

TABLE 3.10

Monomer feed ratio		Time/h	Conversion %
MHpI/g	DHpI/g		
1	9	3	9.5
2	8	2	10.0
3.3	7	2.2	11
5	5	2	9
6	4	2	12

(iv) Poly(MDI + DDI)

Polymer samples were prepared with different feed ratios using 5% emulsifier solutions at 348K and the following conversions were obtained.

TABLE 3.11

Monomer feed ratio		Time/h	Conversion %
MDI/g	DDI/g		
1.5	8.5	0.75	6
2.5	7.5	1.75	6
3.5	6.5	2.0	9.5
5.5	4.5	1.5	6.5
6.5	3.5	3.00	13
7.5	2.5	1.5	15
8.5	1.5	0.75	8

(v) Poly(DMI + DHpI)

Copolymers with different monomer feed ratios were prepared using 5% emulsifier solutions at 328K. The conversions are shown in the table below.

TABLE 3.12

Monomer feed ratio		Time/h	Conversion %
DMI/g	DHpI/g		
0.5	9.5	3	10
1	9	3.5	12
2	8	4	7
3	7	4	13
5	5	4.5	13
8	3	6	8

(vi) Poly(DMI + DDI)

Copolymers were prepared with different monomer feed ratio using 5% emulsifier solutions at 328K and following conversions were obtained.

TABLE 3.13

Monomer feed ratio		Time/h	Conversion %
DMI/g	DDI/g		
1	10	3	8
2	10	10	25
3	10	4.5	7
4	8	12	14
8	4	7	5
10	1	11	13

3.5 REACTIVITY RATIO MEASUREMENTS

The reactivity ratios for the six copolymers systems prepared as described in the previous section were measured by using two different techniques.

In the systems Poly(MBI + DBI), Poly(MBI + DMI) and Poly(MHpI + DHpI), the amount of monoester in each copolymer was estimated by non-aqueous potentiometric titration as follows.

A 25 cm^3 solution of a known weight concentration (approximately 0.2 ∿ 0.4g) of copolymer was made up in a suitable solvent or solvent mixture. Standard M/10 sodium hydroxide solution was made up using CVS(BDH) solution, again in the appropriate solvent or solvent mixture. The details are shown in Table 3.14 below.

TABLE 3.14

Copolymer system	Solvent Composition by volume	NaOH Solution 10% water +
Poly(MBI + DBI)	Methanol	Methanol
Poly(MBI + DMI)	Butanol + DMSO 50 50	Butanol + DMSO 50 40
Poly(MHpI + DHpI)	Butanol & Ethanol 50 50	Butanol + Ethanol 50 40

Solutions were titrated at 298K ± 0.5K with constant stirring using a pH meter (CORNING-EEL Model 7) connected to a Heathkit 10 mV chart recorder. Sodium hydroxide solution was added from a calibrated burette and the pH observed on the recorder. Since the reaction time for neutralisation of acid groups on the copolymer chains was invariably lengthy (up to one half hour in the case of poly(MHpI + DHpI)) the use of a recorder was essential. When there was no further change in the indicated pH, this value was noted and plotted as a function of the volume of sodium hydroxide solution added. The amount of free acid group in any sample of copolymer, and hence the content of monoester, was calculated from the end point of the titration curve.

In the case of Poly(DMI + DHpI) and Poly(DMI + DDI), analyses of the copolymer were carried out using an N.M.R. technique (see section 3.17). The relative amounts of DMI(x) and DHpI(y) or DDI(z) in the copolymer were calculated from the areas of the absorptions at 0.9 - 2.3 τ (A) due to

methylene absorption ($-CH_2-CH_2-$), and 3.4 - 4.5 τ (B) due to methoxy($-OCH_3$) and oxymethylene ($-OCH_2-$). The following equations for Poly(DMI + DHpI)

$$2x + 28y = \text{area of A} \qquad (3.1)$$

$$6x + 4y = \text{area of B} \qquad (3.2)$$

and for Poly(DMI + DDI)

$$2x + 40y = \text{area of A} \qquad (3.3)$$

$$6x + 4z = \text{area of B} \qquad (3.4)$$

were used.

Peak areas were measured both by instrumental integration and by cutting and weighing. In both types of analysis (i.e. titration and n.m.r.) errors are estimated at ca. ± 5%.

The reactivity ratios were calculated from the well-known relation[37]

$$r_2 = r_1 H^2/h + H(1-h)/h \qquad (3.5)$$

where r_1 and r_2 are the reactivity ratios, h is the mole ratio of monomer (1) to monomer (2) in the copolymer, and H the same ratio in the monomer feed. This equation is only valid for low polymer conversions. H^2/h was plotted against $H(1-h)/h$ and r_1 and r_2 determined from the slope and intercept respectively of the resulting straight line graph.

3.6 PREPARATION OF IONOMERS (POLYSALTS)

Ionomers were prepared by reacting low conversion (less than 13%), monoester containing, copolymers with a hydroxide solution (NaOH, KOH or CsOH) using the technique described in section 3.5. After the required amount of hydroxide solution had been added, the solutions were stirred

overnight at 313K. The solvent was then evaporated and the resulting ionomer dried at 313K for 4 days under vacuum.

3.7 VISCOSITY MEASUREMENTS

Polymer solutions for viscometric molecular weight determinations of poly(di-n-alkyl itaconates) were made up and allowed to stand at least 24 hours to ensure complete dissolution. Both polymer solutions and solvents for subsequent dilutions were filtered through G5 glass sinters before use. The specific viscosity (η_{sp}) was obtained at five different concentrations using a modified Ubbelohde viscometer which could be suspended reproducibly by a three point mounting in a thermostat bath controlled within $\pm$ 0.01K.

The intrinsic viscosity [η] was obtained by plotting $\eta_{sp/c}$ against c, where the concentration c is expressed in g cm^{-3} of polymer solution. The viscosity average molecular weight ($\bar{M}_v$) was calculated from the relation

$$[\eta] = K \bar{M}_v^{\alpha} \qquad (3.6)$$

The values of the parameters K and α have been established by Velickovic[25].

3.8 LIGHT SCATTERING AND REFRACTIVE INDEX INCREMENT MEASUREMENTS

3.8.1 Light Scattering Measurements

Light scattering measurements were used to determine the molecular weights of poly(mono-n-alkyl itaconates) and were made using a SOFICA 42000 Photo Gonio Diffusometer at fixed scattering angles between 30° and 135° to the incident beam. For each polymer studied, solutions of different concentrations were made up in 25 cm^3 standard flasks by

adding weighed polymer samples to a suitable solvent and allowing at least 24 hours for complete dissolution. The solutions, and solvent, were clarified by filtering them through Millipore FH or FH2 filters directly into the measuring cells. These were of cylindrical glass construction, carefully cleaned and dried in a dust-free atmosphere, and could be closed by tight fitting PTFE stoppers.

Measurements of the scattered light intensity were carried out at 298K $\pm$ 0.5K using blue (436 nm) light, conventional techniques were employed[48] with benzene used as the standard. In most cases disymmetry corrections were found to be negligible, the weight average molecular weight ($\bar{M}w$) was calculated from the relation

$$\bar{M}w = K/(c/I_{90})_{c=0} \qquad (3.7)$$

where $(c/I_{90})_{c=0}$ was obtained by linear strapolation to zero concentration of c/I_{90} against c. c is the concentration in g cm^{-3} and I_{90} the excess scattered light intensity of the polymer solution over pure solvent at an angle of 90^{o}. The value of K is given by

$$K = \frac{2\pi^2}{N_A \lambda_o^4} \frac{i_B}{R_B} \times r_B^2 \times (dn/dc)^2 \qquad (3.8)$$

where N_A = Avogadros No. = 6.02×10^{23}

λ_o = wavelength in vacuo = 436×10^{-7} cm

i_B = meter setting for benzene = 100

R_B = Raylight ratio for benzene (blue) = 48.4×10^{-6}

r_B = refractive index of benzene

dn/dc = refractive index increment.

3.8.2 Refractive Index Increment Measurements

Refractive index increment measurements were made using a Brice-Phoenix differential refractometer fitted with a PTFE stoppered cell which was thermostated at 298K ± 0.5K. The refractive index difference is determined using the following equation

$$\Delta n = K'\Delta d \qquad (3.9$$

where Δn is the refractive index difference between solution and pure solvent, K' is the calibration constant for the selected wavelength and Δd is the total slit image displacement. The instrument was calibrated at 436 nm using standard aqueous potassium chloride solutions. The calibration curve is shown in figure 3.3, the value of K' was found to be 0.95×10^3 (instrument units). The values of Δn for polymer solutions were obtained at five different concentrations(c) in the range $0.2 \sim 0.004$ g cm^{-3} and the value of the refractive index increment (dn/dc) obtained from the slope of a linear plot of Δn against c.

3.9 TORSIONAL BRAID ANALYSIS

3.9.1 Introduction

Torsional braid analysis (TBA) was developed by Gillham[49-53] from the conventional torsional pendulum. In TBA, the polymer sample is impregnated into a multifilament glass-fibre braid which acts as a support for mechanically weak samples and allows measurements to be made on relatively small (ca. 100 mg) amounts of material.

This approach permits investigation of materials

Fig.3.3 Calibration curve for differential refractometer

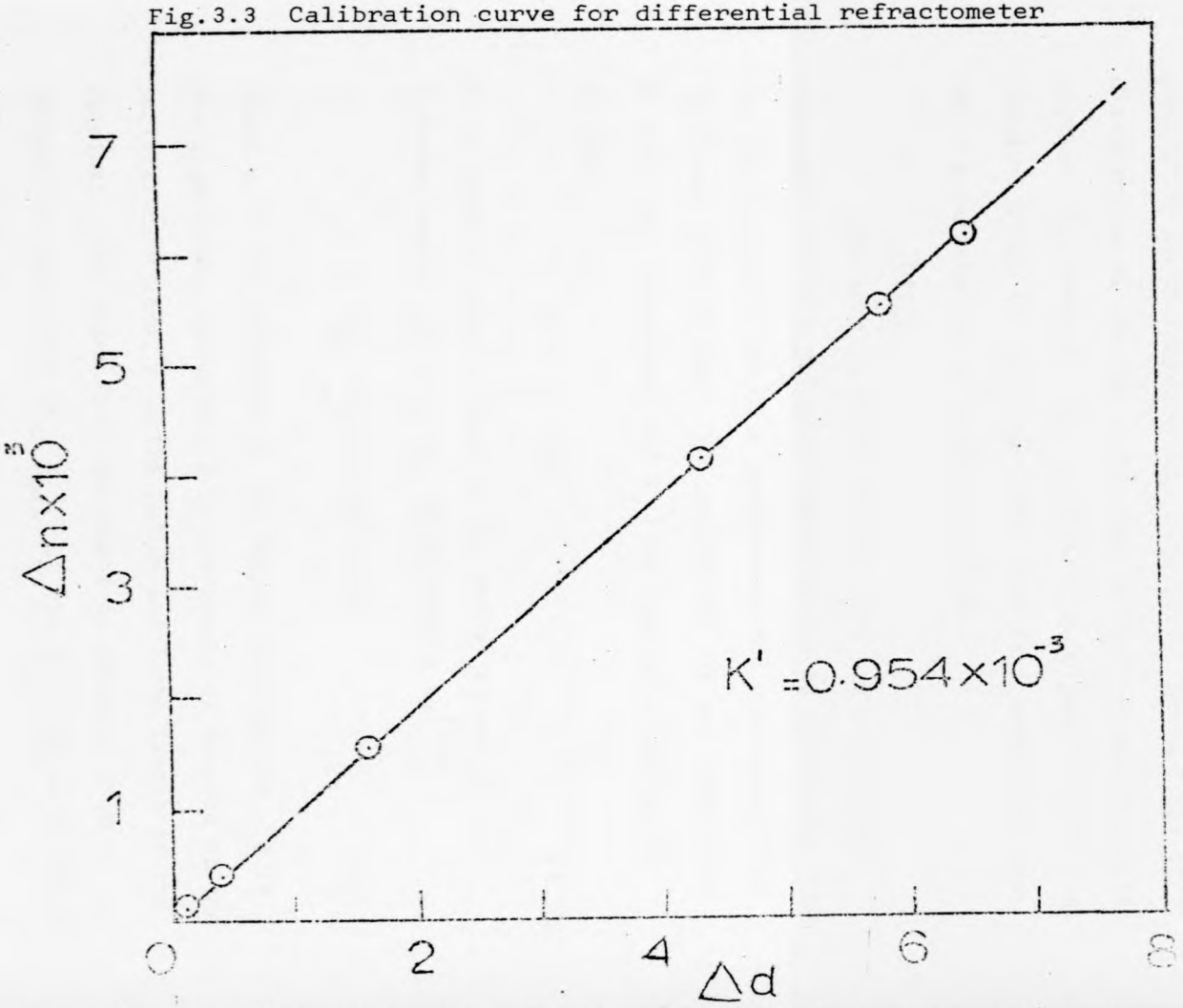

which cannot support their own weight and allows the study of such processes as resin curing and degradation, the behaviour of thermoplastic materials above their melting or softening points and the in situ investigation of the effect of prehistory on thermomechanical behaviour. Perhaps the only disadvantage of the TBA techniques is that it cannot provide absolute measurements (for example of a polymer's mechanical modulus) since the specimen under test is a composite, and not a pure material of known dimensions.

3.9.2 Theory

The complex shear modulus (G*) and logarithmic decrement (Δ) of a polymeric material can be calculated from the damping behaviour of a homogeneous rod undergoing free torsional oscillations. G* consists of the two components G' (the real component) and G" (the imaginary component) so that

$$G^* = G' + iG'' \tag{3.10}$$

G' is directly proportional to the energy stored in the deformed sample and is given approximately by[52]

$$G' = \frac{2LI}{\pi r^4} w^2 (4\pi^2 + \Delta^2) \tag{3.11}$$

where w is the frequency of the damped oscillations, Δ is the logarithmic decrement, I is the moment of inertia of the oscillating system, r is the radius and L the length of the specimen. The logarithmic decrement is obtained from successive amplitudes (A_n, A_{n+1}) of the decaying oscillations and is given by

$$\Delta = \ln A_n / A_{n+1} \tag{3.12}$$

Δ is related to G" and G' by the approximate relation

$$\Delta = \pi G''/G' \qquad (3.13)$$

Storage and loss of energy on cyclic deformation can be characterised by G' and Δ respectively. These parameters are normally plotted as functions of temperature or time.

In TBA the "relative rigidity" parameter ($1/p^2$) where p is the period of oscillation, is used as a convenient measure of modulus (it is simply w^2). This implicitly assumes that any changing contributions from both dimensional and damping characteristics to $1/p^2$ are dominated by changes in the modulus of the polymer.

The mechanical damping index (1/n) is used as a measure of the logarithmic decrement (to which it is directly proportional), n is the number of oscillations between two arbitrary but fixed boundary amplitudes of the decaying vibrations. In TBA, changes in $1/p^2$ and 1/n are interpreted in terms of physical or chemical changes in the polymer supported on its "inert" glass fibre matrix.

3.9.3 Method of Operation

A Torsional Braid Analyzer model 100-B1, based on Gillham's original apparatus and manufactured by Chemical Instruments Corporation (CIC) of New York, was used in this work. A schematic diagram is shown in figure 3.4. Certain modifications were made to this apparatus and are described in detail by Henshall[32]. The glass braids employed were

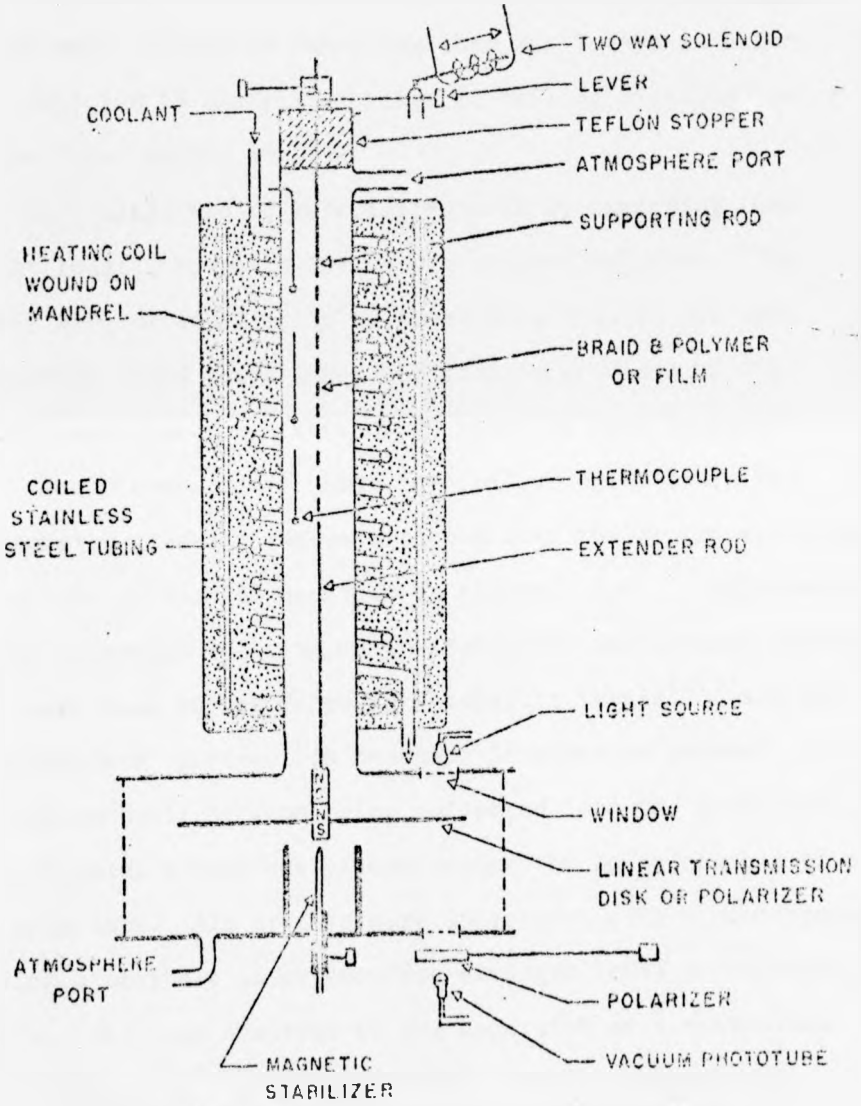

Fig. 3.4 Torsional pendulum and torsional braid apparatus of Gillham (schematic)

supplied by CIC, although at a later stage in the investigation glass braids were fabricated in the laboratory from material supplied by Jones Stroud Insulations, Preston, England (with a considerable saving in cost). These latter braids were cleaned by immersing them for 7 days in chromic acid followed by several washings in boiling distilled water before final drying at 373K.

Glass braids were impregnated by immersing them for at least 2 hours in 10-15% w/v polymer solution. The braids were dried, firstly by suspending them in the open laboratory for 6 hours under the tension provided by 70g weight, and then for a further 24 hours at room temperature in a vacuum oven (again under tension) prior to use. The impregnated glass braids were placed into the centre stainless steel tube of the TBA as shown in figure 3.4 . Adjustments to the extension rods, magnetic stabilizer and optical transducer disc were made as described in Henshall's thesis[32] and the manufacturers' instruction manual. In order to prevent extraneous daylight from being reflected into the photo tube, a black metal screen was placed around the lower chamber of the TBA apparatus. All studies were undertaken with a continuously flowing atmosphere of oxygen-free-nitrogen (OFN) surrounding the sample. This was admitted to the apparatus at a controlled flow rate (20 cm^3 min^{-1}) after first passing through a 1m silica gel drying column.

The CIC TBA apparatus may be operated over the temperature range 83K-573K. Subambient operation requires the circulation of a refrigerant through the concentric jackets that surround the sample chamber (see figure 3.4). In this work the modification described by Henshall was employed in

which OFN at a flow rate of 20 dm^3 min^{-1} is first passed through a cooling coil immersed in liquid nitrogen and then into the instrument. This method avoids the large temperature differentials experienced when the manufacturers' cooling instructions are carried out.

All experimental runs were started after the instrument had been allowed to stabilise at the starting temperature (normally 83K) for at least 15 minutes to allow thermal equilibration of the sample with the sample chamber walls. After equilibration, free oscillation of the sample is initiated and a heating rate of ca. 1 deg min^{-1} maintained as follows:-

Between 83K∿130K.	Flow rate of the cooling nitrogen gas reduced to 2 dm^3 min^{-1}.
Between 130∿273K.	Cooling nitrogen gas flow switched off, and compensating heater switched on. Heater control gradually increased from position four (at 130K) to position ten (at 273K).
Above 273K.	Heating rate controlled at 1K min^{-1} by a Hewlett Packard 220 linear temperature programmer.

The damped oscillations of polymer/braid composite were initiated at 2.5 min intervals throughout the temperature scan and recorded on a Bryans 10 mv strip chart recorder. The temperature was recorded as the output of the centre iron-constanton thermocouple (see figure 3.4) by a second 10 mv chart recorder. This thermocouple had been previously calibrated against a standard copper-constantan thermocouple, mounted in the same position as the sample,

during blank runs at a heating rate of 1K min^{-1}.

3.9.4 Data Analysis

Typical damped waves for a polymer sample are shown in figure 3.5. The mechanical damping index (1/n) was calculated from each such trace obtained (ca. 150∿200 in a typical run) and log 1/n plotted as a function of temperature.

3.10 DIFFERENTIAL SCANNING CALORIMETRY

3.10.1 Introduction

Differential scanning calorimetry (DSC) is a technique of non-equilibrium calorimetry in which the heat flow into or out of a sample and inert reference is measured. Both sample and reference are maintained at the same temperature by altering the electric heating currents to the sample and reference chambers. Heat flow is detected by electronically measuring the differences in the heating current requirements of sample and reference. These are amplified and displayed on the Y axis of an XY chart recorder. The X axis can either be time or temperature.

D.S.C. is probably the easiest and quickest method of measuring the thermal response of polymer systems. However, it is somewhat less sensitive than the TBA technique already described.

3.10.2 Theory

In DSC, if the temperature gradient within the sample can be neglected without serious error, the heat flow into the sample holder can be approximated by[54]

$$dQ/dT = K(T_b - T) \qquad (3.14)$$

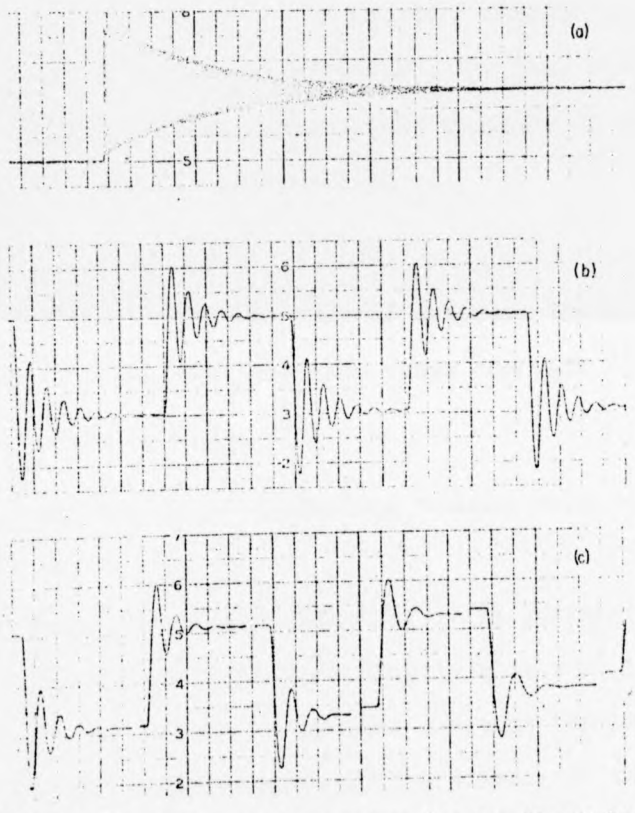

Fig. 3.5 Characteristic output of instrument: (a) glassy state, (b) approach to transition (c) transition region (note drift of neutral position).

where K is the thermal conductivity of the thermal resistance layer around the sample (assumed to be dependent on the geometry but independent of the temperature), T is the sample temperature and T_b the programmed block temperature

$$T_b = T_o + qt \qquad (3.15)$$

where "q" is the heating rate. An equation similar to (3.14) can be written for the reference. The heat absorbed on heating a sample with a constant heat capacity Cp between temperature T_o and T is, by definition

$$Q = mCp(T - T_o) \qquad (3.16)$$

Cp is specific heat and m the mass of sample. The basic equation for DSC can be derived from these concepts[48,55]

$$\Delta T = qCp/K \qquad (3.17)$$

where ΔT is the temperature difference between reference and sample.

When measuring heat capacity, it is generally assumed that changes on heating occur sufficiently slowly so that a steady state is maintained. q is then constant for both sample and reference and equation 3.17 applies. If this is not the case, a simple correction can be made[48]. Specific heat measurements can be obtained with an accuracy of about $\pm$ 2% over a wide temperature range.

3.10.2 Experimental Procedure

In this work a Perkin Elmer DSC2, fitted with a low temperature accessory and capable of measurements in temperature range 100-1000K, was used. The polymer sample to be studied was dried for at least 2 days in a vacuum oven at room temperature. 10∿25mg of the sample were encapsulated

in standard aluminium pans, either in powder form (if the polymer was solid) or as a viscous liquid.

Below 200k helium was used as the purge gas for sample and reference chambers, while above this temperature OFN was used. Additionally a perspex dry box with a constant flow of OFN was mounted on the analyzer deck to minimise condensation in the vicinity of the sample and reference holders during sample changeover.

Temperature calibration was carried out using the standard samples provided by the manufacturer.

3.11 DYNAMIC LINEAR VISCOELASTIC MEASUREMENTS

3.11.1 Theory

When a sinusoidal tensile strain is applied to one end of a polymer sample the resulting sinusoidal stress generated at the other is found to be out of phase with the strain. The polymer is said to exhibit viscoelastic behaviour, i.e. it embodies the characteristics of both a viscous liquid and an ideal elastic solid.

If the instantaneous value at the time t of the sinusoidal elongation strain (γ) of small amplitude is

$$\gamma = \gamma_o \sin wt \qquad (3.18)$$

where γ_o is the maximum value of the strain and w the frequency, then the corresponding stress (S) is given by

$$S = S_o \sin (wt + \delta) \qquad (3.19)$$

where S_o is the maximum value of the stress and δ is the phase angle difference. The relation between S and γ is shown in figure 3.6.

Equation (3.19) may be expanded to give

$$S = S_o \sin wt \cos\delta + S_o \cos wt \sin \delta \qquad (3.20)$$

The peak stress can be resolved into a component $S_o \cos\delta$ which is in phase with the strain (related to the stored energy) and a component $S_o \sin\delta$ which is 90^o out of phase with the strain (related to viscous loss of energy). The ratio of the two, tan δ is the 'dissipation factor' an indication of the relative importance of the viscous contribution as compared to the elastic aspects of the material's behaviour.

Two elastic moduli can be defined[48]

$$E' = (S_o/\gamma_o)\cos\delta \qquad (3.21)$$

and

$$E'' = (S_o/\gamma_o)\sin\delta \qquad (3.22)$$

whose ratio is also the dissipation factor. The complex elastic modulus can be expressed by

$$E^* = E' + iE'' \qquad (3.23)$$

The absolute value of which is

$$E^* = (E'^2 + E''^2)^{\frac{1}{2}} \qquad (3.24)$$

The complex elastic modulus is a function which completely describes the dynamic mechanical behaviour of the material for small tensile strains.

3.11.2 Correlation of Mechanical Damping Terms

In this thesis two methods are being used to obtain damping and moduli; TBA (already described in section 3.9) and linear viscoelastometry. The results of these two techniques can be interrelated quite simply.

In general, one can select a dissipation factor or loss tangent derived from the ratio (G"/G') or (E"/E') to represent the energy conversion per cycle. This leads to the equivalent forms[47]

$$G''/G' = \Delta/\pi \bullet (1/\pi n) \ln (A_1/An) \qquad (3.25)$$

and

$$E''/E' = \tan \delta \qquad (3.26)$$

To a first approximation it is also possible to write

$$(E''/E') = (G''/G') \qquad (3.27)$$

thereby allowing use of the data from either type of measurement to characterize the sample. Moduli can also be related to the viscosity, $G' = w\eta''$ and $G'' = w\eta'$ where η is known as the dynamic viscosity. The approximations $G \simeq G'$ and $E \simeq E'$ can be made when the damping is low.

3.11.3 Preparation of Samples

Polymer samples were analysed in the form of films. These were prepared by a compression molding technique using a hot press designed for this purpose. Polymer samples were placed between two PTFE 1/4 cm. thick plates and a small pressure applied. The heater was then switched on and the press allowed to stabilise at the required temperature for 15 minutes. The necessary pressure to form the film (70 – 100 atm) was then applied for a period of time ranging from one to three hours. From this pressed film a strip approximately 0.1 cm x 2.0 cm x 0.2 cm was cut, using single strokes of a sharp razor and avoiding nicks or rough edges.

3.11.4 Apparatus

A Rheovibron model DDVIIC direct reading dynamic

viscoelastometer (see figure 3.7) supplied by Toyo Baldwin Co. Ltd., Japan, was used. It has the following specifications.

(a) Viscoelastic measurements.

(i)	Dynamic elasticity modulus	$10^6 - 10^{12}$ N m^{-2}
(ii)	tan δ	0.001 - 1.7

(b) Static tensile testing.

(i)	maximum load	1N
(ii)	maximum displacement	2 cm.

(c) Size of sample.

(i)	length maximum	7 cm.
(ii)	thickness maximum	0.5 cm.
(iii)	width maximum	0.5 cm.

(d)	Temperature range	143K — 473K
(e)	Measuring frequencies	3.5 Hz, 11 Hz, 35 Hz, 110 Hz
(f)	Dynamic measurement displacement	$\pm$ 16 x 10^{-4} cm
		$\pm$ 50 x 10^{-4} cm
		$\pm$ 160 x 10^{-4} cm
(g)	Maximum stress	1N
(h)	Maximum stress sensitivity	3.2 x 10^{-2}N

In order to reduce the effects of moisture when samples were being tested at subambient temperature, the Rheovibron (RV) instrument was mounted inside a perspex dry box. This was purged with OFN for at least ½ hour prior to cooling and throughout the subsequent measurements.

Cooling of the sample was achieved by passing refrigerated OFN (as for TBA) though the water cooling coils provided by the manufacturer and which are set into the

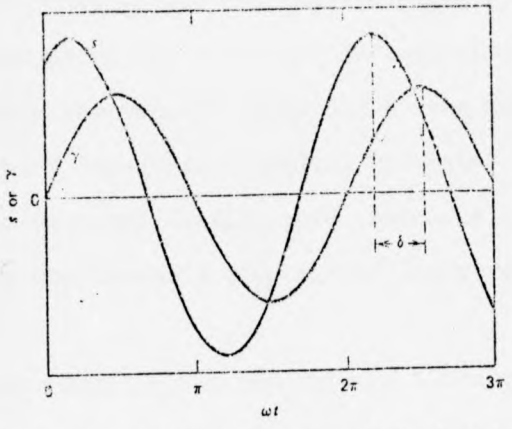

Fig. 3.6 Stress and strain as a function of time in the application of a sinusoidal strain to a viscoelastic specimen.

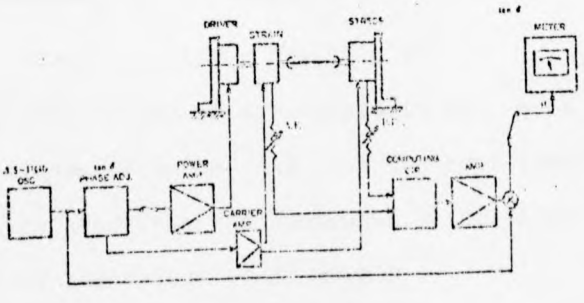

RHEOVIBRON DDV II C

Fig. 3.7 Direct Reading Dynamic Viscoelastometer

instruments heating block. This procedure avoids the unnecessary complication and expense which would have accompanied the commercially available cooling system. The sample temperature was monitored by the output of a copper-constantan thermocouple provided by the manufacturer, using a calibrated "Schneider" digital voltmeter reading to $\pm$ 0.01 mV. The required heating rate (normally ca. 2K min^{-1}) was achieved by continuously varying the input voltage to the heating block.

Polymer samples, in the form of the strips, already described, were mounted in the instrument which was then brought to the starting temperature of the experiment. During cooling, contraction of the sample and metal chucks necessitates that the tension on the sample be constantly monitored to avoid the sample breaking. After heating had been initiated, readings of the dynamic force and tan δ were taken at approximately 2 minute intervals. The dynamic force (D) is an instrumental setting which is related to the sample modulus by the equation

$$E^* = (2\ell/F \times D \times A) \times 10^8 \qquad (3.28)$$

where ℓ is the length of the sample in cm. A is the sample cross section area in cm^2 and F is the amplitude factor which can be calculated from the instrumental settings. Equation (3.28) gives the values of E^* in $N\ m^{-2}$.

The value of tan δ and E^* were plotted as a function of temperature using log-linear graph paper.

3.12 THERMOGRAVIMETRIC ANALYSIS

The work described in this and the following section (3.13) was undertaken in the Chemistry Department of the University of Glasgow with the kind permission of Professor N. Grassie.

3.12.1 Introduction

Thermogravimetric analysis (TGA) is a dynamic technique in which the weight loss of a sample is measured continuously while its temperature is increased at a constant programmed rate. Weight loss can be measured as a function of time at constant temperature if desired. The major use of this technique when applied to polymer systems has been in studies of thermal decomposition and stability.

TGA is most useful when used in conjunction with DSC (see section 3.9) measurements. Both provide a knowledge of the temperature at which a thermal event occurs, but TGA will indicate whether or not the event is accompanied by a weight loss. Gas chromatography, mass spectrometry and infrared analysis can be used to identify the effluent gases, if any.

3.12.2 Experimental Measurements

A Du Pont 951 Thermogravimetric Analyzer attached to a 990 Du Pont DTA unit was used. Previously well dried 10 mg samples were placed in a flame-cleaned boat-shaped platinum sample holder. Thermal degradation was carried out in an atmosphere of OFN at a constant 75 cm^3 min^{-1} flow rate. Normally a 10K min^{-1} heating rate was used. The results are displayed on an X-Y recorder as a graph of sample weight loss against temperature.

3.13 THERMAL VOLATILIZATION ANALYSIS

3.13.1 Introduction

Thermal volatilization analysis (TVA) was first described and developed by McNeil et al. These authors have published a large number of papers discussing studies of polymer degradation by this technique[56-58]. The method has certain advantages over other forms of thermal analysis in the quantity of information that can be obtained from a relatively small number of experiments. Isothermal application of TVA have also been recently described[59].

Unlike other thermoanalytical approaches, the apparatus required for TVA is very simple. The problems of sample shape and atmosphere effects, which can sometimes be very important in other techniques, are avoided in TVA by the use of a relatively large sample area (and consequently small sample thickness) and by high vacuum conditions.

Recent developments in TVA, permitting differential condensation of the volatile products of degradation, have substantially increased the amount of information which can be obtained. For example it is possible to obtain information about the nature of the products without their isolation and subsequent analysis. In some cases the presence of specific substances may be inferred and rates of evolution of two products may, in favourable circumstances, be obtained simultaneously but independently during an experiment.

3.13.2 Principle of TVA

The basic TVA system is shown in figure 3.8a; a Pirani gauge is attached to the system at some convenient

3.13 THERMAL VOLATILIZATION ANALYSIS

3.13.1 Introduction

Thermal volatilization analysis (TVA) was first described and developed by McNeil et al. These authors have published a large number of papers discussing studies of polymer degradation by this technique[56-58]. The method has certain advantages over other forms of thermal analysis in the quantity of information that can be obtained from a relatively small number of experiments. Isothermal application of TVA have also been recently described[59].

Unlike other thermoanalytical approaches, the apparatus required for TVA is very simple. The problems of sample shape and atmosphere effects, which can sometimes be very important in other techniques, are avoided in TVA by the use of a relatively large sample area (and consequently small sample thickness) and by high vacuum conditions.

Recent developments in TVA, permitting differential condensation of the volatile products of degradation, have substantially increased the amount of information which can be obtained. For example it is possible to obtain information about the nature of the products without their isolation and subsequent analysis. In some cases the presence of specific substances may be inferred and rates of evolution of two products may, in favourable circumstances, be obtained simultaneously but independently during an experiment.

3.13.2 Principle of TVA

The basic TVA system is shown in figure 3.8a; a Pirani gauge is attached to the system at some convenient

point between the heated sample and the main cold trap (77K). The volatile products passing through the apparatus produces a response on the Pirani gauge. Materials which are volatile under vacuum at the temperature of the first trap are thus detected. When a series of experiments are carried out with the first trap at different temperatures in each case, then a considerable amount of information about the nature of the volatile products may be obtained.

In the recent versions of TVA, this information is collected in a single experiment by having a number of traps at different temperatures, each followed by a Pirani gauge whose outputs are recorded simultaneously on the same chart paper. If several lines are arranged in parallel, all open simultaneously, such that the sample to gauge distance, and the gauge to main trap distance does not differ from one line to another, then the problem of variation of Pirani response with distance does not arise. The resulting curves are then directly comparable. Such an apparatus was used in this work and is shown schematically in figure 3.8B.

3.13.3 Experimental Procedure

The basic features of the TVA apparatus used are shown in figure 3.8a and 3.8b. The construction and operation have been fully described by McNeil[60]. Briefly, the experimental procedure is as follows.

About 50mg of polymer are put in the sample tube and the apparatus pumped down to the best available vacuum without coolant in the intermediate traps (6, 7, 8 and 9 in the figure). The zero adjustments are then made on the Pirani gauges. Next the intermediate cold trap coolants

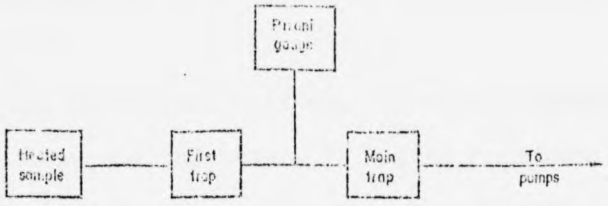

Fig. 3.8a Single line differential condensation TVA system.

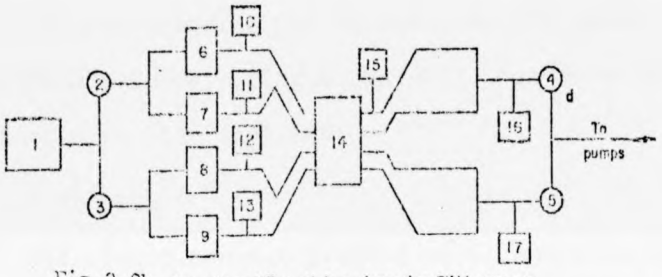

Fig. 3.8b Four line differential condensation TVA system.

1 = heated sample; 2, 3, 4, 5 = stopcocks (large bore, right angle type); 6, 7, 8, 9 = initial cold traps; 10, 11, 12, 13 = Pirani gauge heads; 14 = main cold trap; 15 = exhaust Pirani gauge head; 16, 17 = product collection points.

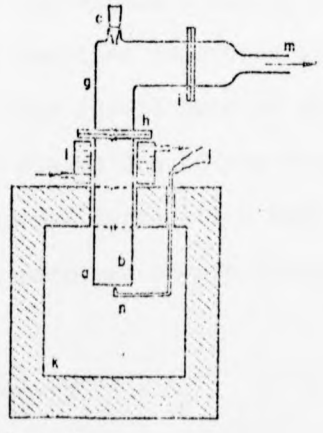

Fig. 3.8c TVA oven, sample tube, lid assembly.

a = sample tube; b = inlet tube; c = ground joint; vessel; g = lid; h, i = flange joints; j = thermocouple leads; k = oven; l = water jacket; m = outlet to trap system and pumps; n = thermocouple junction.

are put in place (i.e. 273K, 228K, 198K and 173K; main trap at 77K).

In normal use, all four lines are opened simultaneously and the sample is heated from room temperature to the required final temperature (usually 298K to 773K) at 10K min^{-1}. The output of each of the Pirani gauges is recorded as a function of temperature or time. Infrared analyses (see section 3.15) were carried out on the volatile gases which collected in the traps, using a gas cell. Non-volatile products and residues were also analysed.

3.14 G.L.C. STUDIES

Gas liquid chromatographic (GLC) analysis was carried out on the products of isothermal degradation of several polymer samples. A Perkin-Elmer F11 hot wire chromatograph fitted with a matched pair of Porapak Q columns was used.

A polymer sample (∿ 10mg) was placed in a specially constructed by-pass loop in the nitrogen supply to one column of the chromatograph. This was then evacuated at 10^{-2} torr for 2-3 hours, after which time an oil bath at the required degradation temperature was placed around the by-pass loop. The volatile products of thermal degradation were then admitted to the GLC by directing the nitrogen supply through the by-pass loop.

3.15 MASS SPECTROMETRIC STUDIES

A JEOL Mass Spectrometer model JMS-D100 linked with a JEOL Gas Chromatograph (model JGC-20R) and data anlysing computer was used to identify the products which distilled from

polymer samples during isothermal degradation. The mass spectrometric technique was used to complement the GLC analysis described in the last section. The degradation products for analysis were obtained as follows.

A polymer sample of ca 20-30 mg was placed in one limb of a U-shaped pyrex container which was then connected with a vacuum line and evacuated for 4 hours at 293K and 10^{-2} torr. It was further evacuated for 2 hours at 313K and then sealed off from the vacuum line. The sample tube was heated to the desired degradation temperature for the required time. Volatile degradation products were distilled, over a period of $\sim$ 24 hours, to the vacant limb of the U-tube using liquid nitrogen as refrigerant. These were then sealed off and stored at 278K until required for mass spectroscopic analysis, which was carried out using standard operating techniques.

3.16 INFRARED ANALYSIS

Infrared analysis (IR) was carried out using a Perkin-Elmer IR spectrophotometer 577 operating in its standard mode. Monomer and polymer samples were studies in one of three forms, film, in solution or as a KBr disc.

Polymer films were cast from 5 — 10% w/v solution onto freshly polished NaCl plates. The films were dried either at room temperature or by using an IR radiant lamp when the solvent was not particularly volatile. Di-n-alkyl itaconates and some degradation products were studied as capillary films between two NaCl plates. Monomer and polymer samples which could not form films were studied in carbon tetrachloride solution using 0.1 cm cells or as KBr discs.

Analysis of gaseous volatile products from polymer degradation studies was carried out using a 10 cm IR gas cell with NaCl windows.

3.17 NUCLEAR MAGNETIC RESONANCE ANALYSIS

Nuclear Magnetic Resonance (NMR) analyses were carried out using a Hitachi-Perkin Elmer R24 High Resolution NMR Spectrometer operating in its normal mode. Monomers (mono-and di-n-alkyl itaconate) were studied as 5 — 10% w/v solutions in deuterated chloroform made up directly in standard NMR tubes. Polymer solutions were first made up in 1 cm^3 standard flasks before being transferred to nmr tubes after complete dissolution had been achieved. The concentrations of the polymer solutions under study were limited by viscosity line broadening effects, but were normally in the range of 5 — 10% w/v. All measurements were carried out at 308K.

Peak areas were determined both by (a) instrumental integration and (b) cutting out and weighing. Peak positions were recorded with reference to the absorption position of tetramethylsilane as the internal standard.

3.18 ELECTRON MICROSCOPIC STUDIES

3.18.1 Introduction

Electron microscopy (EM) has proved to be a powerful tool for the study of polymer morphology. The principle of EM is essentially similar to that of conventional visible-light microscopy; the wavelength of the electron beam used is determined by de Broglie's description of the wave-particle duality of electrons and the focussing system employs

electric and magnetic lenses rather than the usual glass type[48].

3.18.2 Sample Preparation

0.5 — 2 mm thick polymer films were prepared either by solvent casting or using the hot plate press described in section 3.11.3. When the latter technique was employed, the lowest possible temperature and pressure was used in order to minimise damage to the polymer structure from degradation.

Sections of ca. 100 — 150 μm thick were cut from the solvent-cast or pressed films by an L.K.B. Ultratome III using standard procedures. Glass knives were normally used and sections were collected on a water surface. (It was observed that some polymer samples damaged the knife very quickly, a new knife or a diamond knife was used in these cases). The sections were supported on a copper grid and stored in a vacuum dessicator. The grids were typically about 200 — 300 mesh and were not covered with any type of substrate.

3.18.3 E.M. Study

The sample grids were studied using a JEOL JEM 100C Transmission Electron Microscope. Operating in its standard mode this has a 14 nm resolution and a 750,000X maximum magnification. Normally, a 200,000X magnification was employed and the EM plates were enlarged photographically to the required scales.

CHAPTER 4

RESULTS AND DISCUSSION

4.1 POLY(DI-n-ALKYL ITACONATES)

Selected homopolymers were prepared to cover the range of expected physical properties, to establish glass transitions (Tg) and possible sub-transitions by TBA. Additionally, using the samples supplied by Velickovic, the series PDMI to PDDoI was examined using DSC techniques.

4.1.1 Polymerisation Results

The polymers prepared by the techniques described in section 3.3 are listed in table 4.1 along with their viscosity average molecular weights. No detailed kinetic

TABLE 4.1

Intrinsic viscosities and molecular weights of poly(di-n-alkyl itaconates) prepared by emulsion polymerisation.

Polymer	$[\eta]/cm^3g^{-1}$	$\bar{M}v \times 10^{-5}$	DP* $\times 10^{-3}$
Poly(DMI)	0.27	2.68	1.836
Poly(DBI)	0.35	2.58	0.942
Poly(DHpI)	0.25	2.08	0.638
Poly(DDI)	0.25	3.07	0.748

* DP = degree of polymerisation

analysis was made, However, it was observed that the rate of polymerisation rose to a maximum at the dipentyl ester and thereafter fell off slowly. Dimethyl itaconate polymerised very much more slowly than all the others.

4.1.2 TBA and DSC analysis

Results from TBA (see section 3.9) were obtained in the form of thermograms with temperature as the abscissa and mechanical damping index as the ordinate. Transitions

in the polymer sample are estimated from maxima in the damping index and correspond to the activation of particular molecular motions. Since the nominal frequency of the TBA technique is relatively low (ca. 1 Hz), transition temperatures should be broadly comparable to those obtained by a static technique. All samples were run at least twice to ensure consistency of the results.

DSC thermograms have temperature as the abscissa and relative specific heat (Cp) as the ordinate. The onset of cooperative molecular motion in a polymer sample results in a change of Cp which, in this work, is identified by the intersection of the extrapolated base line before the change and the line drawn through the steepest point of base line change. Ideally, in the regions away from a transition, the base line of a DSC thermogram can be set parallel to the temperature axis. For many of the samples tested here, however, curved base lines were obtained and these complicate the interpretation of the thermograms. Samples were scanned repeatedly until reproducible thermograms were obtained.

4.1.3 Results of TBA

The TBA thermograms of the selected polymers are shown in figures 4.1 and 4.2, each being constructed from up to 200 data points collected at 2.5 minute intervals. Since more than one TBA thermogram is shown on one figure, the mechanical damping index scale ($- \log \frac{1}{n}$) is not marked with absolute values of $- \log \frac{1}{n}$, The intervals indicated correspond to a change of 0.2 in the damping index. This applies to figures 4.1 and 4.2 and to all subsequent figures showing TBA

Fig.4.1 TBA thermograms of indicated polymers

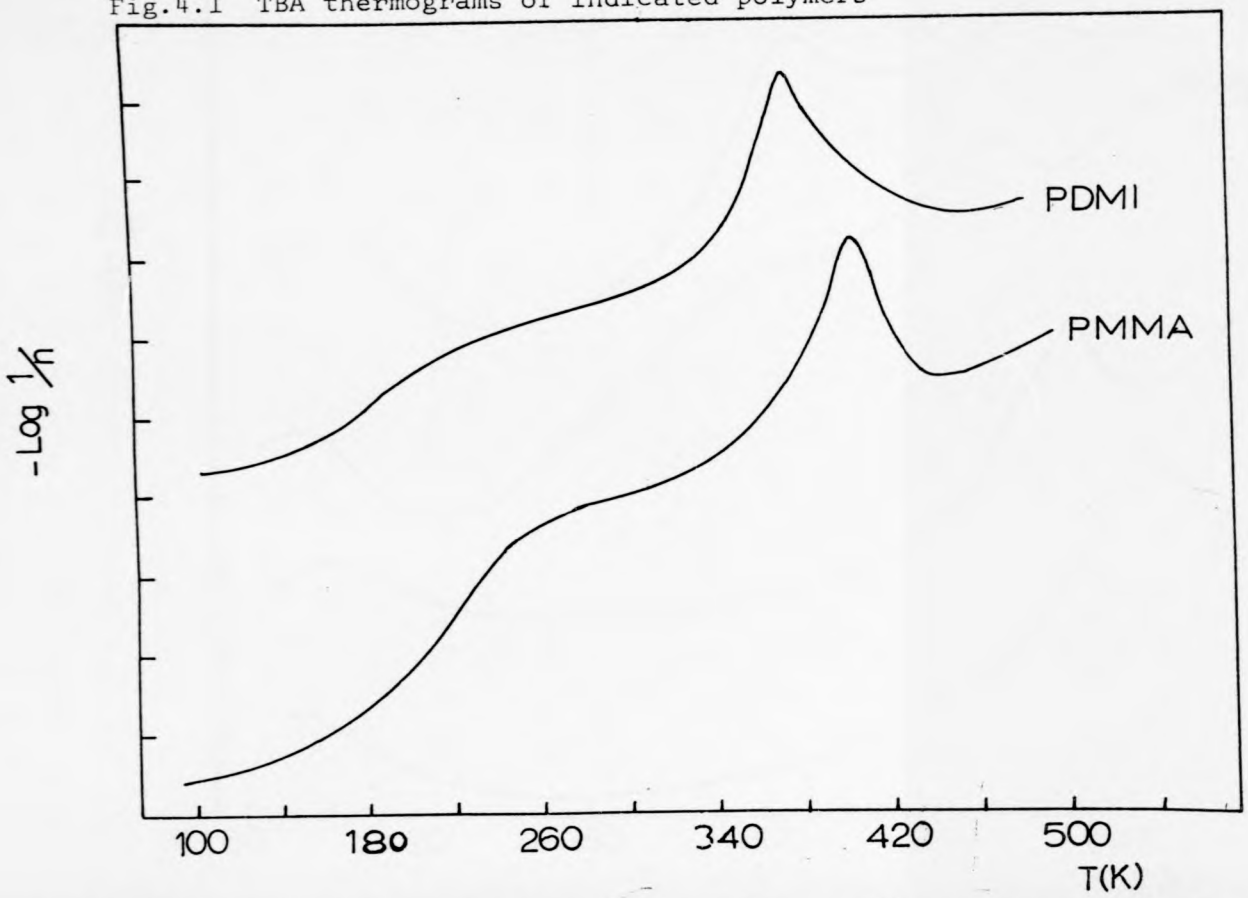

Fig.4.2 TBA thermograms of indicated polymers

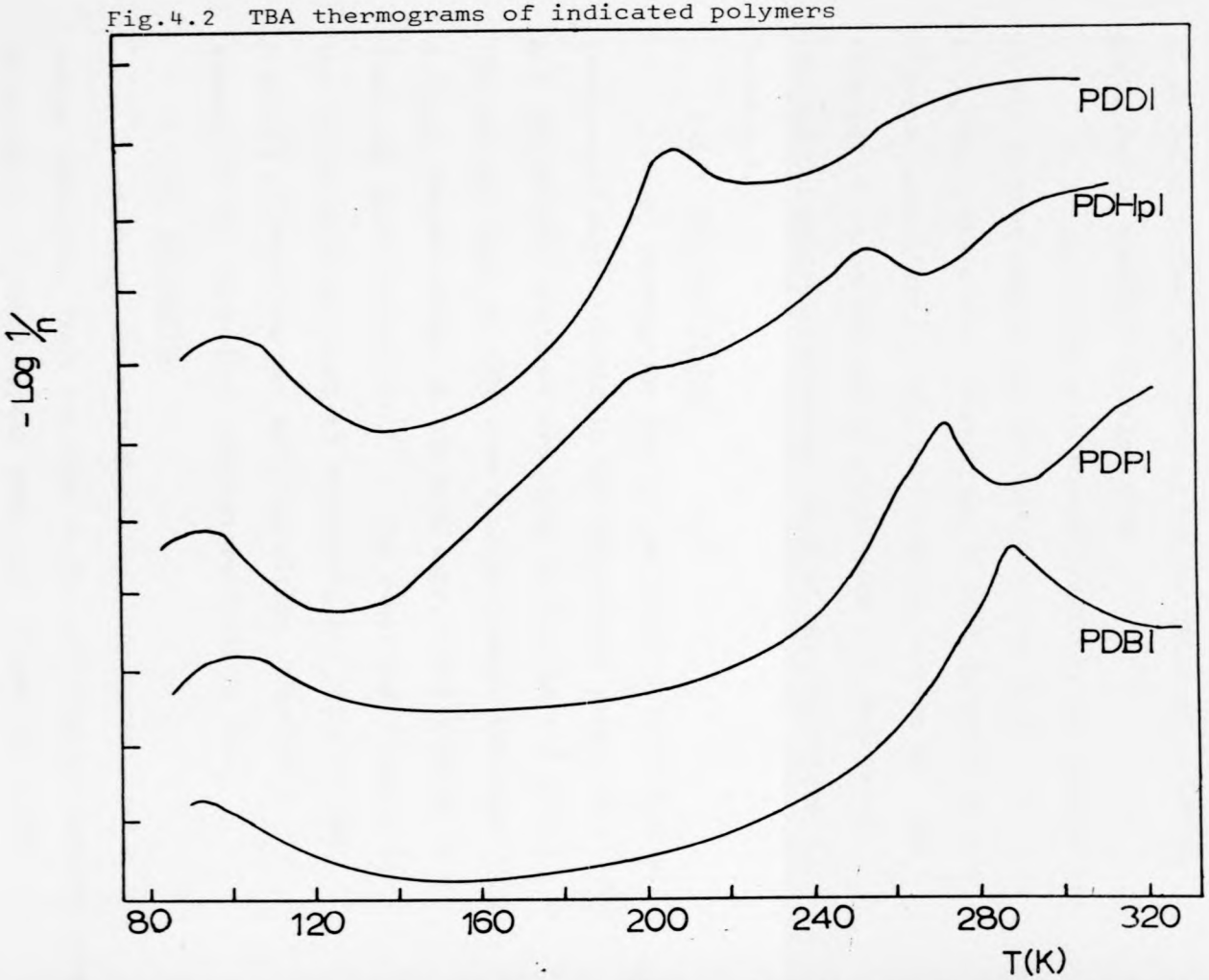

thermograms. The thermogram for a sample of atactic PMMA, which is shown along with that for PDMI in figure 4.1, was obtained for comparison purposes. PDMI can be thought of as being derived from PMMA by substitution of a $-COOCH_3$ group for an α-methyl hydrogen atom.

In accordance with normal practice, the transitions in any polymer sample are identified by the Greek letters α, β, γ, etc., where the α transition is that occurring at the highest temperature, β the next highest, and so on. The temperature range over which transitions are observed in the poly(di-n-alkyl itaconates) studied here are listed in Table 4.2.

4.1.4 Results of DSC

DSC thermograms for the series of poly(di-n-alkyl itaconates) were obtained in the temperature range 100 - 500K and the relevant sections are shown in figures 4.3 to 4.5. The polymers PDMI to PDHI show straightforward behaviour with a single marked change in the base line, corresponding to a classical glass transition[37]. The remaining polymers in the series show more complex behaviour, and point to the presence of more than one main transition. Table 4.3 summarises the transition temperatures found by DSC.

4.1.5. Discussion

Although the poly(di-n-alkyl itaconates) have a unique structure, their relation to the poly(n-alkyl methacrylates) is obvious. It would appear then, that comparisons with published data for this latter series[61] would be a reasonable starting point from which to attempt assignments of observed

TABLE 4.2

TRANSITION REGIONS OBSERVED IN Poly(di-n-alkyl itaconates) AND PMMA BY TBA

Sample	Temperature Ranges of Maxima in Damping Index/K		
	α	β	γ
PMMA	404-405	260-290	-
PDMI	373-374	230-290	-
PDBI	287-288	-	95-110
PDPI	273-274	-	100-110
PDHpI	255-256	195-205	95-110
PDDI	260-275	207-208	100-105

TABLE 4.3

GLASS TRANSITION TEMPERATURE OF Poly(di-alkyl itaconates) AND PMMA

Polymer	DSC Tg/K	TBA Tg/K
PMMA	401	404
PDMI	371	373
PDEI	331	-
PDPrI	307	-
PDBI	285	288
PDPI	278	274
PDHI	265	-
PDHpI	250	252
PDOI	254	-
PDNI	261	-
PDDI	260	255
PDuDI	217	-
PDDoI	228	-

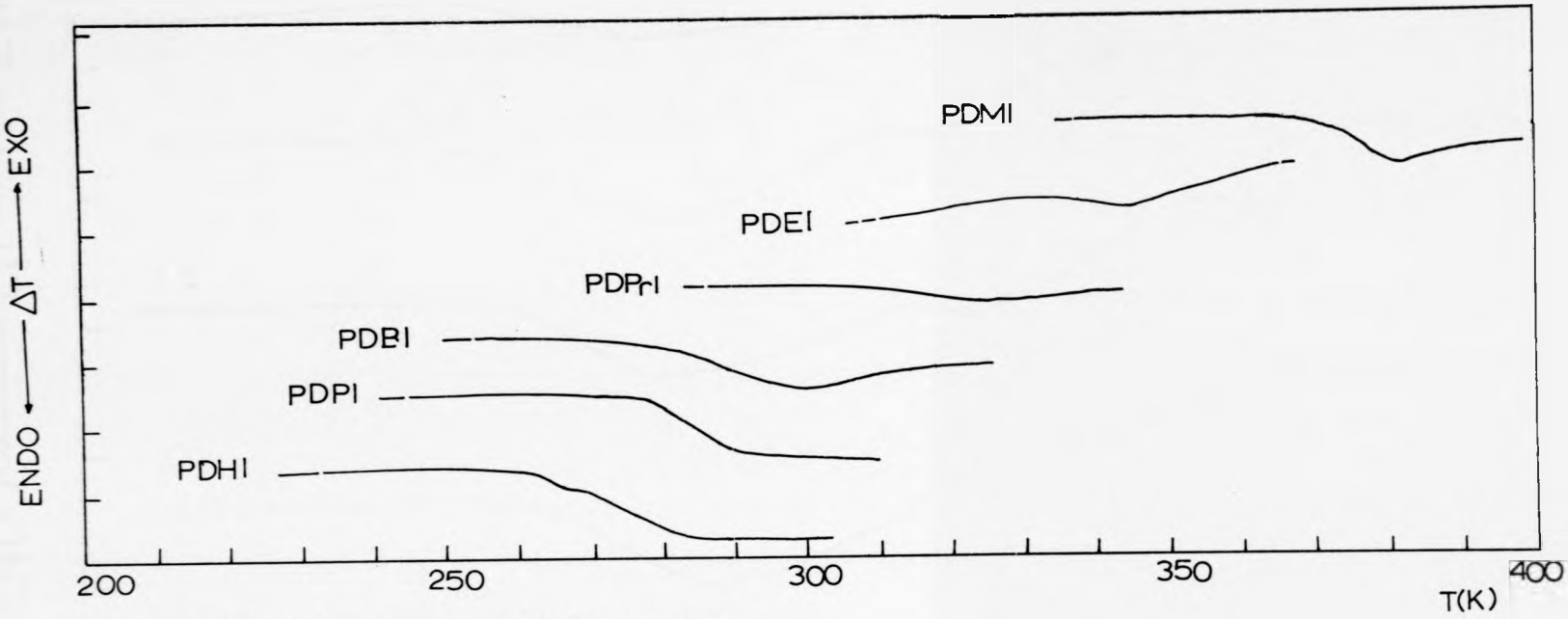

Fig.4.3 DSC thermograms of indicated polymers

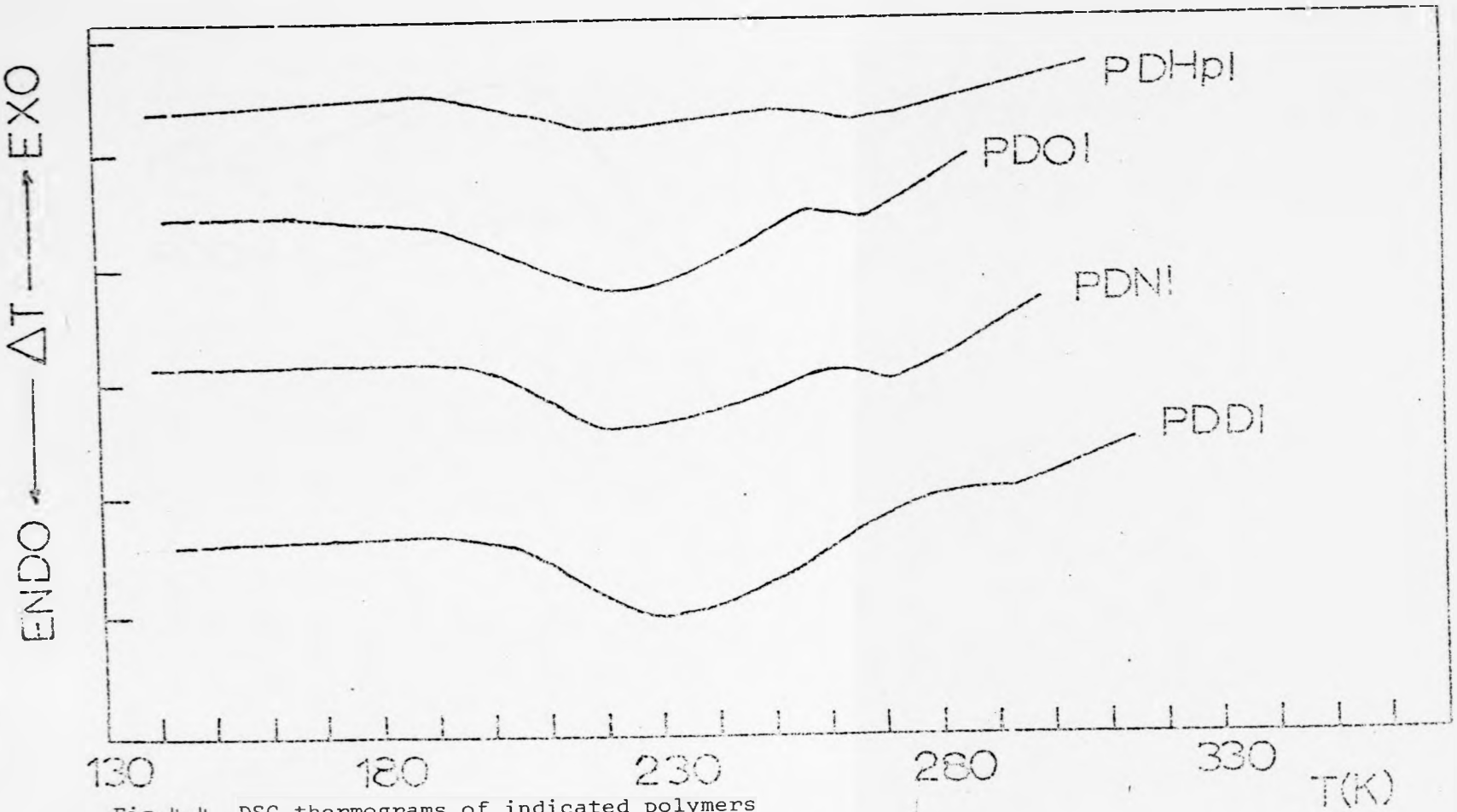

Fig.4.4 DSC thermograms of indicated polymers

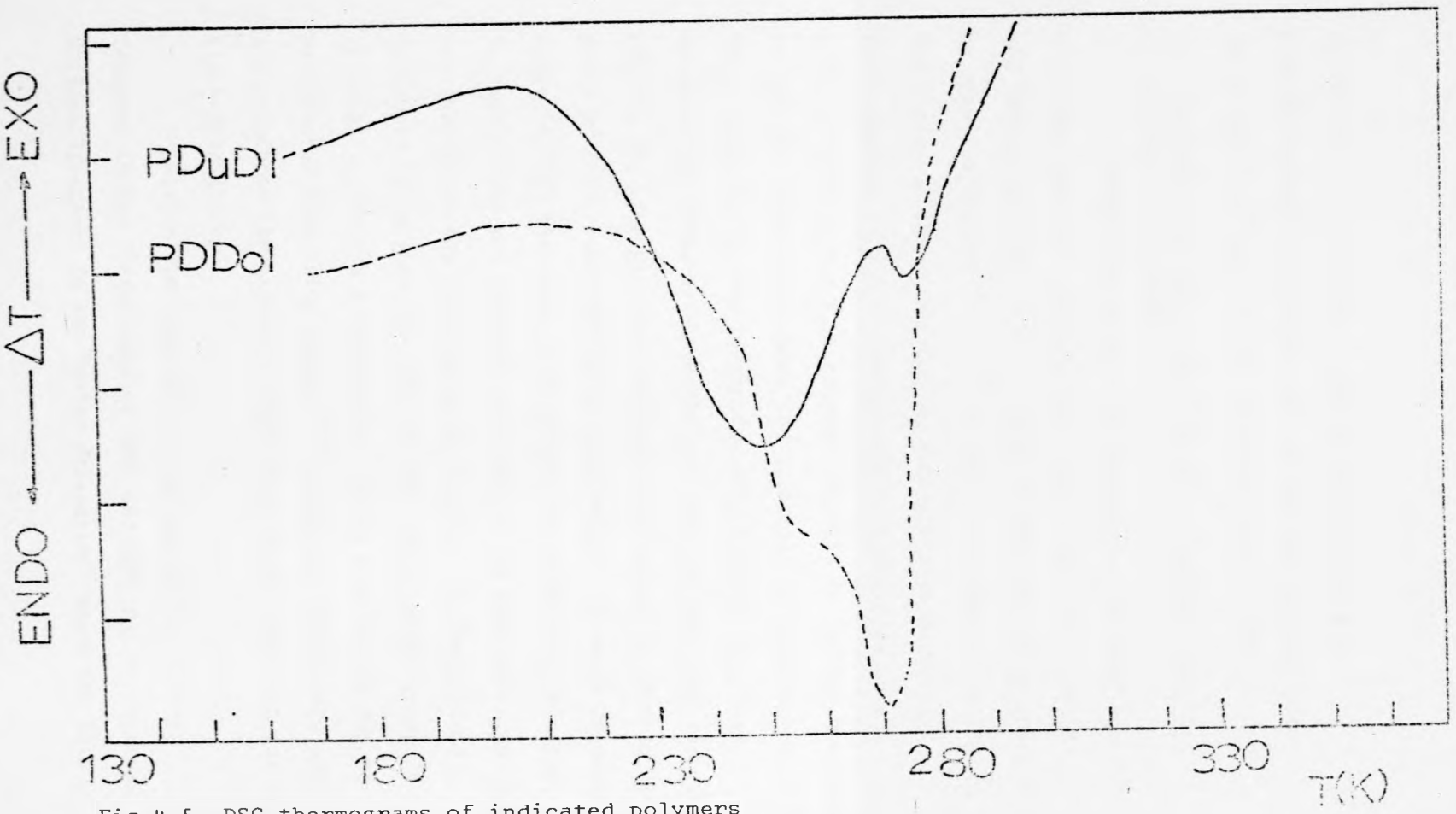

Fig.4.5 DSC thermograms of indicated polymers

transition in the former. Out of convenience the poly(di-n-alkyl itaconates) series has been divided into two groups (a) PDMI to PDHI, and (b) PDHpI to PDDoI.

(a) Polymers with the n-alkyl group containing less than seven carbon atoms

Comparison of the TBA thermograms for PMMA and PDMI shows the expected similarities. The α peak (404 – 405K), and the β "shoulder" (260 – 290K) of PMMA have been identified by previous workers[38,62,63] as the glass transition (Tg) and motion of the ester $-COOCH_3$ side group respectively. The α maximum at 373 - 364K in PDMI is identified as the glass transition for this polymer and this is further confirmed by the DSC trace which shows the classical Tg inflexion at 371K. The β shoulder in PDMI is considerably broader than that observed for PMMA, but nevertheless occupies the same temperature region, and it would seem reasonable to assign it also to ester group motion. A broadening of this relaxation would be expected, since in PDMI the ester side groups are slightly dissimilar, in that one is not directly attached to the main chain and can presumably undergo rotation more readily. In fact, it is difficult to say, in the case of PDMI, which ester group is responsible for the β transition. It is most likely due to rotation of both ester groups[33] which will ultimately add to and reinforce the extensive main chain motion required for the glass transition.

Within the temperature scan employed, no other features in the thermograms of PMMA and PDMI can be observed. Noticeably absent is any "water relaxation" which has been

reported[38] at ∿170K in PMMA; this of course, may be a consequence of the rather rigorous drying procedures employed.

The DSC traces for the remaining polymers under discussion all show obvious glass transitions which decrease in temperature as the n-alkyl side chain increases from ethyl through to hexyl. These are listed in table 4.3. Such behaviour within a homologous series of polymers is not unexpected, and parallels a similar trend in the n-alkyl methacrylate polymers[38,61]. An explanation given for such behaviour[38,61] is that, as the length of a side group increases, neighbouring polymer chains are "pushed" further apart, thus decreasing the steric hindrance to backbone rotations. The effect is similar to that produced by the addition of plasticizers[37]. Such a hypothesis is supported by observations[61] on poly(n-alkyl methacrylates) where the density shows a systematic decrease with increasing length of the side chain. "The molecular packing factor", calculated by Ishida et al.[64] from the densities, exhibits a similar trend. According to these workers, this density decrease is consistent with a similar decrease in the magnitude of the interchain interactions as determined from the cohesive energy densities.

The TBA thermograms for PDPI and PDBI each show (figure 4.2) a pronounced maximum in damping and confirm the allocation of the DSC Tg values in these polymers. The physical nature of PDPI and PDBI at ambient temperature is as expected from such results; PDBI is rubbery, PDPI is a viscous liquid. Also obvious from the TBA results is the apparent absence of a β-type transition. Since this transition

is thought to originate in ester linkage motions it should, in principle, be observed throughout the entire series of poly(di-n-alkyl itaconates). It is assumed, in the cases studied here, that the β transition is overlapped by the glass transition. Similar behaviour is also observed in poly(n-alkyl methacrylates).[65]

The TBA thermograms for PDBI and PDPI do, however, exhibit a second transition located at relatively low temperature, i.e. around 100K (labelled γ in table 4.2). This peak is quite pronounced but is observed only when the side chain length is greater than three carbon atoms[32]. From the evidence presented so far, it can be assumed that these polymers are predominantly amorphous and it is proposed that these low temperature peaks originate in a common mechanism - the so-called "crankshaft rotation" of short polymethylene segments in non-crystalline phases, mentioned in chapter 2. Schatzki[66,67] has suggested that such relaxation will be present whether the $-CH_2-$ sequences are in the side groups, as in the higher poly(alkyl methacrylates), or in the polymer backbone, as with polyethylene. On this argument one can postulate that, in the systems studied here, the motion arises from the $-CH_2-$ sequences in the alkyl side groups, since it is only observed when the side chain contains more than three carbon atoms.

(b) Polymers with the n-alkyl group containing more than six carbon atoms

When the side chain contains seven or more carbon atoms, both the TBA and DSC thermograms become more complex.

One feature, however, remains common to all the polymers in the series[32], that is the ~ 100K relaxation first observed at PDBI and ascribed to crankshaft motion in the side chain. The presence of this peak is confirmed here by the TBA thermograms for PDHpI and PDDI shown in figure 4.2. It is proposed that this peak is also due to crankshaft motion in these polymers, and indeed in all the poly(di-n-alkyl itaconates) where the side chain contains more than three carbon atoms.

The problem of the remaining features in the higher poly(di-n-alkyl itaconates) is not easily resolved. Examination of the DSC thermograms shows that there is a distinct "Tg-like" inflexion followed by a second feature which is rather obscured by a rapidly curving base line. In PDHpI and PDDI the TBA thermograms also show two obvious transitions corresponding to those observed by DSC (compare figures 4.2 and 4.4).

Analysis of the second, higher temperature, feature is rather subjective; in PDHpI to PDDI it has been analysed as a glass transition base line change and the temperatures obtained listed in table 4.3. However, in PDDoI the second feature is quite definitely identifiable as a melting endotherm[68], and that in PDuDI could also be given this interpretation. This leads to the inevitable conclusion that PDDoI is no longer completely amorphous, but contains regions of crystalline order[69-72]. This order must be associated with ordering of the side chains, which have now sufficient length to adopt the necessary packing arrangement

favoured in crystalline linear paraffins[73]. In PDuDI a similar situation may be present, here any side chain crystallinity, giving rise to the higher temperature feature in the DSC thermogram, is much less well developed.

In each of the remaining polymers discussed in the section, it appears that there are two glass transitions. This implies that there are two types of amorphous regions within the polymer. These are proposed as being due to (a) the main polymer backbone and (b) the side chains. In other words, when there are more than six carbon atoms in the side chain the polymer can no longer be considered as a homopolymer but rather as a graft copolymer[70]. The lower temperature transition in the DSC thermograms of PDHpI to PDDI are assumed to be due to the onset of motion within the side chain regions, while the higher temperature features result from main chain relaxation. The apparently greater intensity of the DSC base line shift for the former transition is less surprising when the ratios of carbon atoms in the side chain to those in the main chain is considered. For example, in the PDDI repeat unit there are sixteen carbon atoms located in the side chains, but only five associated with the main chain and ester linkages. If all of the latter participate in the main chain relaxation, the ratio of carbon atoms undergoing molecular motions in the side chain, compared to the main chain, is 16:5, or approximately 3:1.

For the PDDoI and PDuDI polymers the situation is changed by presence of crystallinity in the side chain phase. The lower temperature DSC feature in these polymers must then be the glass transition associated with the main chain motion.

Fig.4.5(a) Effect of side chain length on the glass transition of poly(di-n-alkyl itaconates)

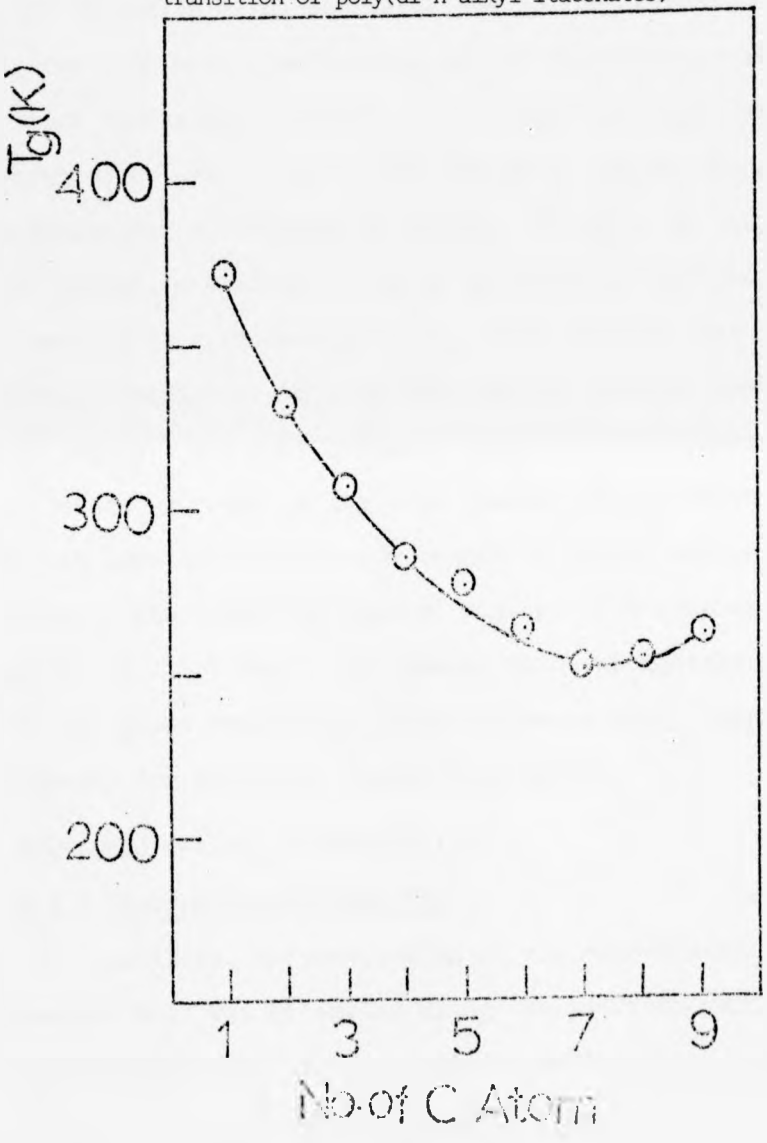

The values of the glass transition, plotted as a function of side chain length, are shown in figure 4.5(a) for the entire poly(di-n-alkyl itaconate) series. From dimethyl to diheptyl the value of Tg decreases due to the decrease in the steric restrictions to main chain motion caused by greater separation of the main chains. Intuitively one might expect an assymptotic lower limit to the decrease, beyond which side chain length has no noticeable effect. However, in this present series, a minimum in Tg is observed at the diheptyl ester and the Tg's thereafter rise. This implies that some additional restriction to main chain motion becomes operative in this region. The most probable origin of the effect here is an increasing order in the side chains, which eventually results in crystallinity when a length of twelve carbon atoms is reached. The effect of ordered regions within an amorphous polymer is to "tie" down the segments which ultimately give rise to the glass transition, hence increase their energy requirements for wholesale cooperative motion.

4.2 POLY(MONO-n-ALKYL ITACONATES)

4.2.1 Polymerisation Results

Initially, polymerisation of the mono-n-alkyl esters of itaconate acid was attempted using the solution techniques outlined in section 3.2. This proved unsatisfactory, possibly due to system heterogeneity, in that polymerisation rates were extremely slow and led only to low molecular weight products. A typical rate profile for the polymerisation of MMI in solution is shown in figure 4.6(a). Using the bulk polymerisation technique (section 3.2), reasonably high molecular weight polymer could be

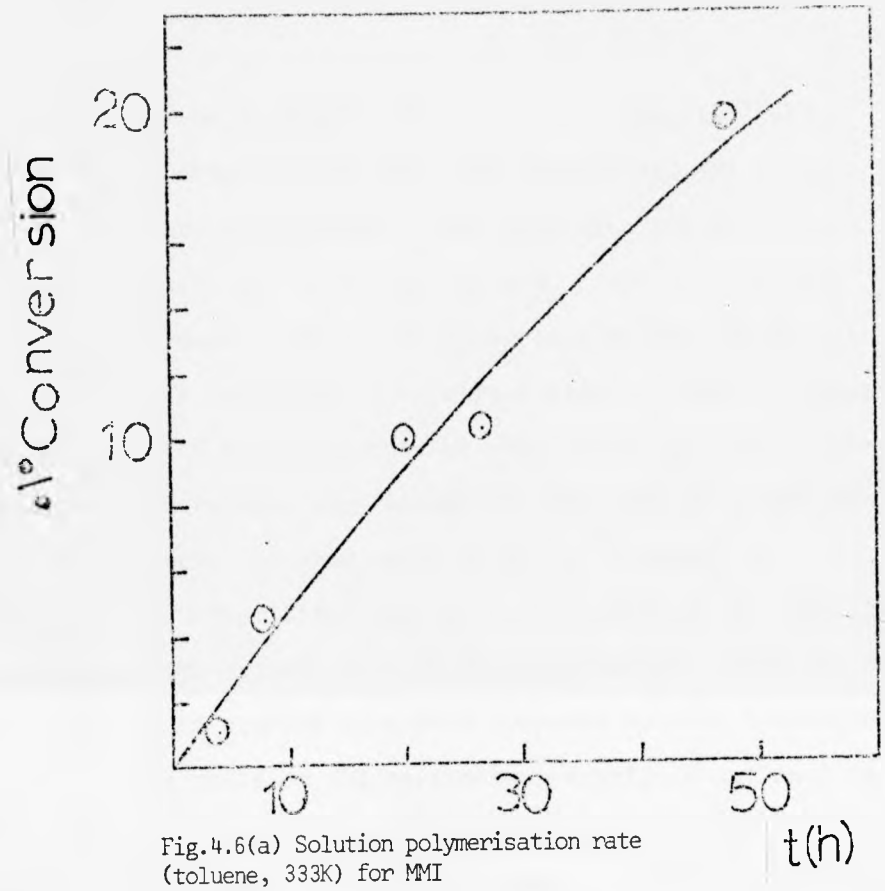

Fig.4.6(a) Solution polymerisation rate (toluene, 333K) for MMI

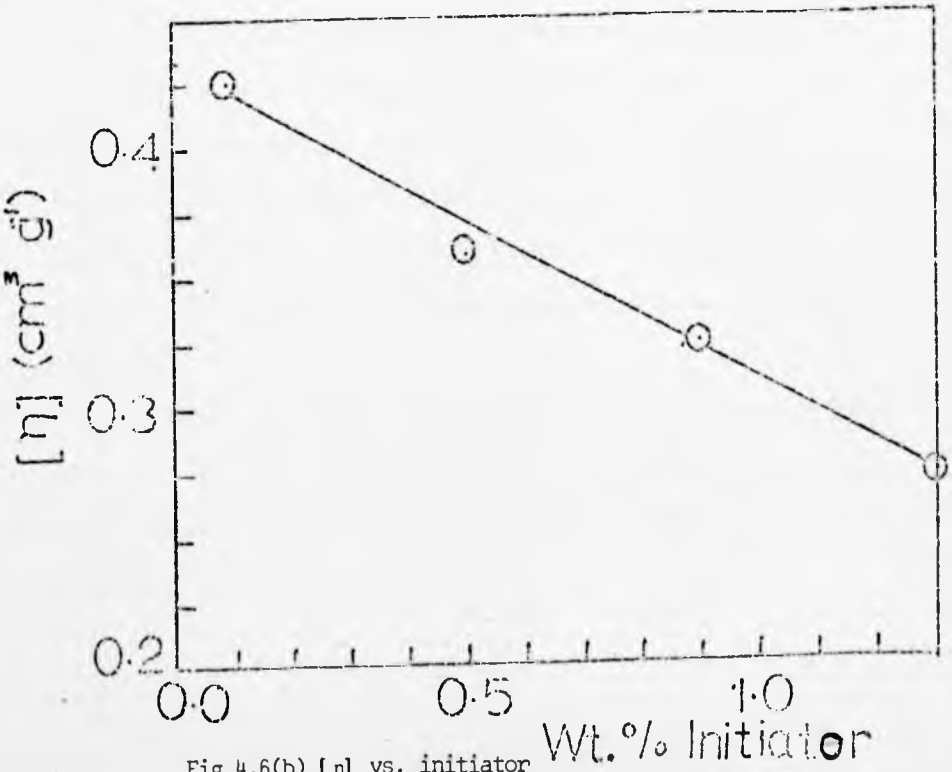

Fig.4.6(b) [η] vs. initiator concentration for PMMI (DMSO, 298K).

obtained and the dependence of intrinsic viscosity ([η]) on initiater concentration for bulk polymerised MMI is shown in figure 4.6(b). However, this technique was not wholly satisfactory for the following reasons. (a) The reaction rate was extremely fast making conversion control difficult (conversion is important in copolymer studies) and (b) because of the elevated melting points of several of the monomers, reaction temperatures high enough to alter the structure of the polymer were required (this is fully discussed in section 4.5). The latter problem can be overcome by optimizing conditions with respect to time and temperature. Only the PMMI and PMEI samples studied here were prepared by bulk techniques.

The emulsion polymerisation techniques outlined in section 3.3 were selected for the preparation of the remaining mono-n-alkyl polymer and copolymer samples used in this study. Emulsion polymerisation was found to give higher molecular weights, easily controlled rates, structurally pure polymers and has additional advantages in terms of general experimental convenience. The weight average molecular weights of the series of poly(mono-n-alkyl itaconates) studied were determined by light scattering measurements (section 3.8) and are listed in table 4.4 along with the corresponding refractive index increments.

DSC thermograms were obtained for all the polymers in this series, while TBA thermograms were obtained for the following representative polymers; PMMI, PMBI, PMHpI, PMOI, PMNI and PMDI.

TABLE 4.4

MOLECULAR WEIGHTS DETERMINED BY LIGHT SCATTERING MEASUREMENTS

Polymer	Solvent	Refractive Index Increment (298K)	$\bar{M}w \times 10^{-5}$	DP $\times 10^{-3}$
PMMI	Methanol	0.142	1.78	1.238
PMEI	Methanol	0.176	4.368	2.771
PMPrI	Ethanol	0.130	10.01	5.820
PMBI	Ethanol	0.125	3.090	1.661
PMPI	Ethanol	0.122	8.811	4.406
PMHI	Butanol	0.090	9.137	4.270
PMHpI	Butanol	0.0938	4.854	2.129
PMOI	Butanol	0.0966	4.415	1.824
PMNI	Butanol	0.0897	6.623	2.587
PMDI	Butanol	0.0875	8.843	3.275

TABLE 4.5

Transition Regions in Poly(mono-n-alkyl itaconates) from TBA Thermograms

Polymers	Temperature Range (K) of Maxima in Damping Index				
	α	β	γ	δ	ε
PMMI	435-440				
PMBI	430-435	240-245	190-195	90-95	
PMHpI	435-438	248-255	195-200	90-95	
PMOI	440-445	248-252	190-195	90-95	
PMNI	438-445	358-362	250-260	195-200	90-95
PMDI	440-445	325-330	255-260	195-200	90-95

4.2.2 Results of TBA studies

For each polymer studied, two or three thermograms are shown. Thermogram (I) shows the response of a freshly made polymer/braid composite which was then recooled to ~ 80K and run again to give thermogram (II). In some cases the braid was thermally recycled a third time to give thermogram (III).

The thermograms obtained are shown in figures 4.7 - 4.12, and the transition regions (indicated by maxima in the damping index) are summarised in table 4.5. The Greek letters α, β, etc. are again used to indicate the transitions.

4.2.3 Results of DSC studies

The DSC thermograms were obtained at a scan rate of 40K min^{-1} from 100 to 500K. The portions which show transitions are reproduced for several representative polymers in figure 4.13 (the omitted portions are completely featureless). All the poly(mono-n-alkyl itaconates), apart from PMDI show only one feature, an endothermic reaction whose onset is about 430K. The additional feature on the PMDI DSC thermogram has been analysed as a glass transition base line change at 315K.

4.4 DISCUSSION

The poly(mono-n-alkyl itaconates) are radically different from the corresponding di-n-alkyl polymers, not only chemically, but to a large extent in their physical properties. At room temperature all the former are hard, brittle solids while only those of the latter which have less than four carbon atoms in the side chain are in the glassy state, the remainder being mainly viscous liquids. It is obvious that the inclusion of carboxyl group in itaconate polymers has a drastic effect on molecular motions.

Fig.4.7 TBA thermograms for PMMI

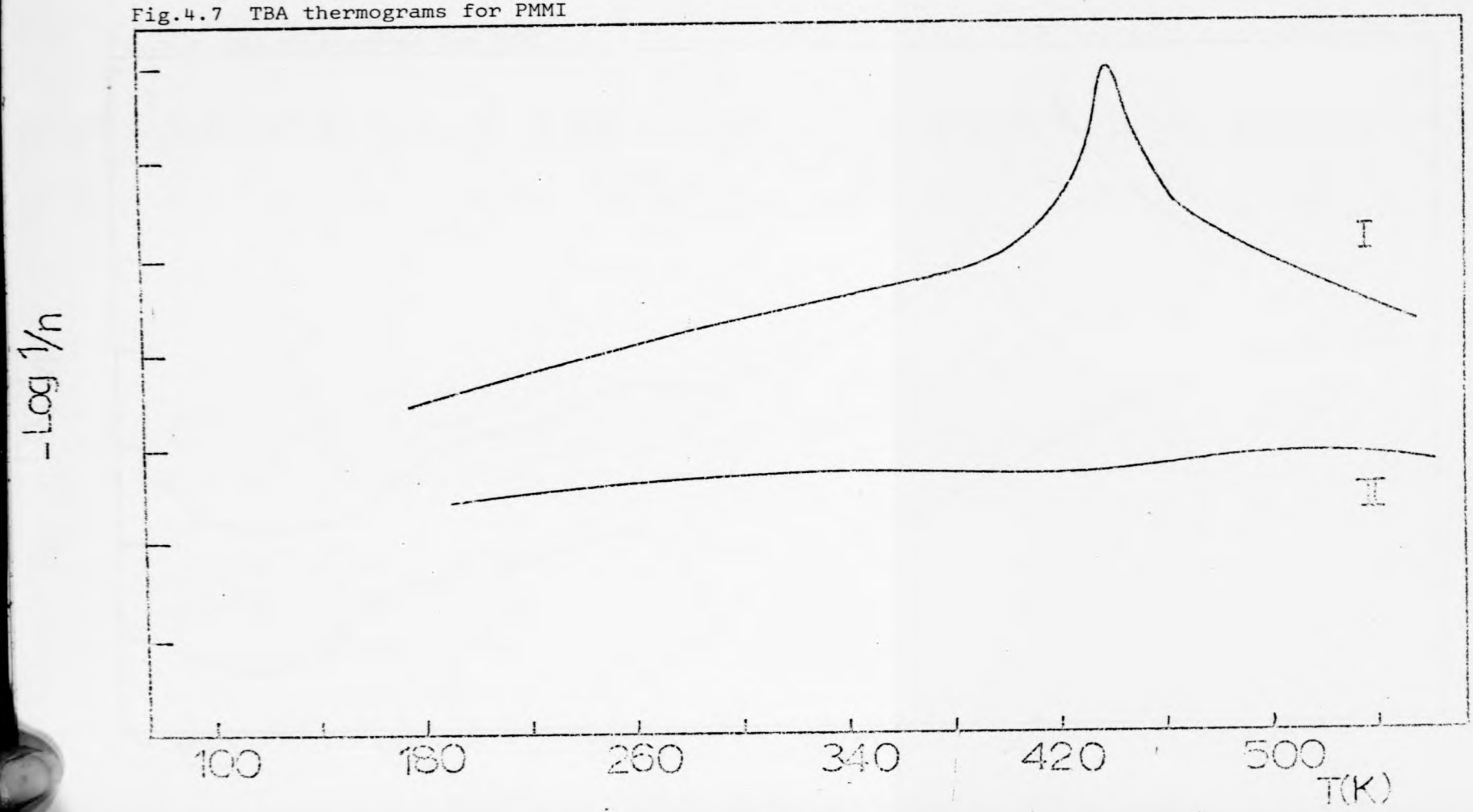

Fig.4.8 TBA thermograms for PMBI

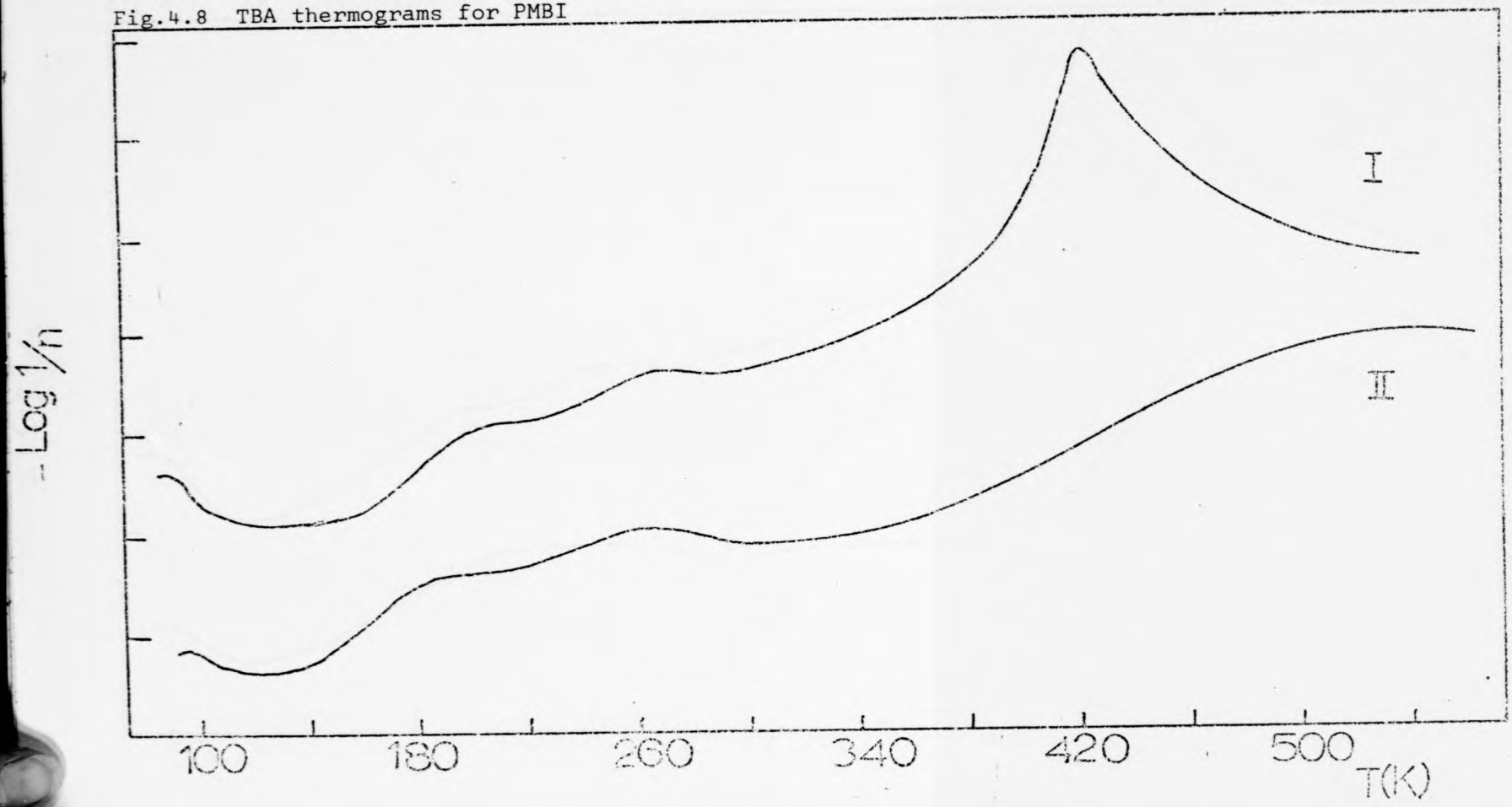

Fig.4.9 TBA thermograms for PMHpI

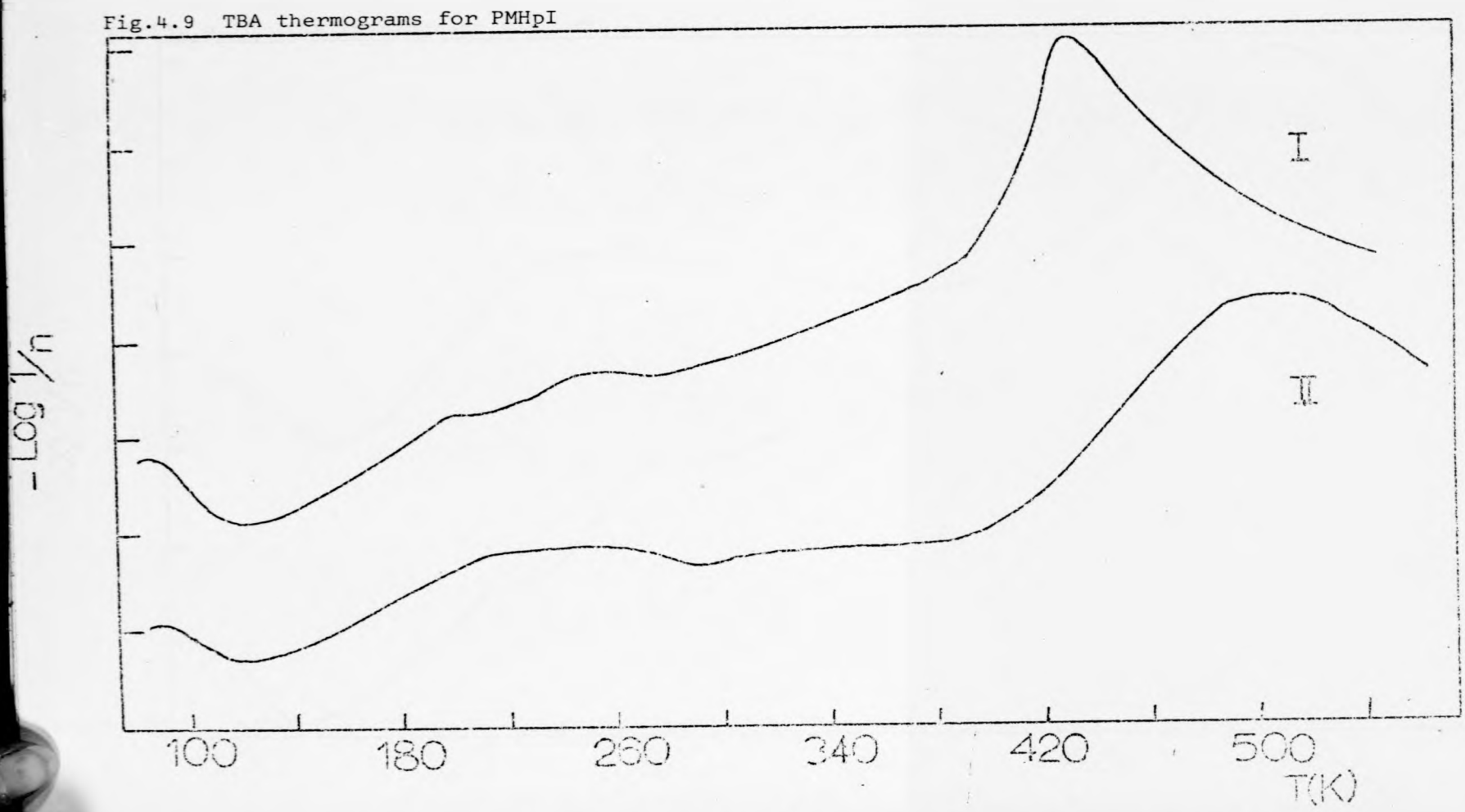

Fig.4.10 TBA thermograms for PMOI

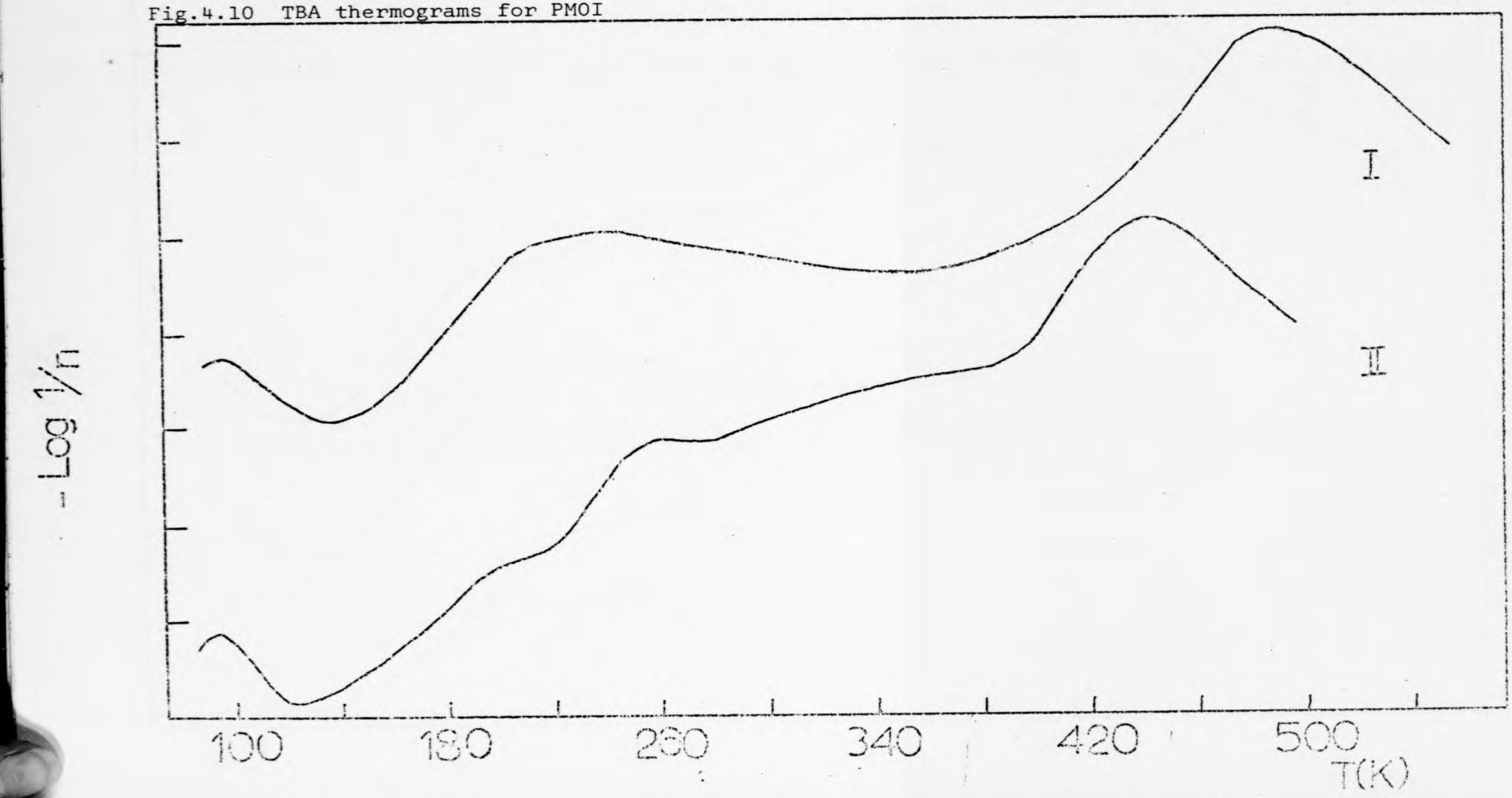

Fig.4.11 TBA thermograms for PMNI

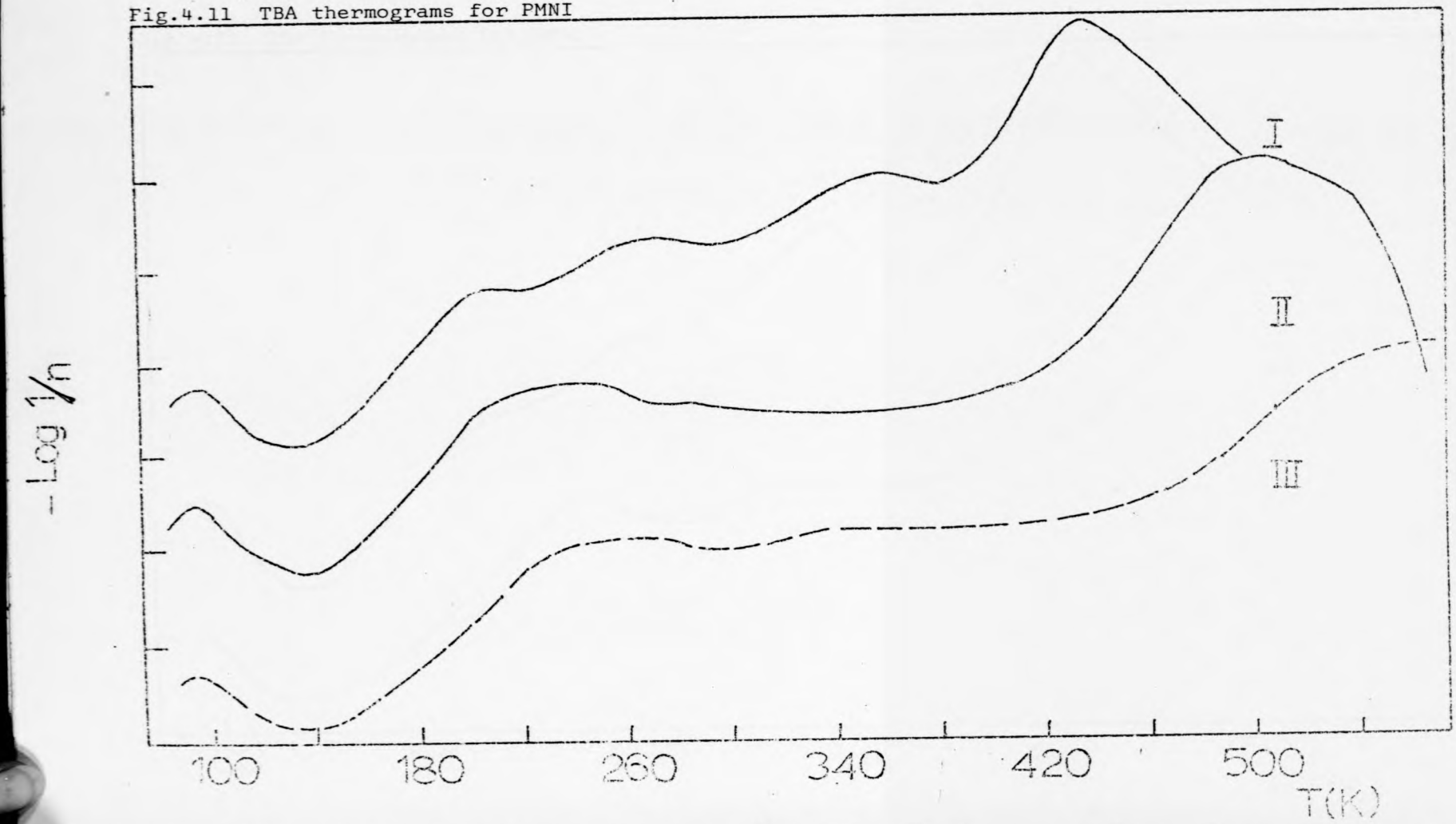

Fig.4.12 TBA thermograms for PMDI

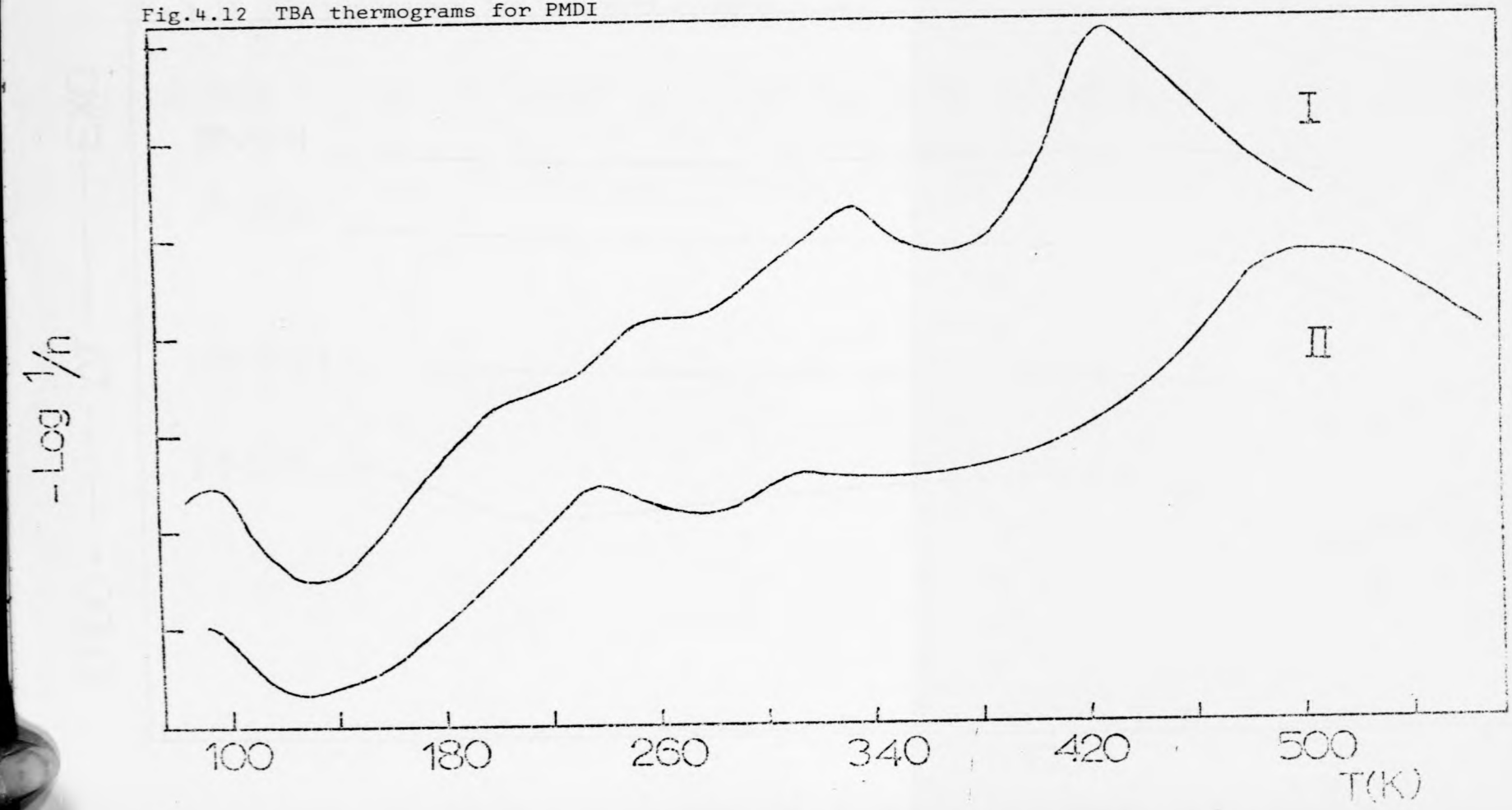

Fig.4.13 DSC thermograms for indicated polymers

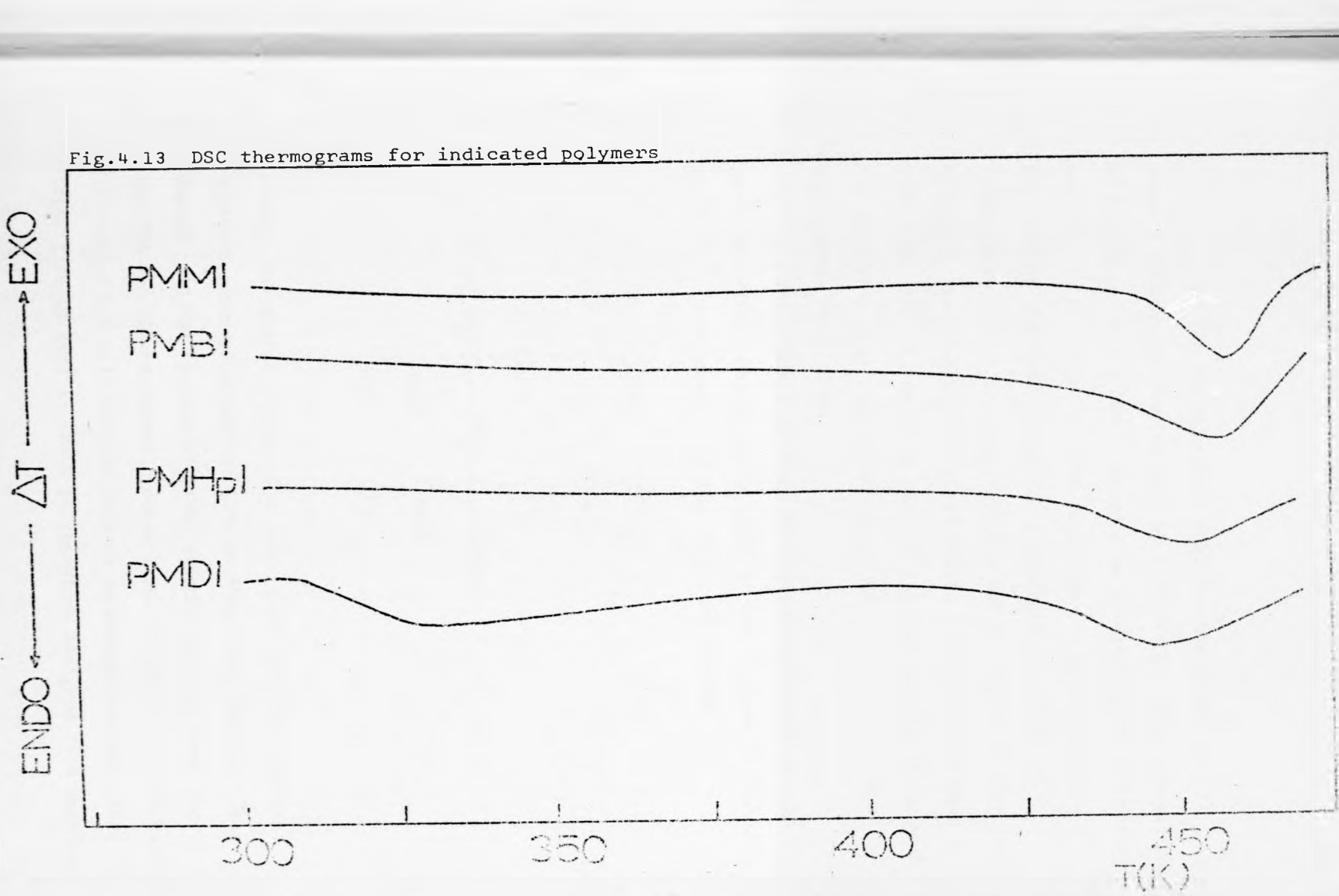

The TBA thermogram of PMMI for the first run (I) shows a pronounced damping peak at 435 – 440K. This transition is indicated on the DSC thermogram as a melting-like endotherm centred ∿450K. However, this transition is <u>not</u> reproduced when either the PMMI TBA braid is thermally recycled (thermogram II) or the sample in the DSC is thermally recycled, (giving an absolutely featureless trace). Additionally when a sample of PMMI is heated to 435K it suddenly expands to around ten or twenty times its original volume, and forms an open structured, white foam.

The transition ∿440K is obviously related to some gross structural change which involves the release of gaseous products. Consideration of the structure of PMMI

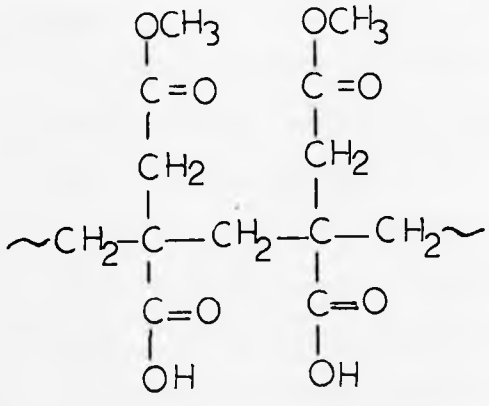

reveals the possibilities of a dehydration reaction between adjacent carboxyl groups to give an anhydride linkage. This change, and the release of water vapour, could account for the TBA and DSC responses around 440K. Evidence to be presented in section 4.5 will confirm this to be essentially the case. The transition in PMMI at ∿440K is therefore assigned to a chemical

change (dehydration) resulting in an irreversible alteration in the polymer's structure.

This contradicts earlier published work[31] on the thermal behaviour of PMMI prepared in the presence of zinc chloride. This polymer is reported to exhibit a melting transition at 418 – 421K. In order to resolve this contradiction, a sample of PMMI was prepared by this method and it did indeed show a melting-like behaviour at this temperature. However after purification by a six-fold reprecipitation, the melting-like behaviour disappeared. The only transition to be observed was the non-repeatable dehydration reaction at ∿440K already mentioned. It must, therefore, be concluded that this reported melting point is due to impurities (perhaps zinc chloride or absorbed water?) in the polymer.

The DSC thermograms of all the remaining polymers in the series also show a endothermic reaction at ∿440K. After the side chain length reaches three carbon atoms this reaction appears to become less facile, in that thermally recycled samples will continue to show the transition, albeit with less intensity and at a slightly higher temperature. PMDI can in fact be cycled five times before the thermogram shows negligible change occurring at ∿440K.

The TBA thermograms shown in figures 4.7-4.12 confirm the behaviour of the dehydration transition observed by DSC. For example, PMOI shows a marked transition in thermogram I at 440K and on thermal recycling (thermogram II) this has moved to ∿490K. With the shorter side chain length in PMBI the dehydration observed in (I) is much less obvious

in the second run (II) showing that the reaction can go much nearer to completion in one stage.

More interesting, however, is the appearance of other transitions in the TBA thermogram (I) of higher mono ester polymers. These occur at 240-250K, 190-195K and 90-95K in PMBI, and at very similar temperatures in the remaining polymers studied by TBA. The transition at 90-95K corresponds almost exactly in temperature with that ascribed to crankshaft motions in the side chains of poly(di-n-alkyl itaconates). It seems reasonable that this molecular motion is also responsible for the 90-95K transition in the poly(mono-n-alkyl itaconates).

The two transitions between 190-250K cannot be unambiguously assigned on the evidence presented here. It is perhaps not unreasonable to suggest three possible causes, (a) ester linkage rotation somewhat related to the n-alkyl methacrylate[38] series, (b) carboxyl group rotation, or (c) absorbed water[38] associated with the hydrophilic carboxyl groups. The 240-250K peak lies closest to the temperature range of ester group rotation in the methacrylate polymers. Since the ester linkage in mono alkyl itaconates is less sterically hindered by the main chain (it has an intervening $-CH_2-$ group), it is not unreasonable to speculate that rotation of this ester link is responsible for the relaxation at 240-250K.

A further additional transition occurs in TBA thermograms of PMNI (at ∿360K) and PMDI (at ∿330K). The latter transition is also observed in the DSC thermogram of PMDI at

315K and has been assigned to the glass transition in this polymer. Although the transition at 360K in the TBA thermogram of PMNI cannot be confirmed by DSC, presumably because of its proximity to the dehydration temperature, this is also assigned as the glass transition. In the poly(mono-n-alkyl itaconates), therefore, glass transitions must be at temperatures well above the dehydration temperature. Only when the side chain is sufficiently long (nine carbon atoms) does it occur below the dehydration range.

4.3 COPOLYMERS

Selected copolymer systems were prepared by the combination of two di-n-alkyl itaconates or a di-n-alkyl itaconate and a mono-n-alkyl itaconate. It was hoped that these would cover as broad a range of physical properties as possible and provide copolymers suitable for the preparation of ionomers (see next section).

4.3.1 Reactivity ratios

During copolymerisation of two monomers, the rates at which the separate monomers add to the growing radical chain determines the composition, and hence the properties of the resulting copolymer. The order, as well as the ratio of the amounts, in which the monomers add is determined by their relative reactivities in the chain growth step. This is in turn influenced by the nature of the growing radical chain end and on which monomer added previously. Among the possibilities are random and regular alternating addition, as well as block formation.

All the copolymer systems studied here were prepared by the emulsion techniques described in section 3.3. Their composition was analysed by (a) titration of the free carboxyl groups, if one comonomer was a mono-n-alkyl ester (except poly(MDI + DDI)), or (b) by N.M.R. if both comonomers were di-n-alkyl esters (see section 3.5). A typical set of titration curves for the copolymer system poly(MHpI + DHpI) is shown in figure 4.14.

The complete composition analysis for the five series of copolymers studied is shown in the appendix. The corresponding plots of $F(1-f)/f$ against F^2/f (see section 3.5) are shown in figure 4.15 and 4.16 and reactivity ratios are shown below in Table 4.6.

TABLE 4.6

Reactivity Ratios of Emulsion Polymerised n-alkyl Itaconate Esters

M_1	M_2	T/K	r_1	r_2	$r_1 r_2$
MBI	DBI	428	0.74	0.82	0.61
MHpI	DHpI	431	1.59	0.58	0.92
MDI	DDI	448	-	-	-
MBI	DMI	428	0.82	0.86	0.70
DMI	DHpI	428	1.4	0.7	0.98
DMI	DDI	428	1.15	0.52	0.76

A reactivity ratio is the ratio of the rate of addition of a given radical to its own monomer compared with the rate of addition of the radical to the other monomer. A value of $r > 1$ means that the radical

Fig.4.14 Titration curves for PMHpI

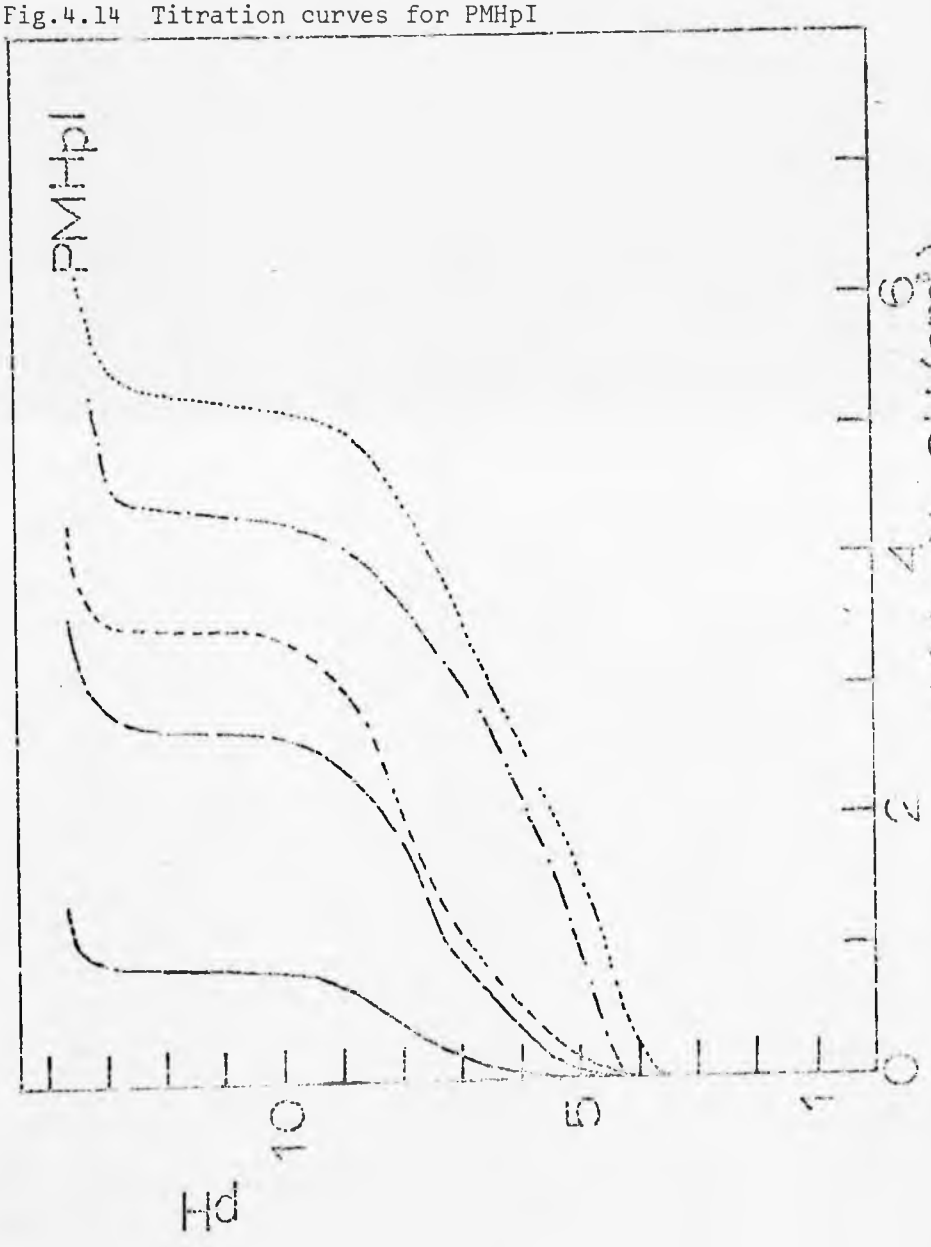

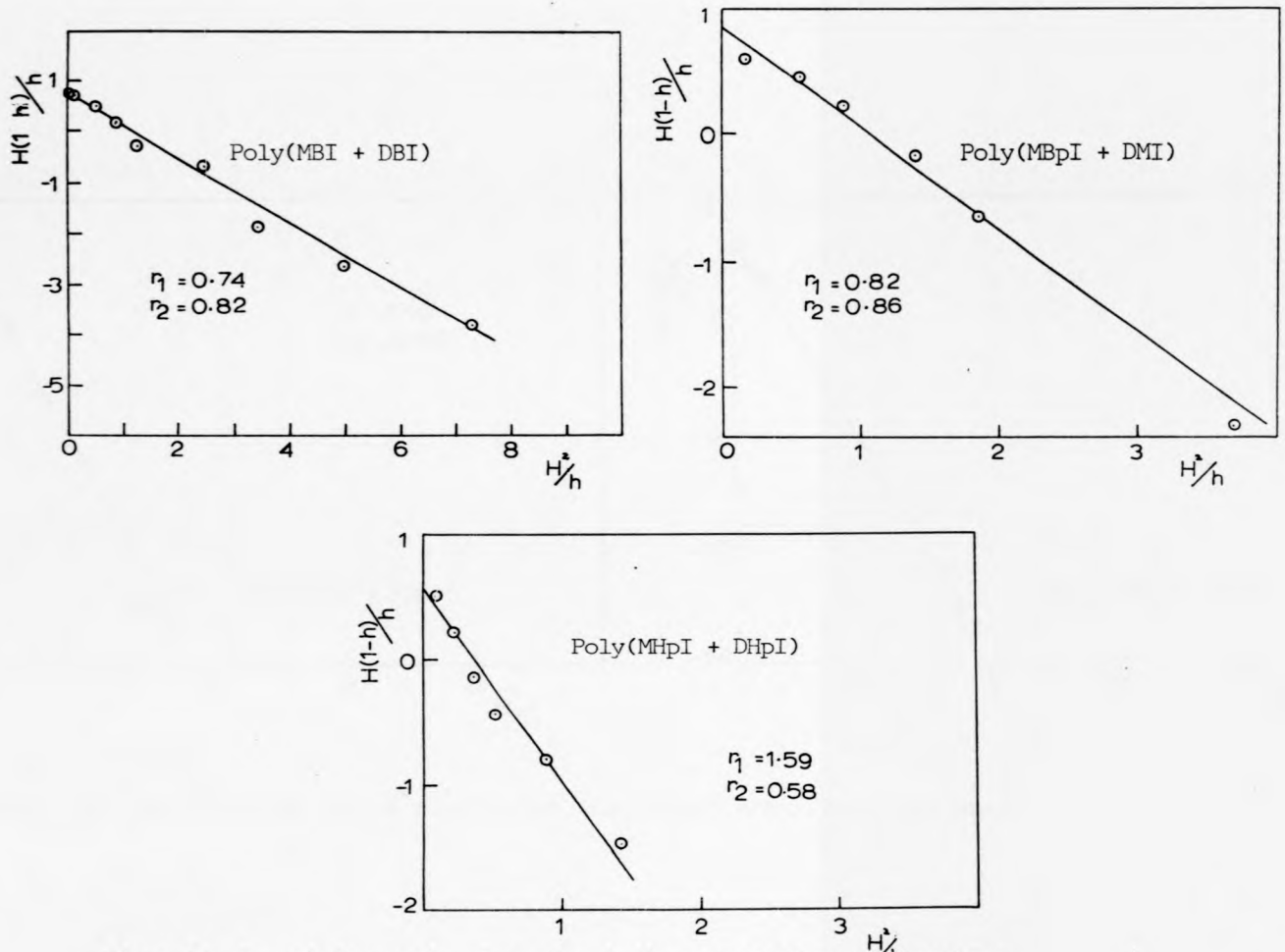

Fig.4.15 Reactivity ratio plots for indicated copolymer systems

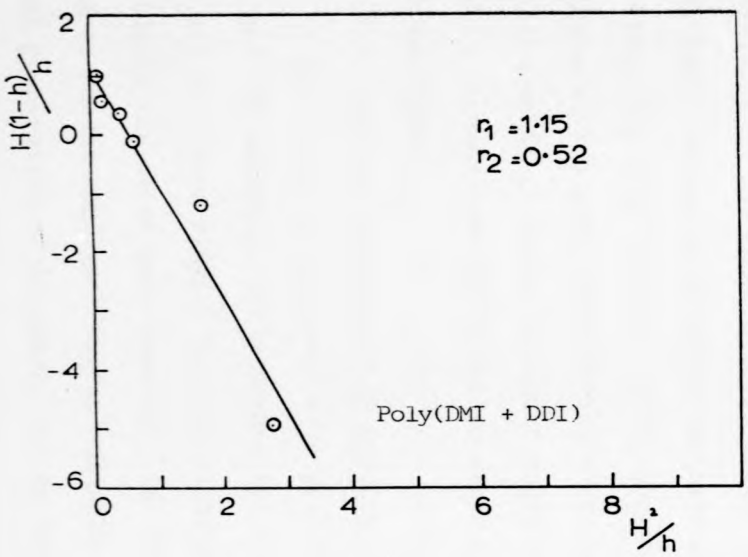

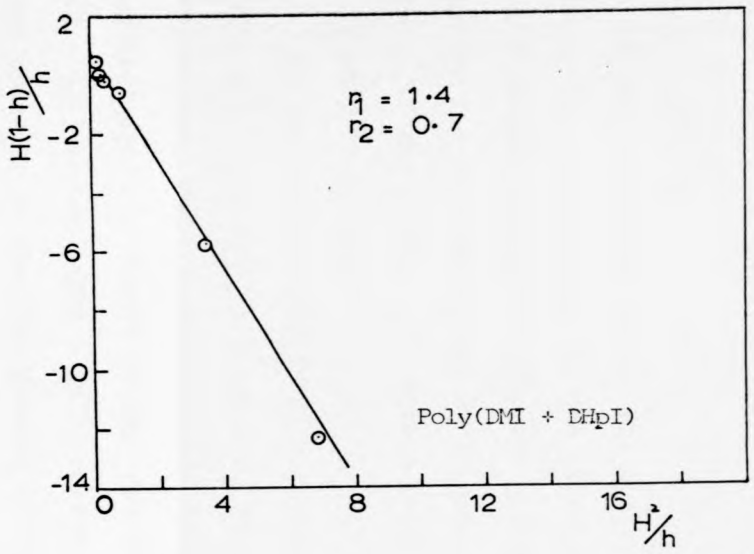

Fig.4.16 Reactivity ratio plots for indicated copolymer systems

prefers to add to its own monomer while a value less than unity indicates a preference for the other monomer. The closer the product r_1r_2 is to zero the greater is the tendency for the monomers m_1 and m_2 to alternate in the copolymer. If the product r_1r_2 equals unity, the copolymer system is said to be ideal[37].

In the cases of Poly(MHpI + DHpI), and Poly(DMI + DDI) $r_1 > 1$, $r_2 < 1$ and r_1r_2 is less than unity. This implies that these systems are not ideal and there is a composition drift in favour of MHpI and DMI respectively. Poly(MBI + DBI) and Poly(MBI + DMI) are more favourable copolymer systems, in that the growing chain radical adds preferentially to the other monomer faster than to its own, and only short sequences of either monomer will form. It may also be observed from Table 4.6 that, when a short chain ester copolymerises with long chain ester, there is always a composition drift in favour of short chain ester, and consequently it becomes more difficult to avoid the formation of a block copolymer.

4.3.2 Physical Properties of Copolymers

Two types of copolymer were prepared for study by TBA and DSC analysis, (i) mono-n-alkyl + di-n-alkyl esters and (ii) di-n-alkyl + di-n-alkyl esters. Type (i) were studied for three main reasons, (a) to obtain a reasonably random copolymer system suitable for the eventual preparation of ionomers, (b) to determine whether a copolymer with good elastomeric properties can be made by

combining the brittle properties of poly(mono-esters) with the viscous liquid behaviour of longer chain poly diesters, (c) to attempt to locate the Tg of poly(mono-esters) by extrapolation above their dehydration temperatures. Type (ii) was studied in an attempt to elucidate the more complex thermal behaviour which occurs when poly(di-n-alkyl esters) have n-alkyl side chains with more than six carbon atoms.

4.3.3 Copolymers of Mono- and Di-n-Alkyl Itaconates.

(i) Poly(MBI + DBI)

Figure 4.17 shows TBA thermograms for this copolymer system. This displays the expected gradation between the two homopolymers. The peaks ∿430K in PMBI and in the copolymers are assigned to dehydration and, as expected, the relative intensity decreases with increasing content of DBI. The glass transition in PDBI is located at ∿285K and a similar transition is observed in the lower four thermograms (see Figure 4.17), but these are located at increasing temperatures, and have been assigned the glass transitions temperature for these copolymers. The lowest temperature peaks at ∿100K in every thermogram are again assigned to crankshaft motion in the n-alkyl side chains. The two transitions in PMBI at ∿250K and ∿190K have already been noted (see section 4.2) and are also apparent in copolymers with greater than 15% MBI content.

DSC studies were carried out on each member of this copolymer series, but in only a few instances was there any indication of glass transition baseline shift. The values of Tg observed by both DSC and TBA are summarized in Table 4.7.

Fig.4.17 TBA thermograms for the poly(MBI + DBI) system

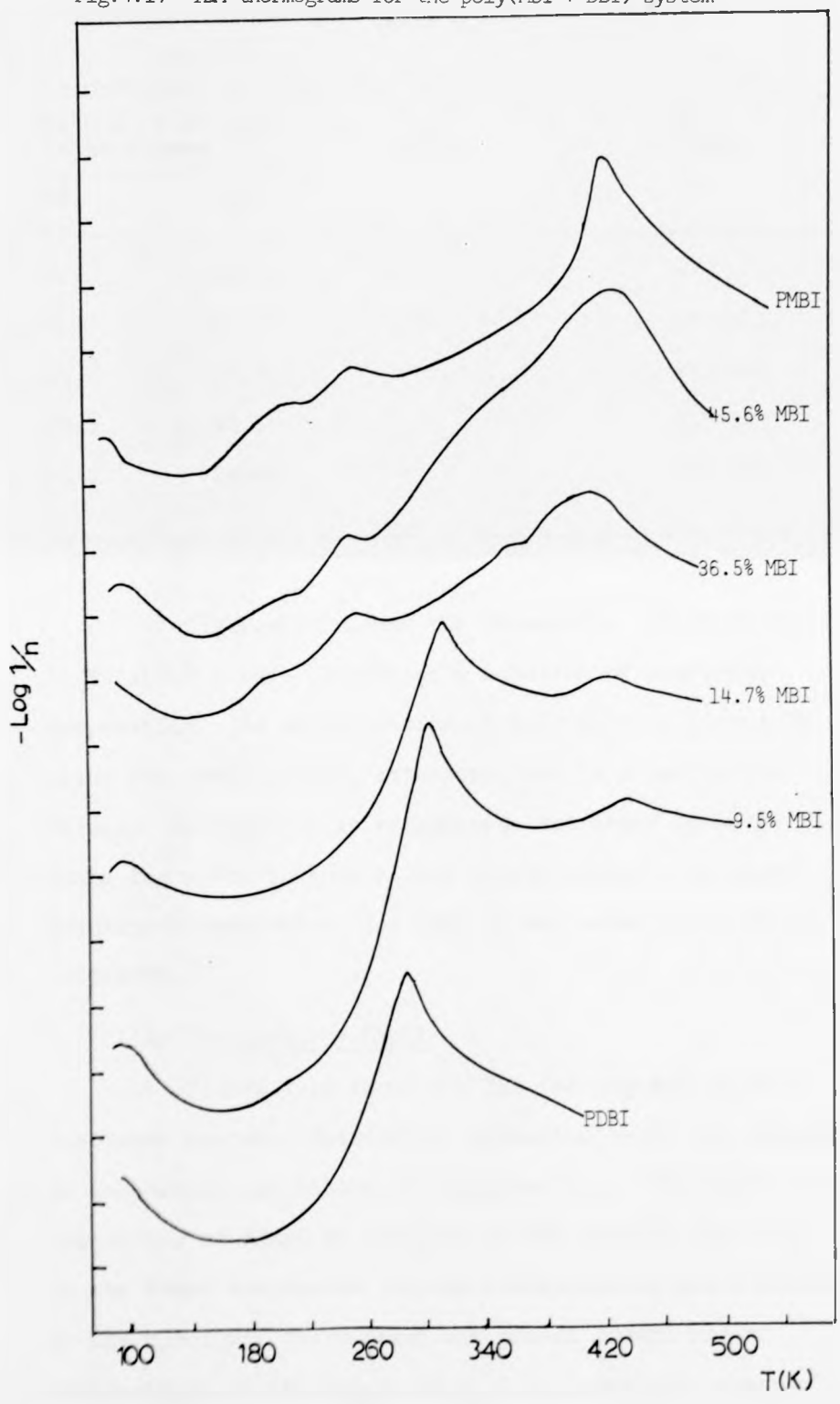

TABLE 4.7

Mole % of monomer in copolymer		Tg/K (DSC)	Tg/K (TBA)
MBI	DBI		
5.7	94.3	287	-
9.5	90.5	294	297-301
14.7	83.3	-	310-313
36.5	63.5	-	353-357
45.6	54.4	-	376-380

Figure 4.18(a) shows the observable values of Tg in Poly(MBI + DBI) plotted as a function of copolymer composition. An extrapolation of this data to give a Tg value for PMBI has been attempted, and is shown in the figure. Although it is recognised that there is large scope for error in such a long extrapolation, the glass transition temperature for PMBI is estimated to be about ∿460-470K.

(ii) Poly(MHpI + DHpI)

Figure 4.19 shows the TBA thermograms of this copolymer system. Transitions appearing ∿430K are assigned to dehydration as in the poly(mono-ester). The glass transition of PDHpI is assigned to the peak at 250-253K in the lower thermogram and the corresponding glass transitions in the copolymer thermograms are pushed toward higher temperatures as the amount of MHpI is increased, eventually

Fig.4.18(a)

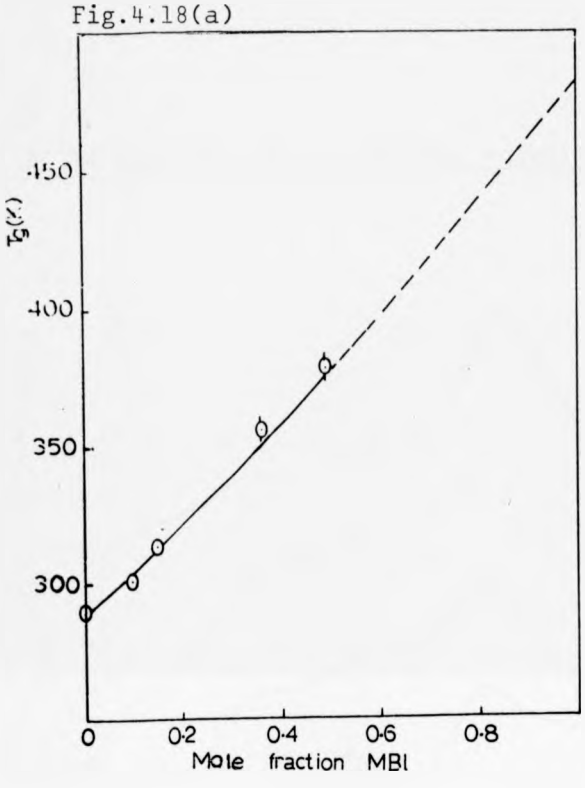

Fig.4.18(b)

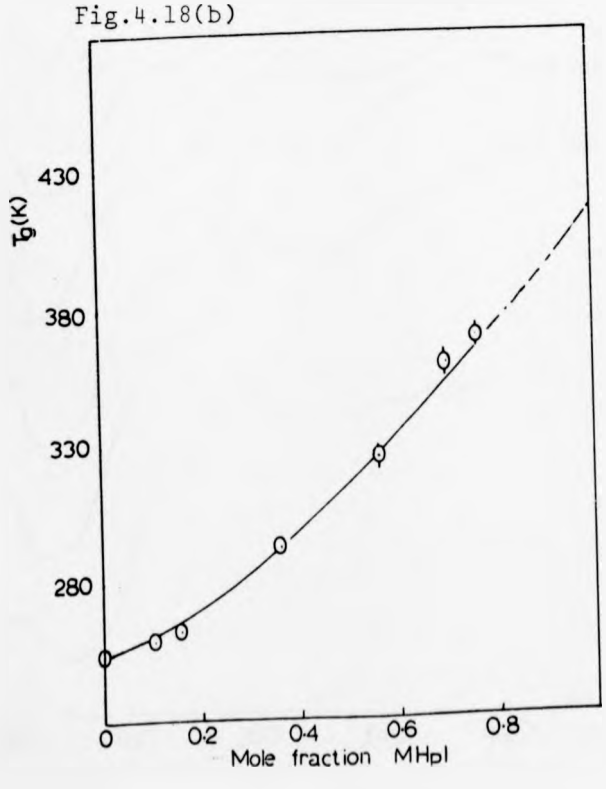

Fig.4.19 TBA ther-ograms for the poly(MHpI + DHpI) system

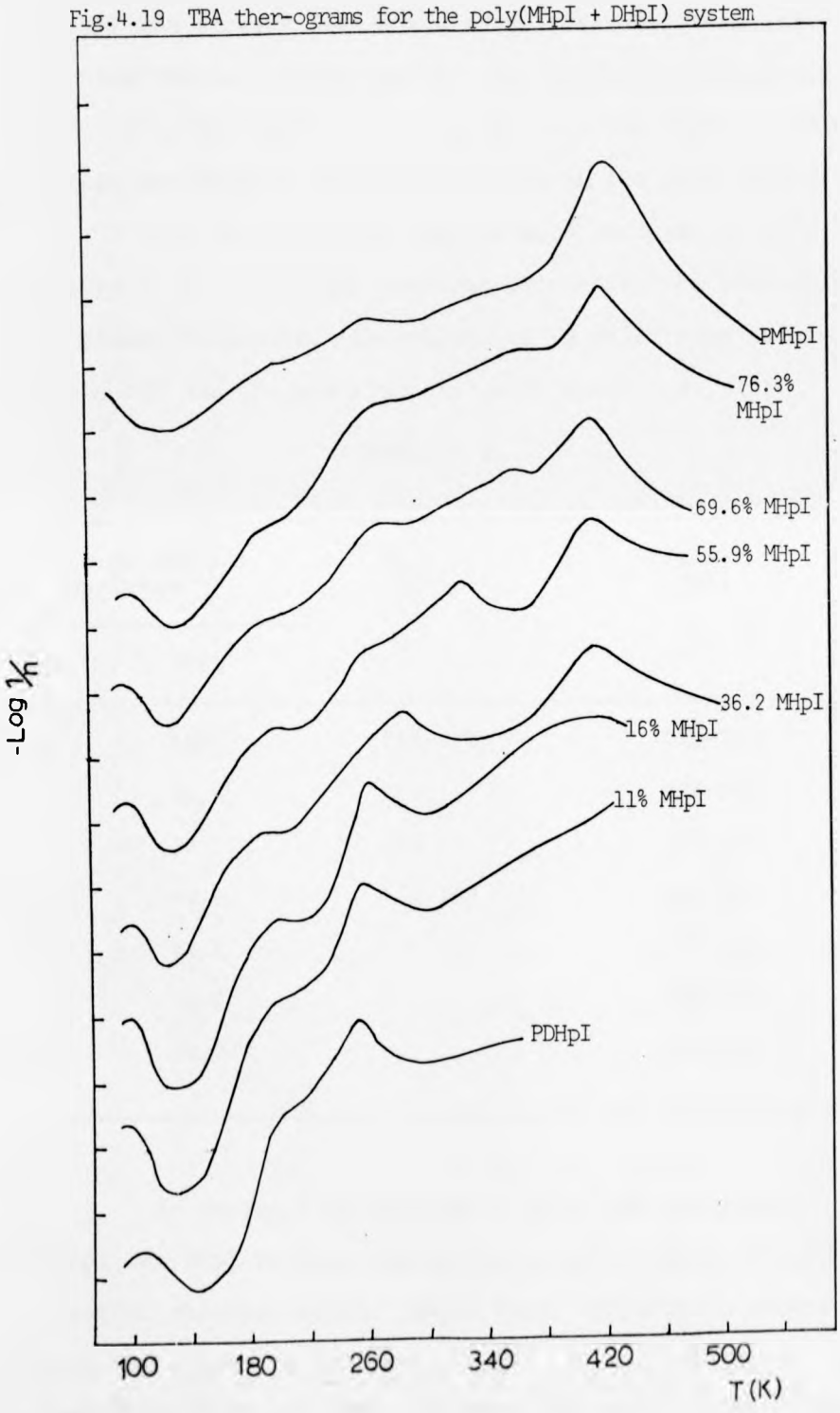

to disappear under the dehydration peak. The peak at ∿200K in PDHpI has already been assigned to a second glass transition involving the ester side chains, this gradually diminishes in intensity as the MHpI content increases. The peak at ∿100K is again assigned to crankshaft motion in the side chain.

All the copolymer samples were analysed by DSC, but only a few showed any features which could be identified as a glass transition. The values of Tg which were observed by both DSC and TBA are shown below in Table 4.8.

TABLE 4.8

Mole % of monomer in copolymer		Tg/K (DSC)	Tg/K (TBA)
MHpI	DHpI		
0	100	249-250	250-253
11	89	254	256-259
16	84	258	260-262
36.2	63.8	275-282	284-286
55.9	44.1	-	324-326
69.6	30.1	-	360-365
76.3	23.7	-	373-383

In contrast to poly(MBI + DBI), the copolymer of MHpI and DHpI retains thermoplastic behaviour up to ∿70% content of the mono-ester. Above this, dehydration occurs before the softening transition (Tg). By extrapolation (figure 4.18(b)), Tg for PMHpI is estimated to be in the range 405-415K.

(iii) Poly(MDI + DDI)

No composition analysis was obtained for this copolymer series. Attempts to analyse the carboxyl group content by titration failed because the neutralisation reaction proved so slow as to make accurate location of the end point impossible. Presumably the structure of the copolymer results in the long n-alkyl side chains forming a cage around the -COOH group, effectively shielding these from reaction. NMR analysis also proved impractical (at least in the time available during this study) as no suitable solvent could be found. As an alternative to titration and NMR analysis, carbon, hydrogen combustion analysis were obtained for the copolymers. Unfortunately this technique was not sufficiently sensitive to observe the small differences in C,H content and allow copolymer compositions to be calculated. In view of these difficulties the compositions quoted for this copolymer series are those of the feed.

TBA thermograms for this series of copolymers are shown in figure 4.20 along with the percent MDI in the feed. The behaviour of the copolymer is not altogether compatible with an assumption that they are random in nature. The transition at ∿320K in PMDI and at ∿255K in PDDI have been identified as Tg for each of the homopolymers respectively. These peaks are also present, at very much the same temperatures, in the copolymers. This could be the result of block formation with the consequent aggregation of the different blocks into essentially separate domains of PMDI

Fig.4.20 TBA thermograms for the poly(MDI + DDI) system

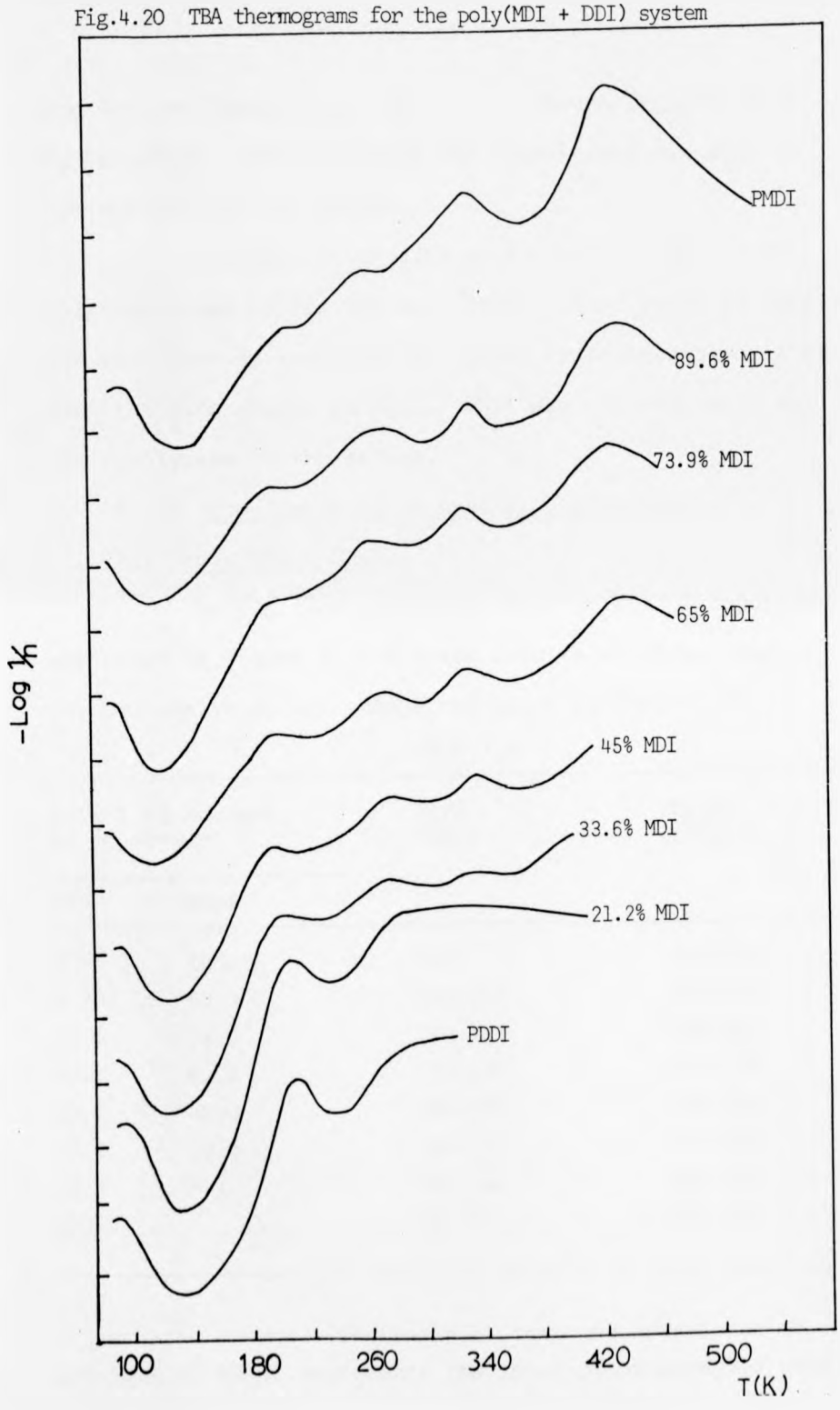

and PDDI of large enough size to retain their individual Tg behaviour. The remaining TBA transitions can also be interpreted in this manner.

Although DSC studies were also carried out on this copolymer series the only feature that could be identified was that already assigned to a glass transition associated with the side chains in PDDI. This was observable in all the copolymers of the series.

4.3.4 Copolymers of Di-n-alkyl Itaconates

(i) Poly(DMI + DHpI)

The TBA thermograms for this series of copolymers are shown in figure 4.21 and the results of these, and of the DSC analysis, are summarised below in Table 4.9.

TABLE 4.9

Mole % of monomer in copolymer		Tg/K (DSC)	Tg(K) (TBA)
DMI	DHpI		
0	100	250	250-253
8.7	91.3	251-252	252-254
22.0	78.0	260-261	260-263
37.2	62.8	275-276	275-277
53.7	46.3	290-291	292-294
70.7	29.3	315-316	315-318
91.9	9.1	343-344	348-349
100.0	-	371-372	373-374

It has been assumed (section 4.1) that the transition at 250-253K in PDHpI represents the onset of cooperative main

Fig.4.21 TBA thermograms for the poly(DMI + DHpI) system

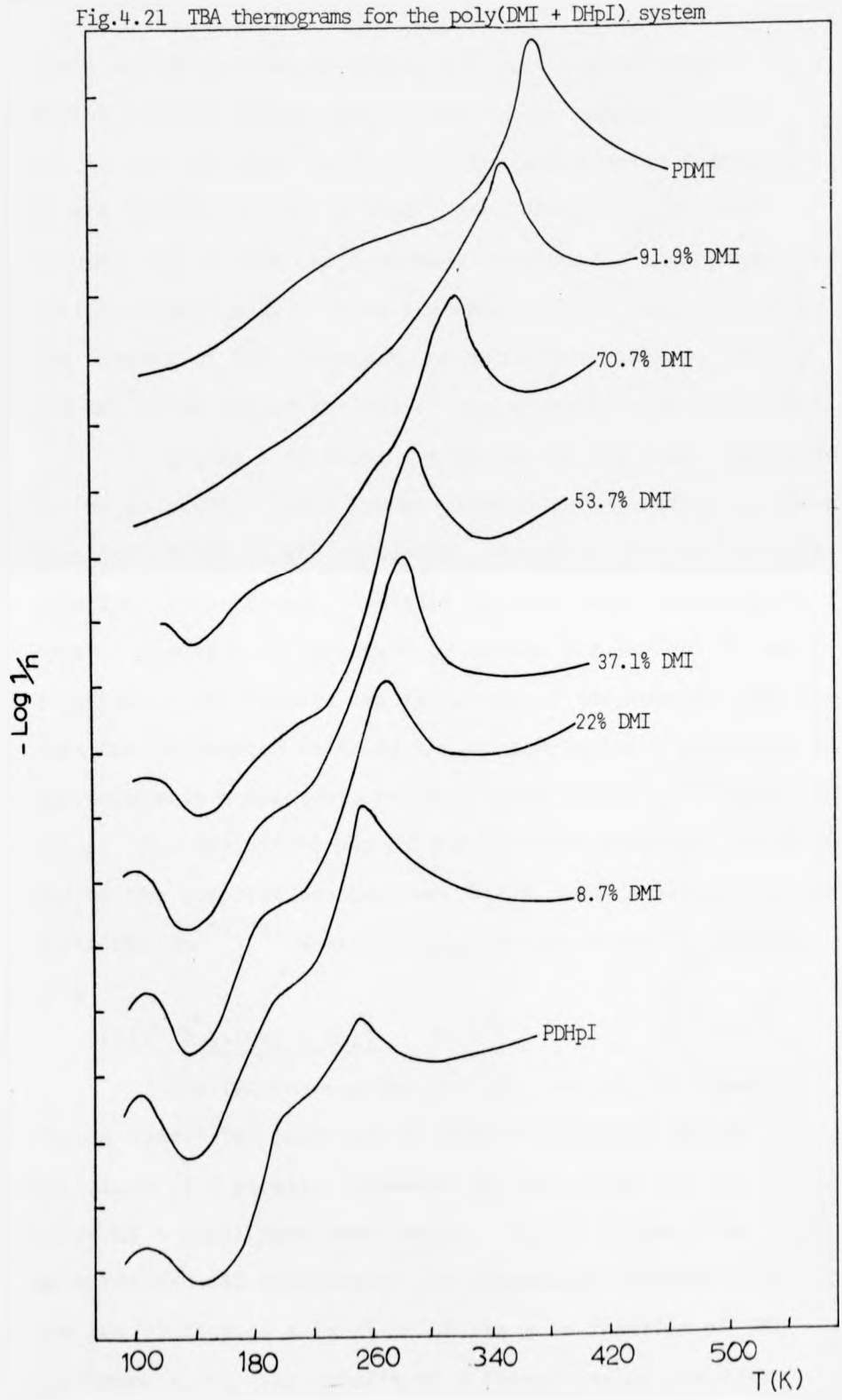

chain motion and the resulting TBA peak can be traced moving towards higher temperature as the composition of DMI in the copolymer increases. The other major transitions in the TBA thermogram of PDHpI, at ∿200K and ∿100K, were assumed due to side chain relaxation and side chain crankshaft motion respectively. These gradually became less intense as the content of DMI increases, as would be expected, if they are due to molecular motions of the n-heptyl side chain only.

Figure 4.22 shows the values of the glass transitions in the poly(DMI + DHpI) system plotted as a function of the mole fraction of DMI in the copolymer. A smooth, but non-linear, relationship is found. Analysis of this data, according to the form of equation 2.1 proposed by Gordon and Taylor[43] was attempted. The results are tabulated in the appendix and show that the calculated value of the Gordon-Taylor K-parameter is approximately a constant, but only over a limited composition range. The deviations may be due to block formation at either end of the composition spectrum, but a more detailed sequence distribution[74,75] analysis would be necessary to confirm this.

(ii) Poly(DMI + DDI)

The TBA thermograms for this series are shown in figure 4.23. The features of these thermograms can be explained by a parallel argument to that given for the poly(DMI + DHpI) copolymer series. The Tg values from both TBA and DSC measurement are summarised in table 4.10 and are plotted as a function of the mole fraction of DMI in figure 4.24. The results of a Gordon-Taylor analysis

Fig.4.22

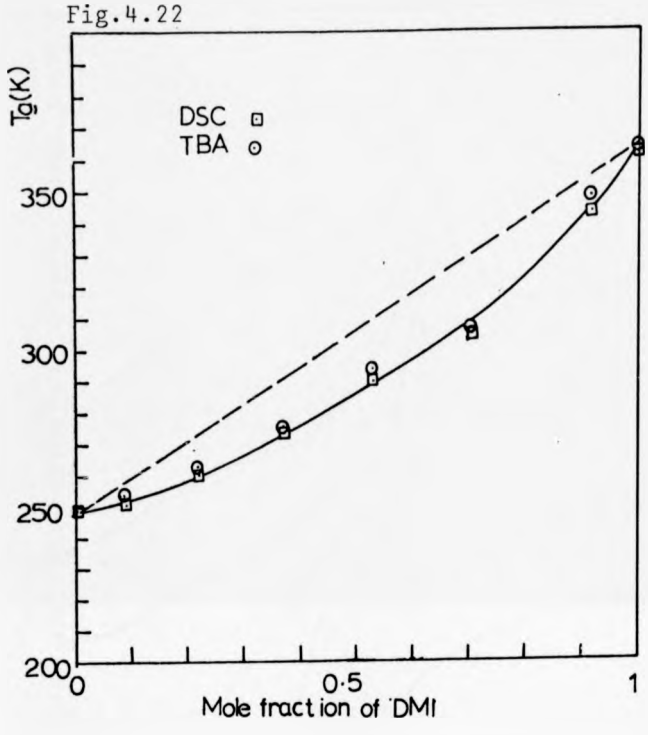

Fig.4.24

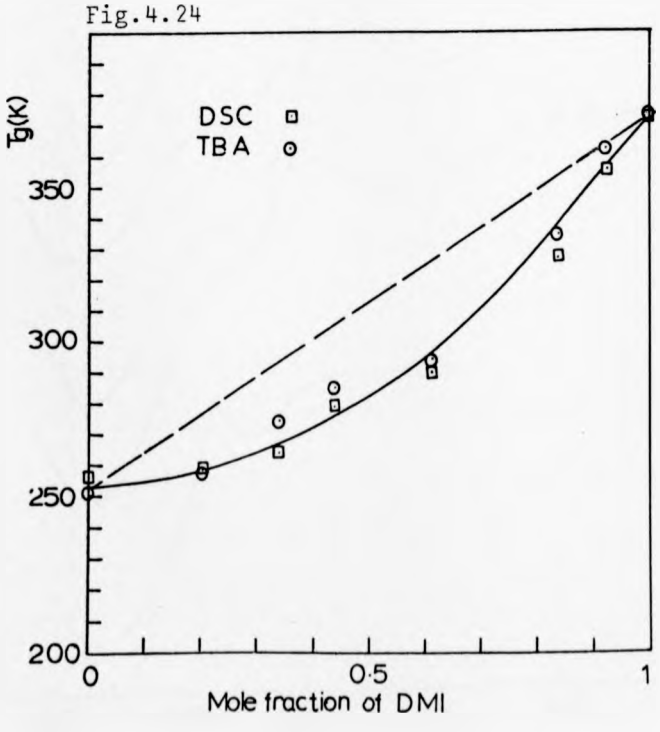

Fig.4.23 TBA thermograms for the poly(DMI + DDI)

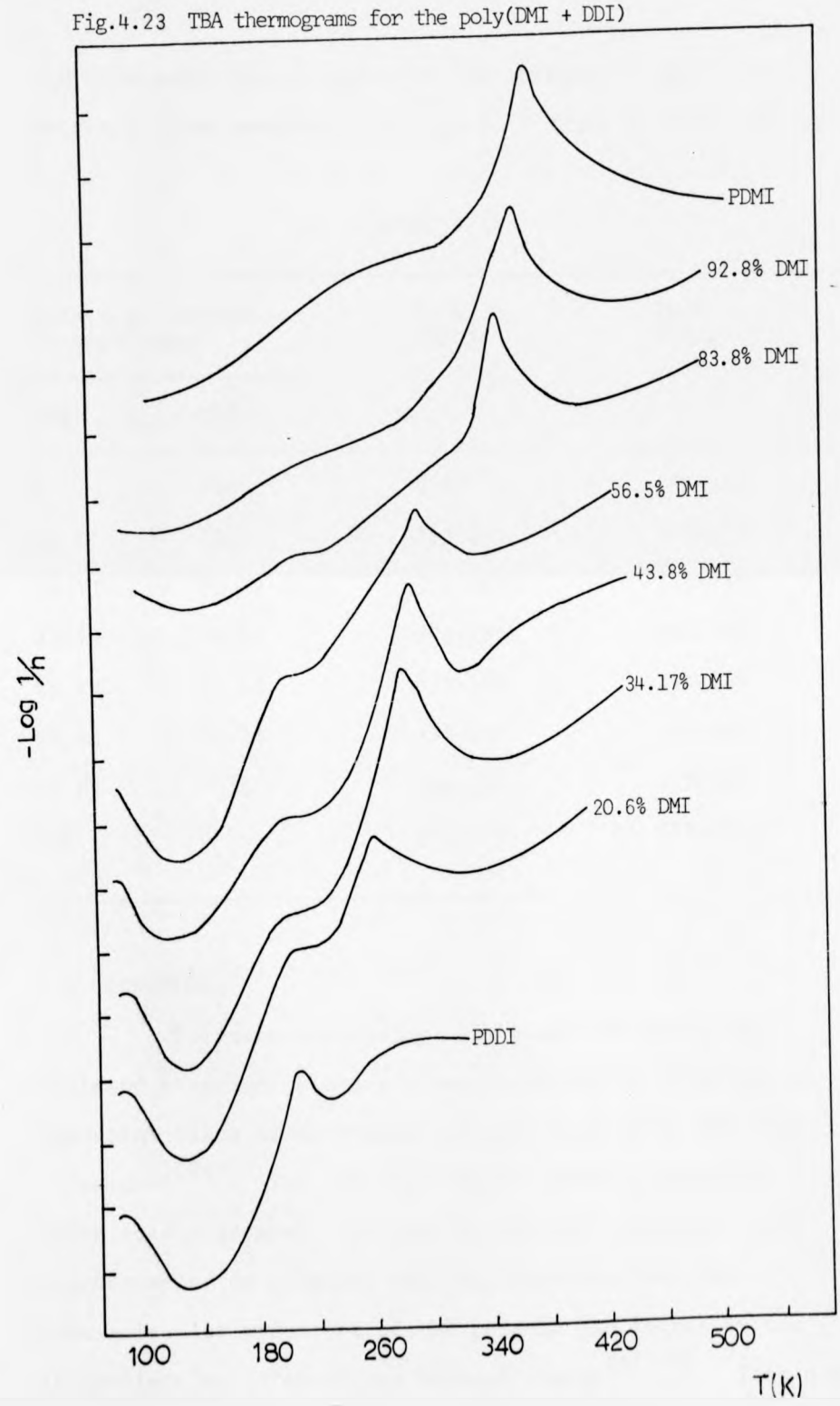

for this data is also shown in the appendix. Again for only a limited composition range is K found to be a constant.

TABLE 4.10

Mole % of monomer in copolymer		Tg/K (DSC)	Tg/K (TBA)
DMI	DDI		
0	100	∿260	255-260
20.6	79.4	262-265	260-262
34.17	65.83	265-267	275-277
43.78	58.22	278-280	285-287
56.47	43.53	287-289	293-295
83.84	16.16	337-340	345-347
92.84	7.16	358-359	362-363
100	0	371-372	373-374

4.4 IONOMERS

Polymers containing salt groups at relatively isolated positions along a linear hydrocarbon chain are an important class of materials and have been given the name "ionomers"[76]. The introduction of carboxyl groups (or other acidic groups), followed by partial ionisation with various mono- or divalent cations, disturbs both the supermolecular structure of the polymer and increases the intermolecular interactions between chains[77,78]. This has a marked effect on the physicomechanical and physicochemical

properties of the polymer[79]. In addition to Van der Walls forces and hydrogen bonding, thermally reversible ionic interactions are introduced. Consequently, in the solid state ionomers are reminiscent of cross-linked polymers, but, at sufficiently high temperatures, they can exhibit normal viscoelastic behaviour. The formation of a network of ionic bonds provides ionomers with a number of desirable properties, such as high strength, rigidity, transparency, good solvent resistance and adhesive properties[45].

Studies of ionomers, to date, have concentrated mainly on salts of ethylene-carboxylic acid copolymers, especially ethylene-acrylic acid copolymers[79-81], and syrene based copolymers[82,83]. In this work the term "ionomer" is extended to cover copolymers of a mono- and a diester of itaconic acid, containing up to 30 mole % of the former comonomer, whose carboxyl groups have been partially or fully ionised. The two systems chosen for study are poly(MBI + DBI) and poly(MHpI + DHpI). Since the resulting ionomers contain relatively long side chains, they should be somewhat different from those already reported in the literature.

Two types of ionomer were prepared (a) from copolymers of a certain known content of carboxyl groups, all of which are subsequently ionised and (b) from copolymers with a fixed 30 mole % content of carboxyl groups which are then partially ionised to a known extent. Type (a) are referred to as "fully ionised polymers" and type (b) are identified by the stated percentage ionisation of the total acid group content.

4.4.1 TBA and DSC Studies

The glass transition temperatures of sodium salt ionomers based on several fully ionised copolymers of MBI + DBI and MHpI + DHpI were determined by both TBA and DSC. The results are gathered in table 4.11 below and the TBA thermograms are shown in figures 4.25-4.27 along with those of the parent unionised copolymers. In each case the

TABLE 4.11

Copolymer and mole % composition	Tg/K			
	Parent Copolymer		100% Na salt	
	DSC	TBA	DSC	TBA
Poly(MBI + DBI) 5.7 94.3	287	-	289	-
Poly(MBI + DBI) 9.5 90.5	294	300-302	297	304-307
Poly(MHpI + DHpI) 11 89	254	256-258	256	257-259
Poly(MHpI + DHpI) 16 84	258	261-263	262	265-267

Tg of the ionomer is increased by 2-3K depending on the amount of carboxylate groups present, in concordance with the observations of other workers[82,84-86]. Accompanying the increase in the value of Tg is a relative reduction in the damping index, at temperatures greater than Tg, when ionomer is compared with the parent copolymer. (This is most apparent in the poly(MHpI + DHpI) systems.) In this

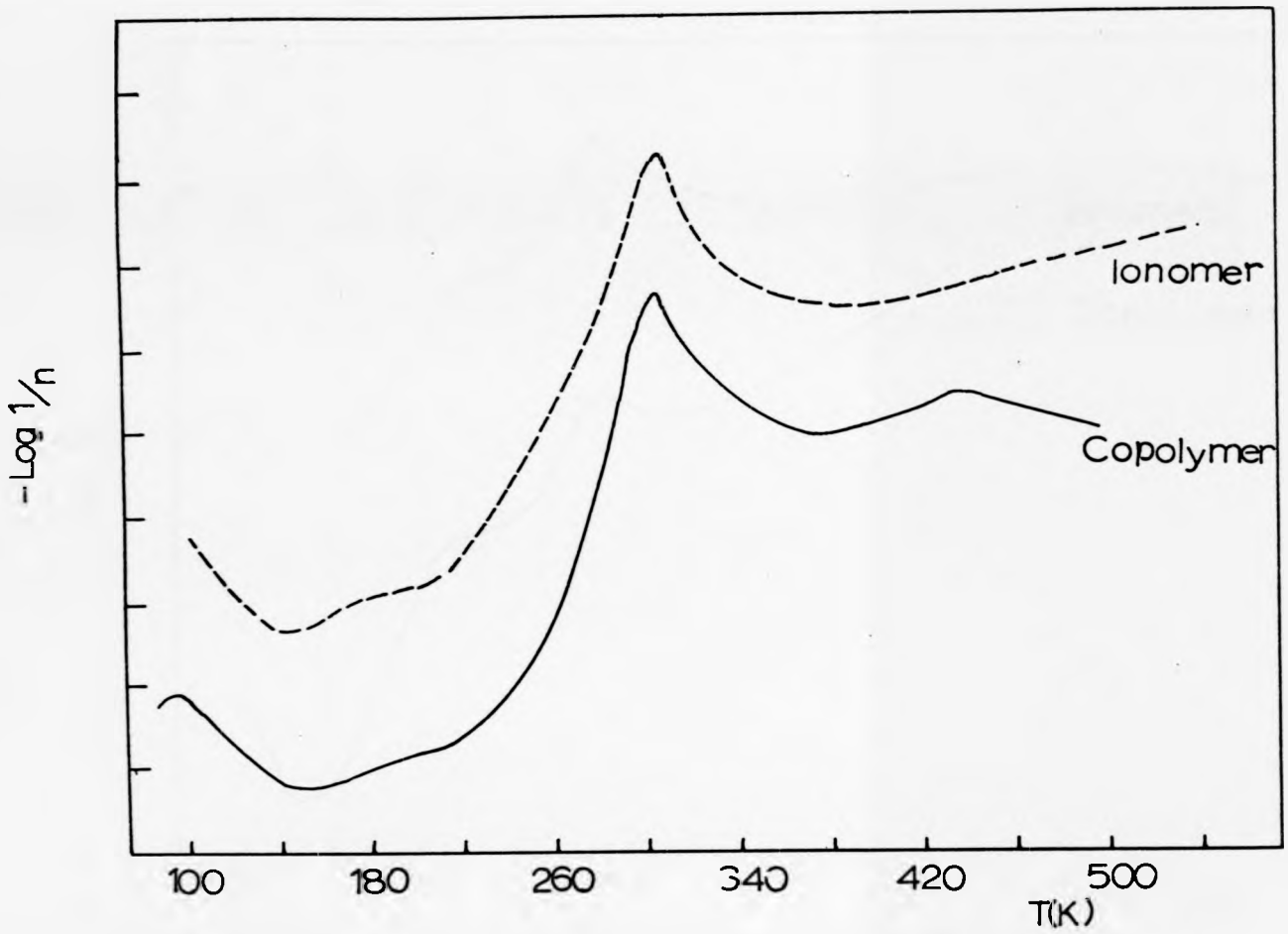

Fig.4.25 TBA thermograms for unionised and ionised poly(MBI + DBI)
9.5 90.5

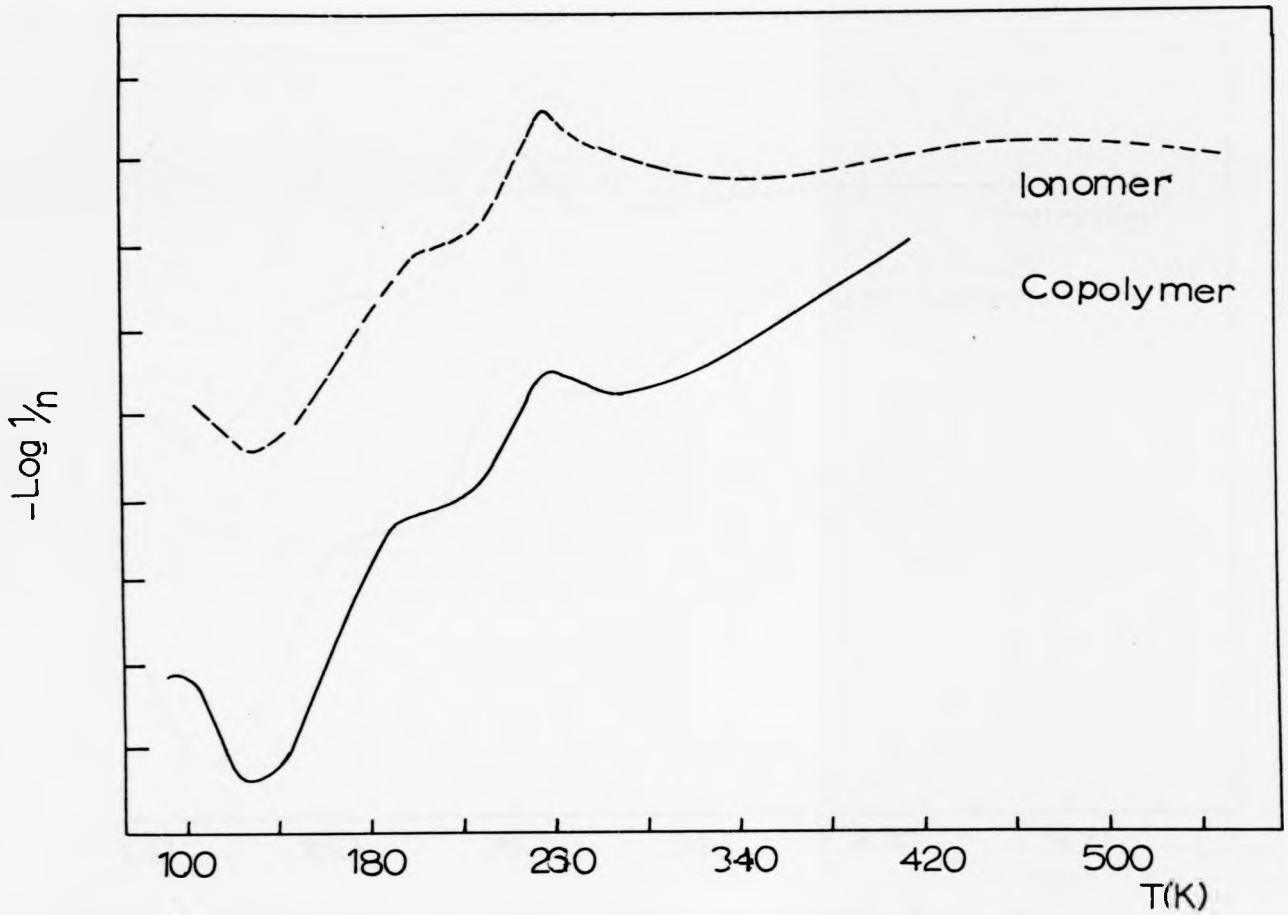

Fig.4.26 TBA thermograms for unionised and ionised poly(MHpI + DHpI)
11 89

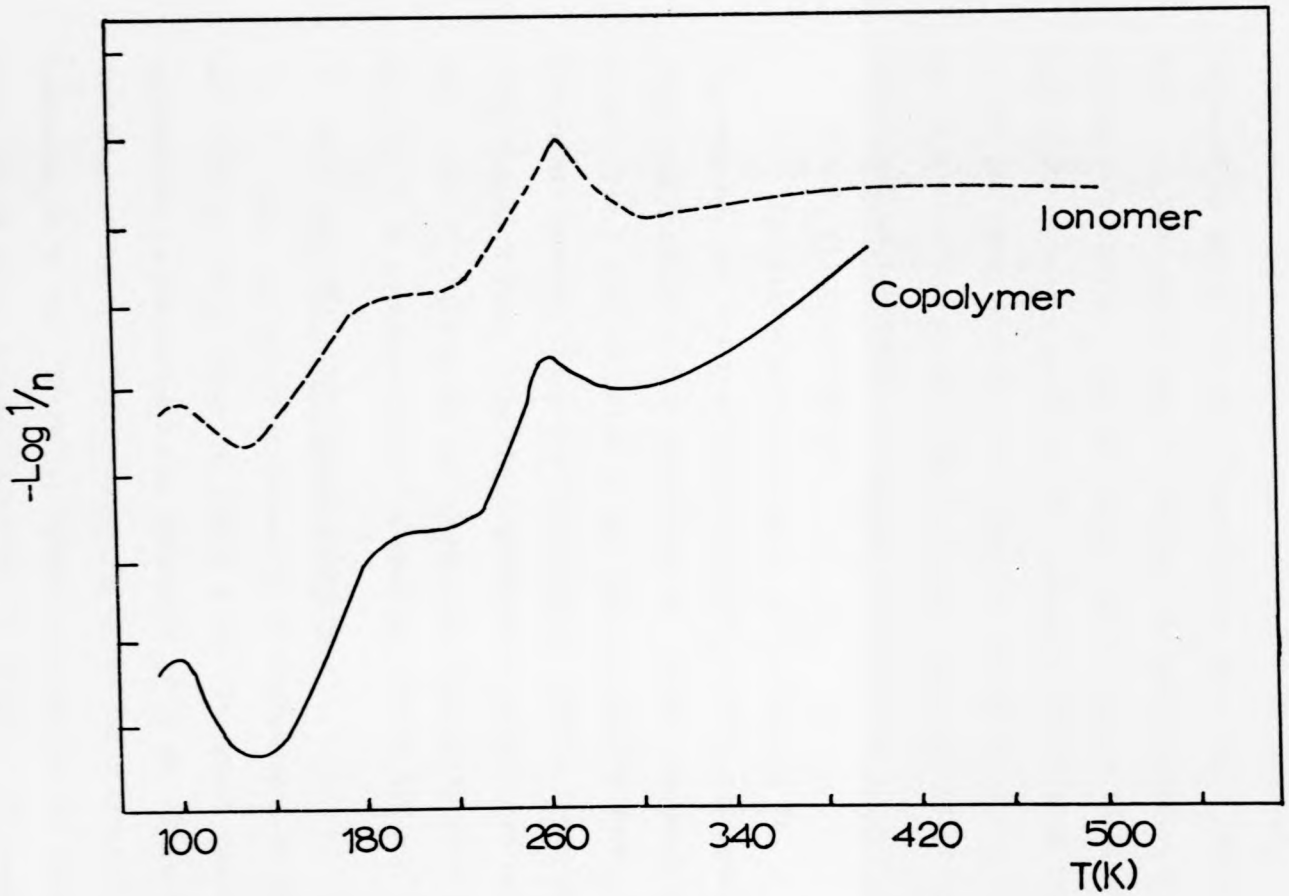

Fig.4.27 TBA thermograms for unionised and ionised poly(MHpI + DHpI)

region, rubbery, rather than viscous liquid, response is being exhibited by the ionomer.

Such behaviour is consistent with the concept of ionic cross-links acting against the onset of unrestricted cooperative motion of the polymer chains above Tg. Apart from this, the TBA thermograms of ionomer and parent copolymer differ very little. All the major features below the glass transition appear unperturbed by ionisation indicating that, in the polymers studied, the formation of any ionic regions has little effect on the glassy state or does not occur to any significant extent.

4.4.2 Viscoelastometry

The viscoelastic response, as a function of temperature, for the two systems mentioned above was measured using the Rheovibron (RV) apparatus at a fixed frequency of 35 Hz. Tan δ and the value of the elastic modulus were determined several times for each sample, using a fresh polymer strip for each run. Only the reproducible results are reported here. The RV thermograms are constructed from 60-80 data points taken at 2-3K intervals and at a heating rate of $\sim$2K min^{-1}.

(a) Poly(MBI + DBI)-based ionomers

For comparison purposes the RV thermogram of PDBI was obtained and is shown in figure 4.28. The glass transition temperature is estimated to be $\sim$308-310K at 35 Hz. This is $\sim$20K higher than that obtained by TBA which has a nominal frequency of $\sim$1 Hz. There is, however, an element of doubt about the Tg value determined by RV. At temperatures greater than Tg, the unsupported polymer strip begins to "draw" rapidly

and prevents accurate tensioning prior to reading tan δ. This is the cause of the rapidly increasing value of tan δ above Tg.

The RV thermograms for two samples of Poly(MBI + DBI) containing, respectively, 5.7 mole % and 9.5 mole % MBI, fully ionised as the sodium salts, are shown in figures 4.29 and 4.30, along with the traces for the unionised parent copolymers. Considering the modulus curve first, it is apparent that ionisation has resulted in only a small increase in the modulus in the glassy region, but in a relatively large increase in the rubbery region. The major effect, in the rubbery region, is consistent with the formation of cross-links having an ionic origin[83]. It is not, however, possible to say anything about the state of aggregation (if any) of the ions from these results.

The tan δ curves for each ionomer show that Tg is little altered (as already indicated by TBA and DSC) but that a relative reduction in damping does occur on ionisation, at about 20K above Tg. The origin of this effect is not immediately obvious.

(b) Poly(MHpI + DHpI)-based ionomers

Tan δ and modulus curves for fully ionised (sodium salt) copolymers of MHpI + DHpI containing 11 mole %, 16 mole % and 20 mole % of the monoester are shown in figures 4.31 to 4.33. Essentially the same behaviour is observed as with the n-butyl ester-based ionomers, i.e. a slight increase in modulus in the glassy region and a much more marked increase

Fig.4.28 RV thermogram for PDBI

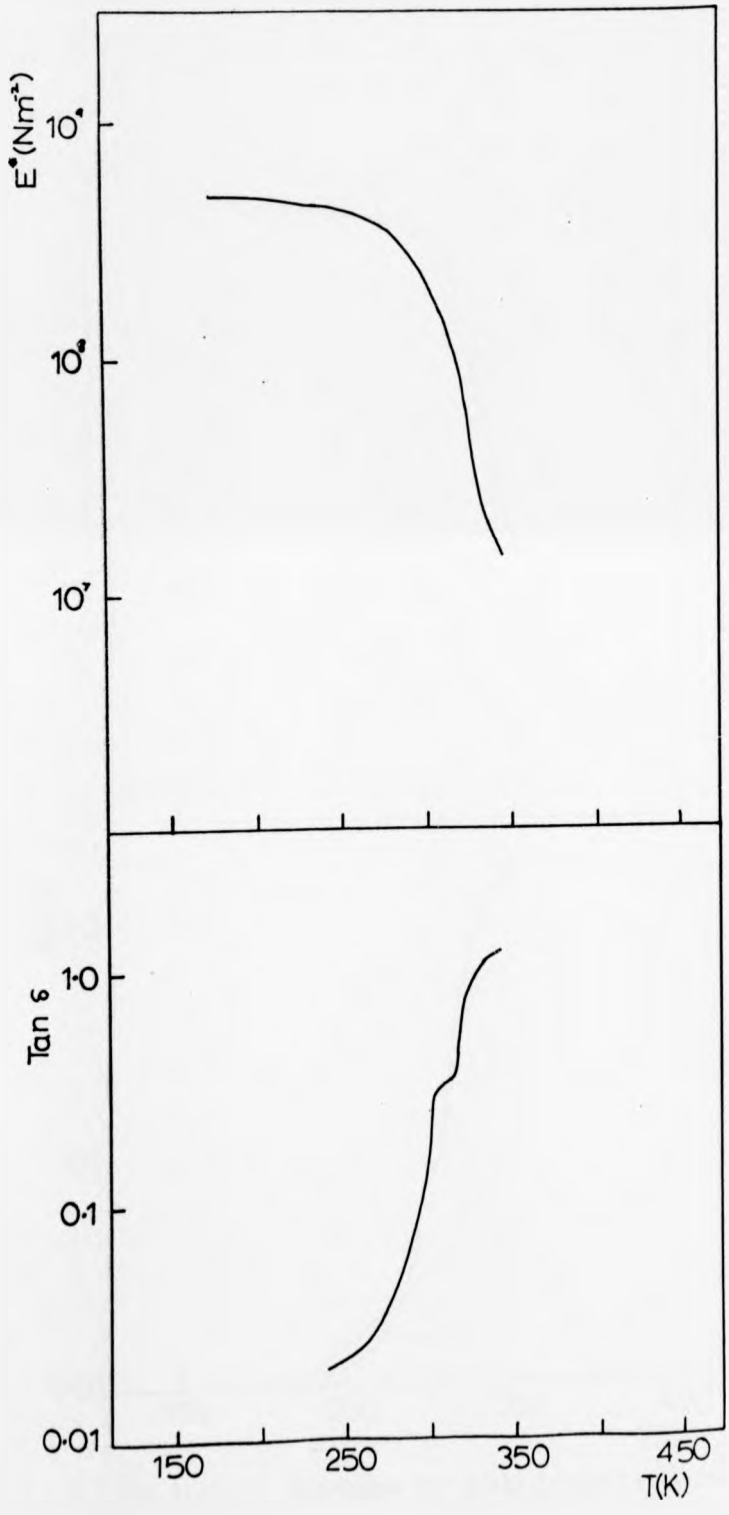

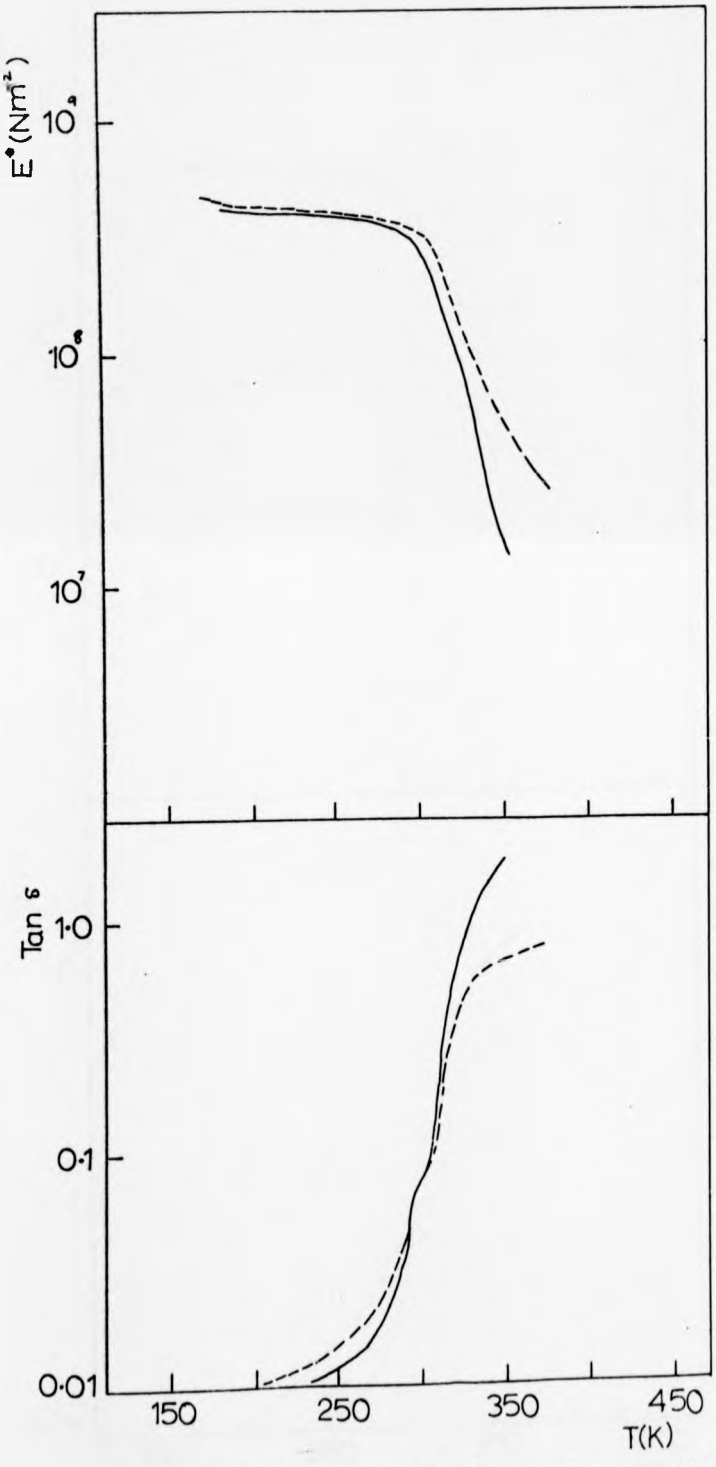

Fig.4.29 RV thermogram for fully ionised poly(MBI + DBI)
5.7 94.3

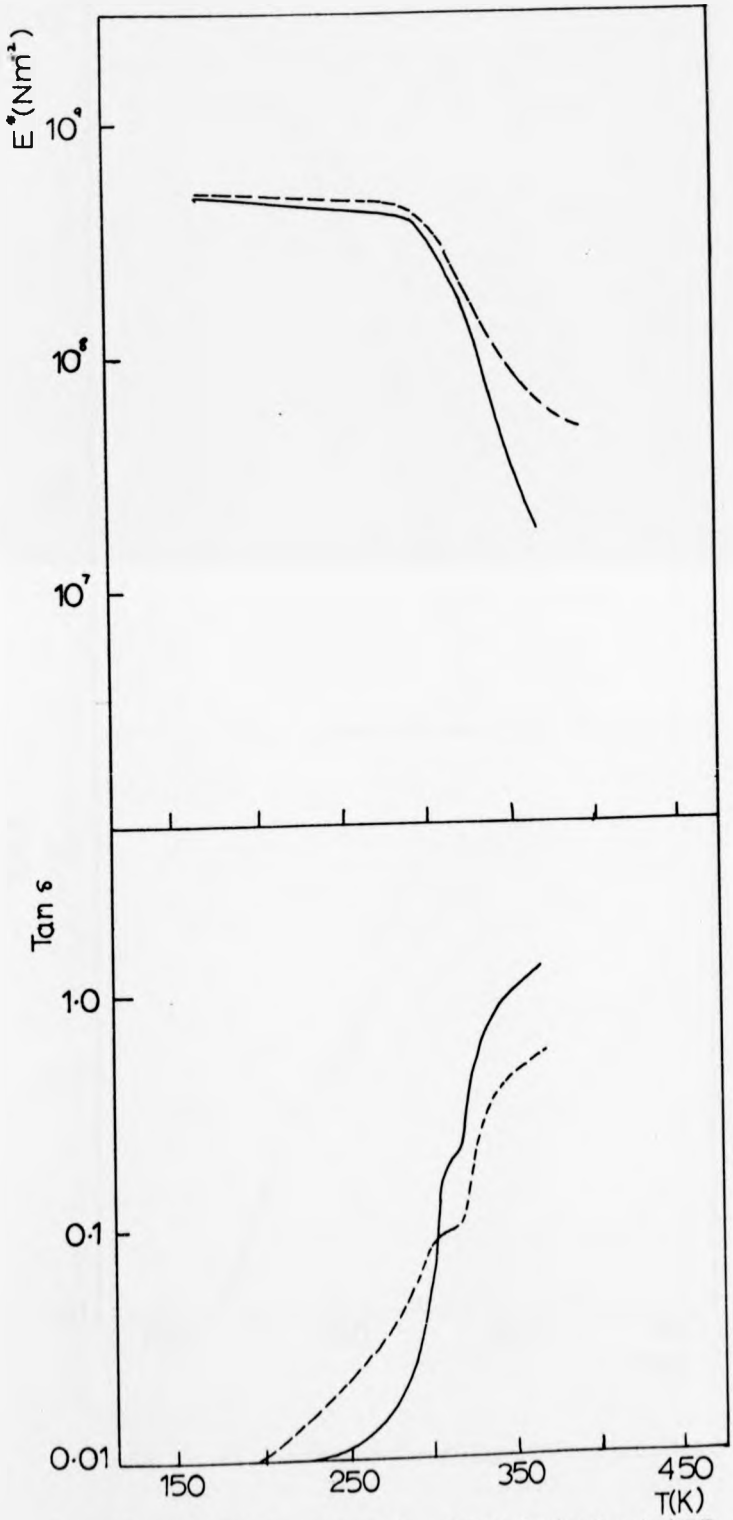

Fig.4.30 RV thermogram for fully ionised poly(MBI + DBI)
9.5 90.5

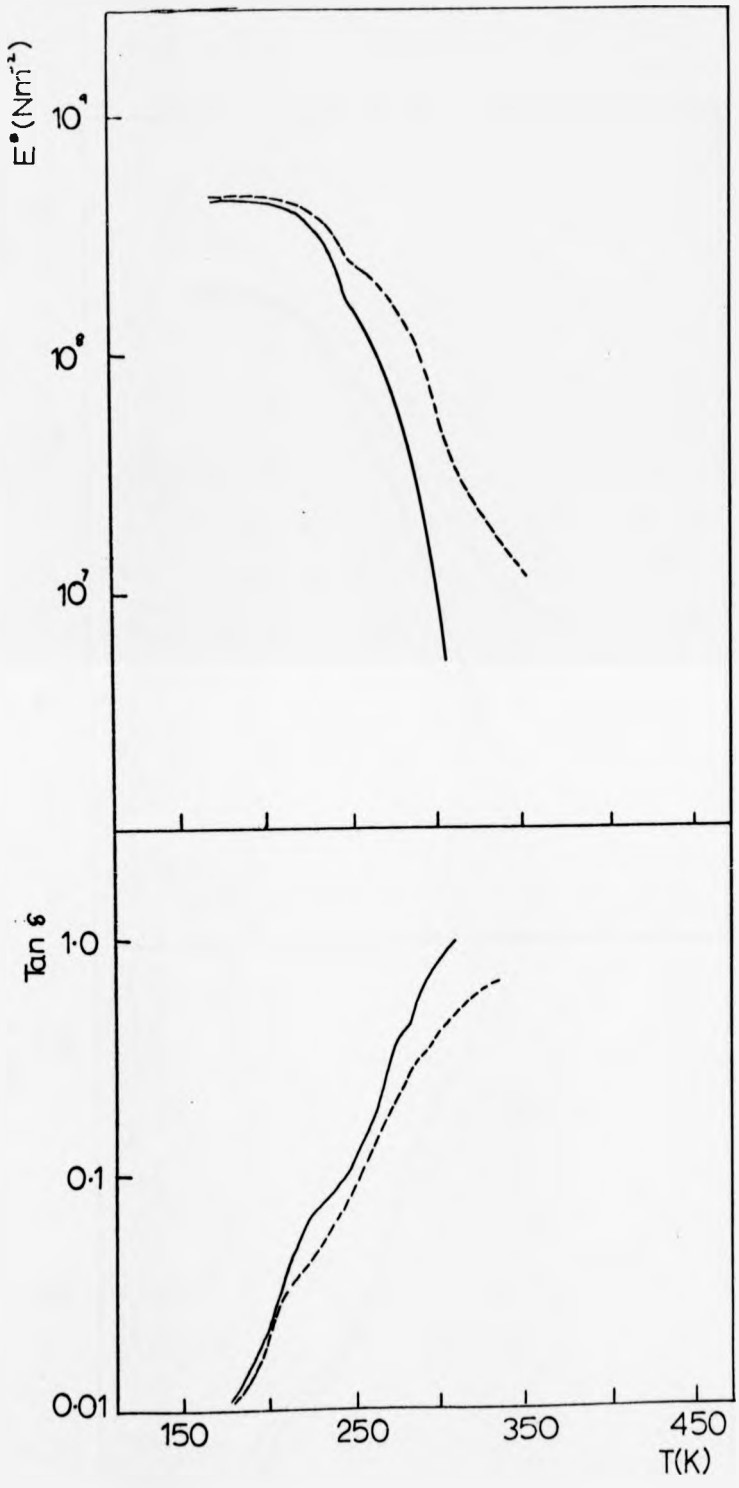

Fig.4.31 RV thermogram for fully ionised poly(MHpI + DHpI)
11 89

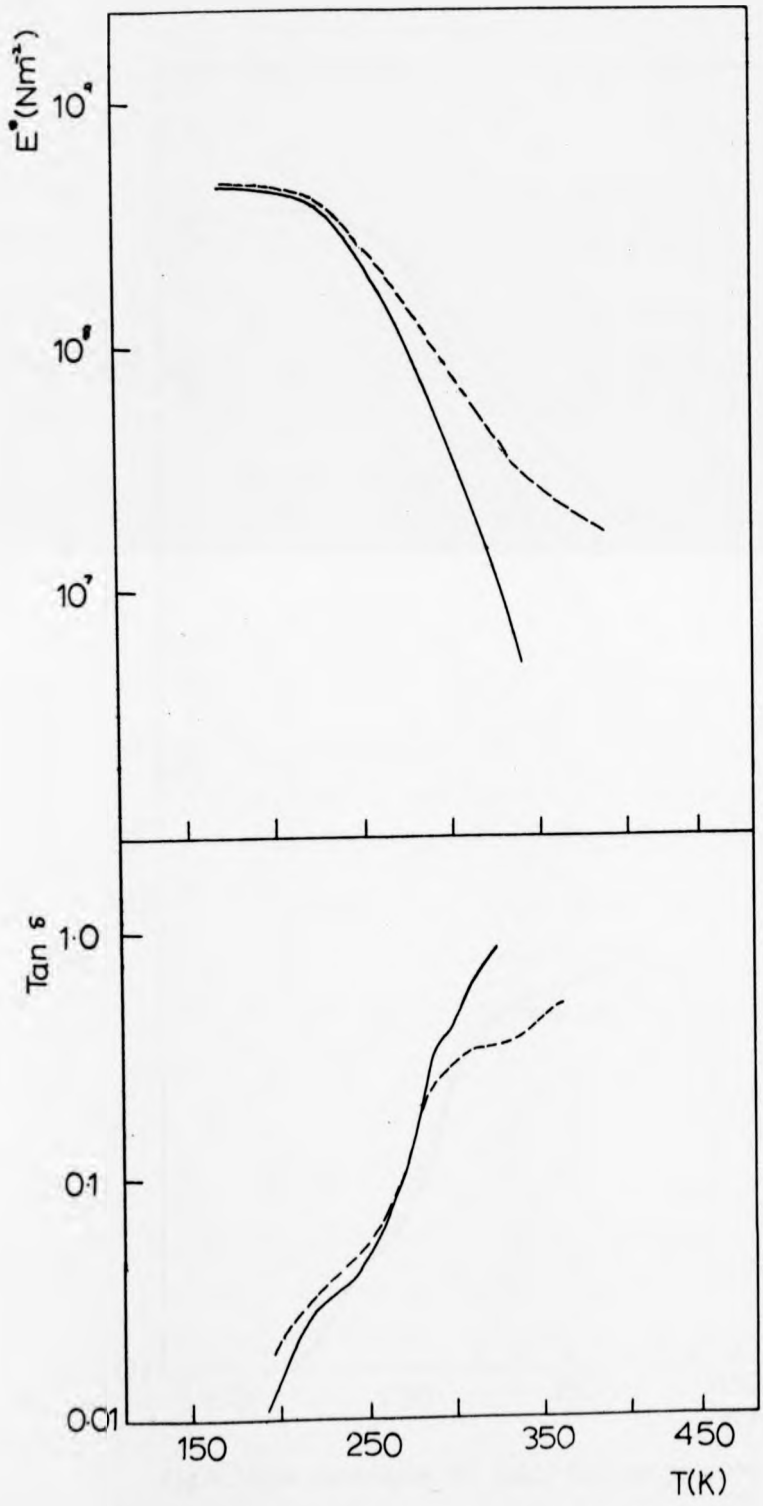

Fig.4.32 RV thermogram for fully ionised poly(MHpI + DHpI)
16 84

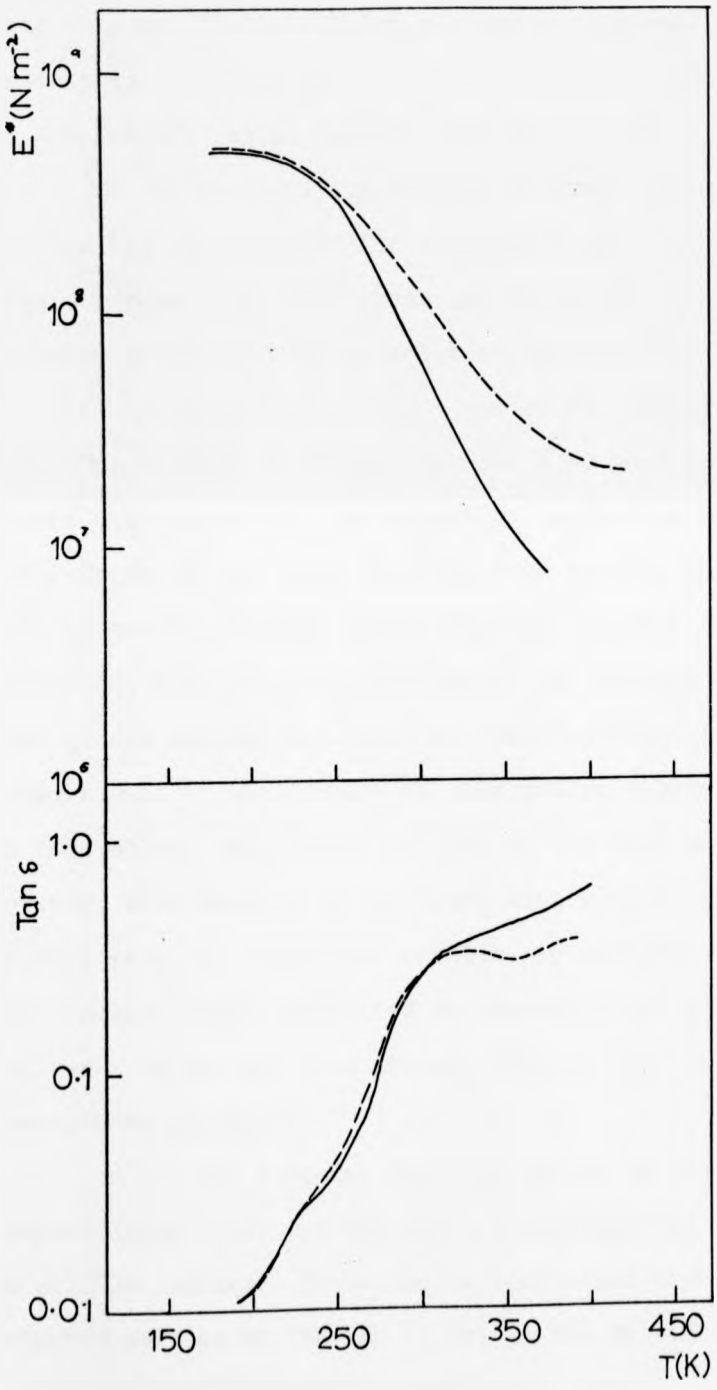

Fig.4.33 RV thermogram for fully ionised poly(MHpI$_{20}$ + DHpI$_{80}$)

in the rubbery region. Indeed, it is only with the ionomers that an identifiable rubbery plateau is apparent. As the percentage incorporation of ions is increased this stabilisation of the rubbery region becomes more pronounced.

The physical appearances of these ionomers at room temperature are worth noting. Compared with the viscous liquid parent copolymers these are the tough, non-tacky, leathery materials with an enhanced optical clarity.

The modules and tan δ curves for ionomers based on Poly(MHpI + DHpI) containing 30 mole % of MHpI are shown in figure 4.34 and 4.35. The extent of ionisation of the acid groups present was varied to give five samples whose sodium salt contents are shown on the figure. As with the previously discussed, fully ionised copolymers, the modulus increases in both glassy and rubbery regions. This increase appears to be proportional to the content of salt groups and is quite dramatic in the rubbery region when all 30% of the MHpI units are ionised. However, when samples of copolymer with greater than 30 mole % of MHpI were fully ionised, brittle, intractible products were formed. These exhibited no thermoplastic behaviour and could not be moulded into strips, even at 400K and ∿70 atmospheres pressure.

The tan δ curves for this series of ionomers are comparatively clear and two major transitions can be observed in all the samples. These can be identified with the transitions detected earlier by TBA (at ∿1 Hz) in the Poly(MHpI + DHpI) series; the lower being assigned to a glass transition of the side chain regions, and the upper to the onset of cooperative

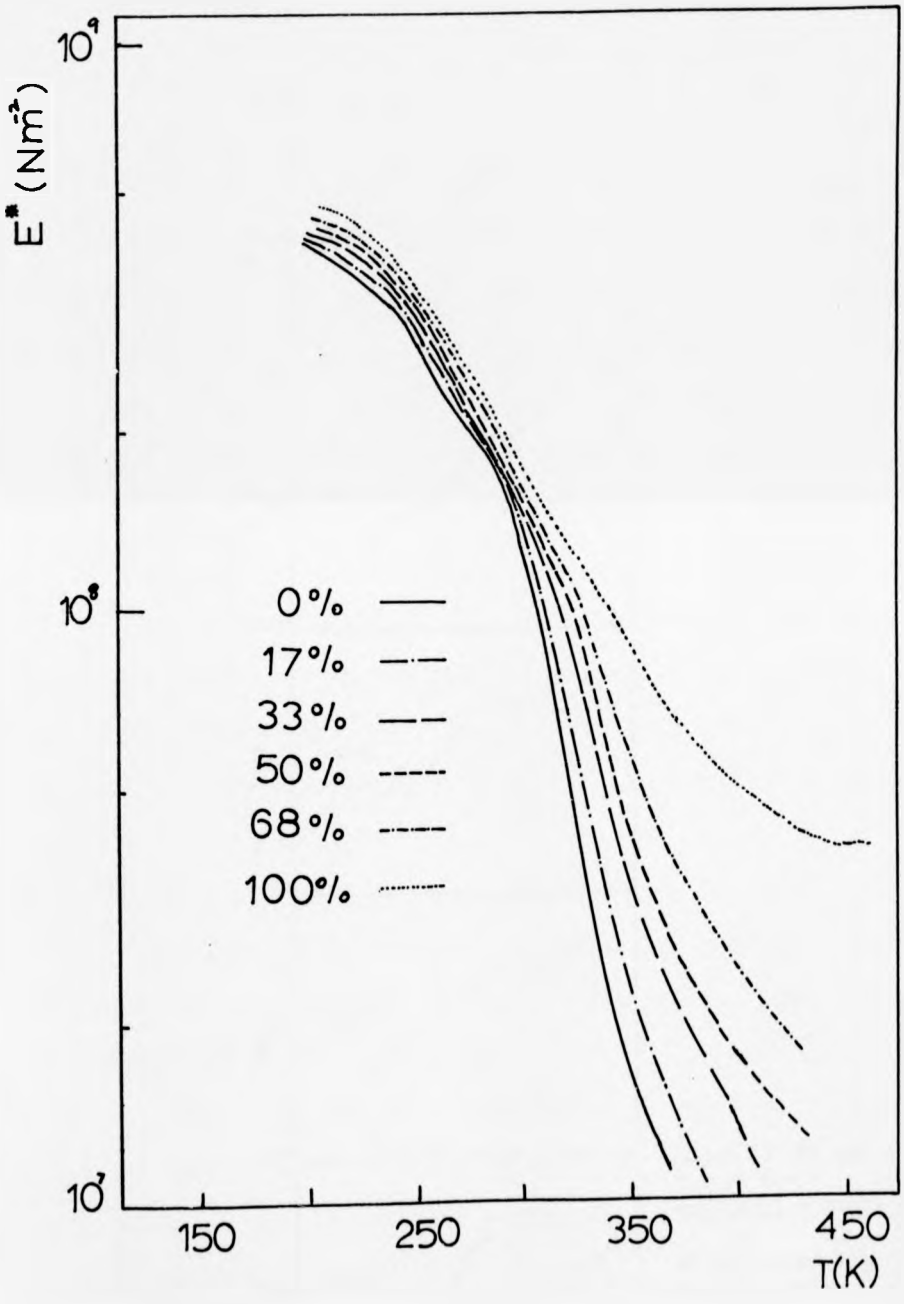

Fig.4.34 RV modulus curves for poly(MHpI$_{30}$ + DHpI$_{70}$) at indicated %age neutralisation

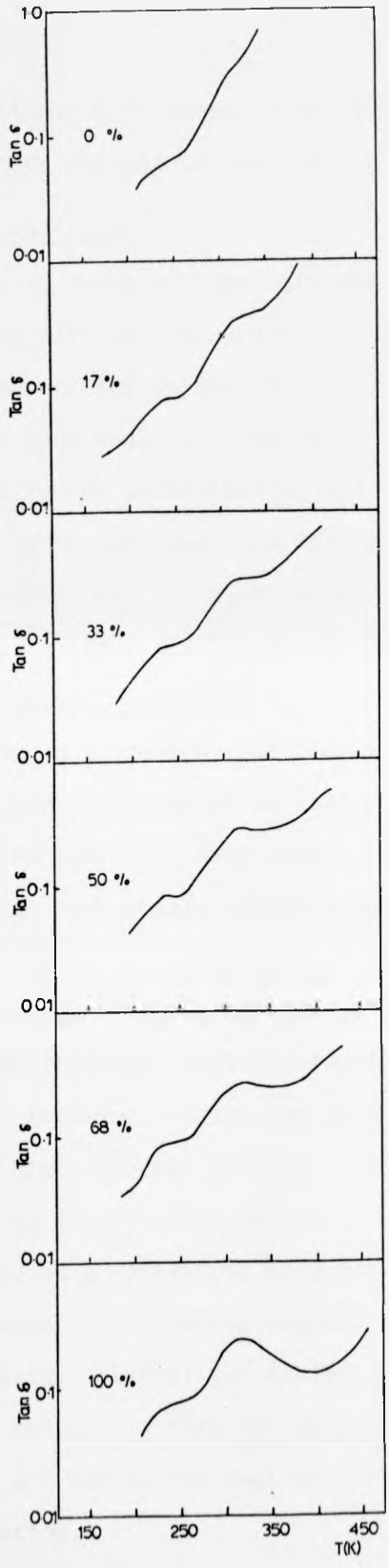

Fig.4.35 RV tan δ curves for poly(MHpI + DHpI) 30 70 at indicated %age neutralisation

main chain motion. Both change very little in temperature as the salt group content changes from zero to 30 mole %.

4.4.3 X-ray Studies

Limited x-ray studies were carried out on several ionomer samples with the cooperation of the Departments of Chemistry at Manchester University and Queen's University, Belfast. Both wide angle and low angle diffraction studies were made, but proved inconclusive, and the results are not reported here. The only negative results that may be relevant were the absence of any low angle peaks which are proposed to be characteristic of ionic cluster formation[87].

4.4.4 Electron microscopy

Electron microscopy was carried out on a variety of copolymers and their sodium or caesium salts. A number of micrographs were taken for each sample, only those having the minimum electron beam damage and showing reproducible structures are presented here.

In every case, the electron micrograph reveals the presence of two different regions, found in both unionised copolymers and ionomers. These are dark areas, corresponding to relatively high electron density, and light areas, corresponding to low electron density. It has been suggested[88,89] that carboxylic acid containing polymers, polymers which consist of components differing significantly in polarity, and ion-containing polymers all exhibit more than one phase. It would seem reasonable that the dark and light areas found in this study are due to two regions differing markedly in their constitution.

Plates 4.1 to 4.4 show the electron micrographs of PDBI, Poly(MBI + DBI) with 9.5 mole % MBI content, and the fully ionised sodium and caesium salts of the copolymer. These four micrographs show a gradation in appearance; PDBI exhibits a very diffuse pattern of light and dark while the caesium salt of poly(MBI + DBI) has a very sharply defined structure. The copolymer and its sodium salt are intermediate in appearance, the salt being slightly better defined.

Plates 4.5 and 4.6 show the electron micrographs of fully ionised (caesium salts) of poly(MBI + DBI) samples containing 30 mole % and 55 mole % MBI respectively. Here the formation of two regions is very marked and is accompanied by what appears to be a "lining up" of the dark areas in the 30 mole % ionomer, and distinct aggregation of these areas at 55 mole %.

The micrographs of sodium salts ionomers based on poly(MHpI + DHpI) containing 30 mole % MHpI are shown in plates 4.7 to 4.10. Although less obvious than the n-butyl-based ionomers, these show a similar gradation in appearance. The parent, unionised, copolymer is diffuse while increasing ionisation leads to a sharping and enhanced definition of the light and dark areas. However, even when all the carboxylic acid groups are ionised, there is no evidence of the lining up effect observed with the previous series of ionomers at high ion concentration.

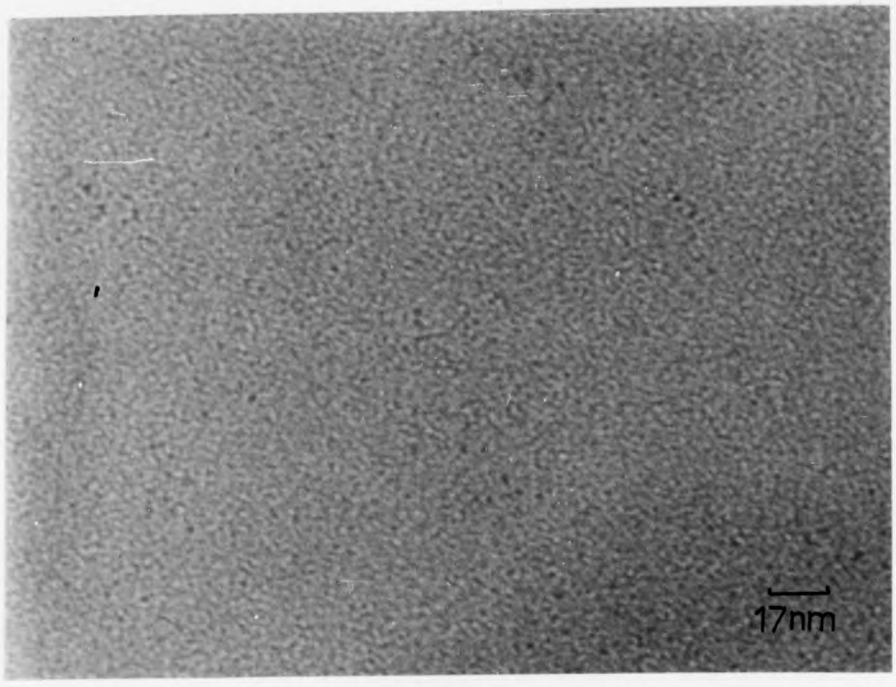

Plate I E.M. of PDBI

Plate II E.M. of Poly(MBI + DBI)
9.5 90.5

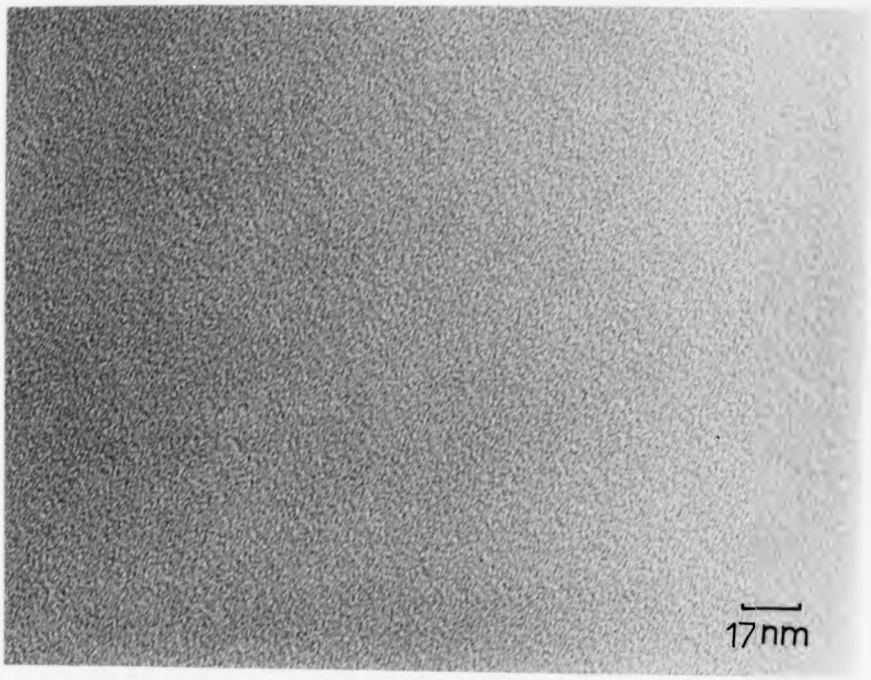

Plate III E.M. of Na salt of Poly(MBI + DBI)
9.5 90.5

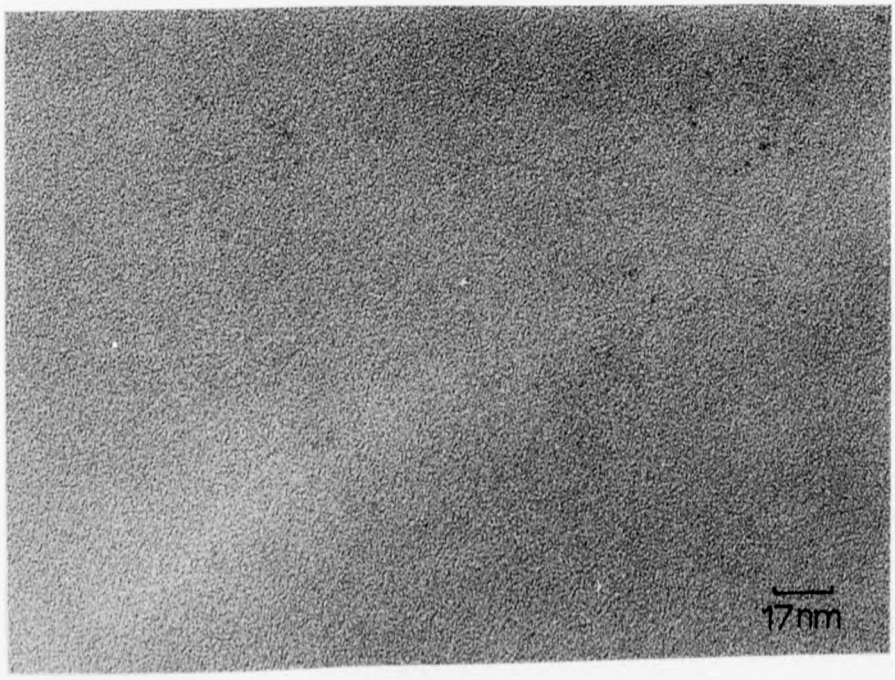

Plate IV E.M. of Cs salt of Poly(MBI + DBI)
9.5 90.5

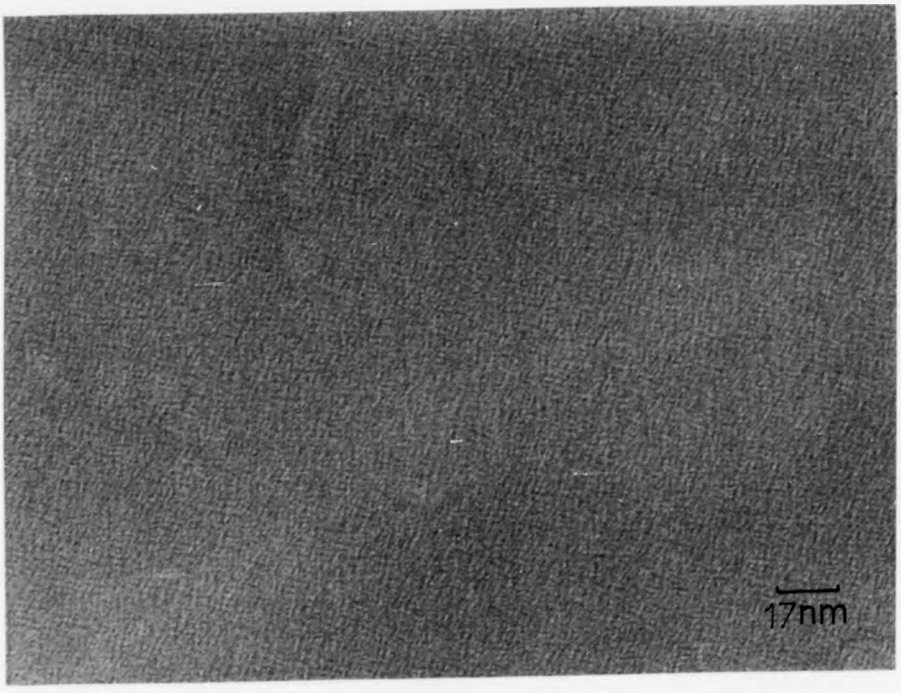

Plate V E.M. of Cs salt of Poly(MBI$_{30}$ + DBI$_{70}$)

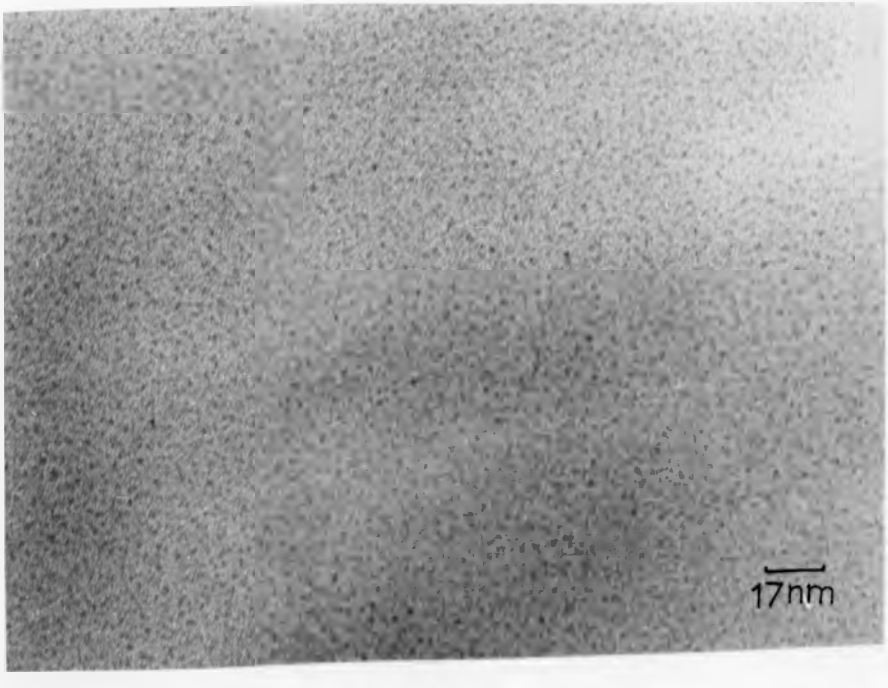

Plate VI E.M. of Cs salt of Poly(MBI$_{55}$ + DBI$_{45}$)

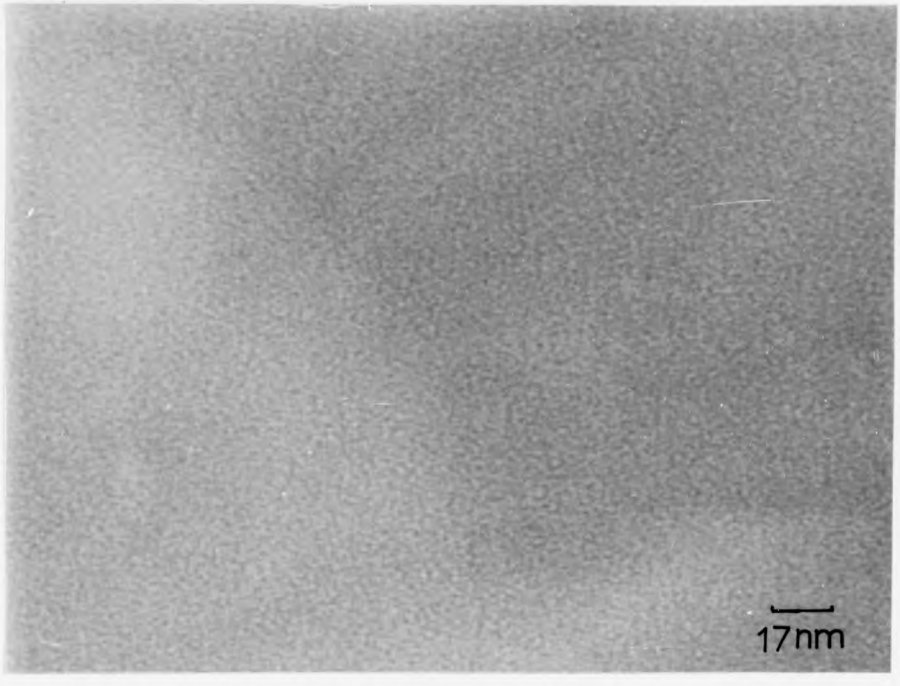

Plate VII E.M. of Poly(MHpI + DHpI)
30 70

Plate VIII E.M. of Na salt of Poly(MHpI + DHpI)
30 70
16% neutralised

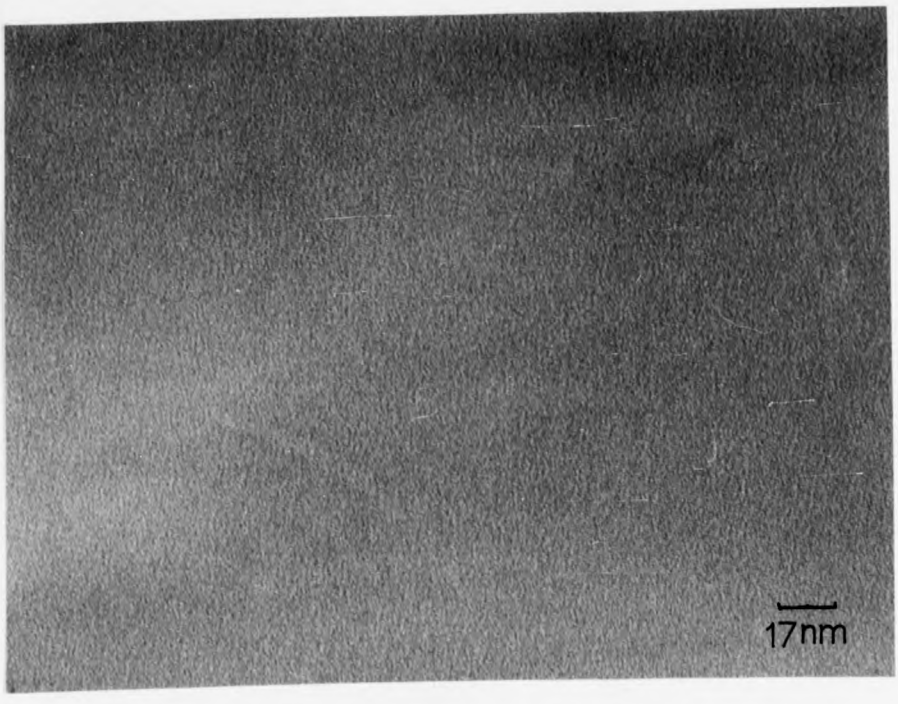

Plate IX E.M. of Na salt of Poly(MHpI + DHpI)
30 70
50% neutralised

Plate X E.M. of Na salt of Poly(MHpI + DHpI)
30 70
100% neutralised

4.4.5 Morphological Models of Ionomers

One of the important features of ionic polymers is the state of aggregation of the ionic groups. The question whether these are distributed at random, or aggregated into domains has attracted both experimental and theoretical work[45,79,90-92]. To date, this has resulted in three distinct morphological models for an ionomer, which are described in the following paragraphs and are illustrated diagrammatically in figure 4.36. It should be noted that all the models are based on experimental work involving crystallisable copolymers and hence describe three phase systems, i.e., amorphous, crystalline and ionic phases.

(a) The "homogeneous" model.

It is readily shown that the simplest form of aggregation, the ion pair, has a high probability of forming in media of low dielectric constant[45]. The homogeneous model of an ionomer consists of an amorphous and a crystalline phase. Acid groups and their ion pair metal salts are assumed to be randomly distributed as dimers in the amorphous phase. Evidence[86,93,94] supporting this model comes from N.M.R., X-ray studies and studies of glass transition shift with composition.

(b) The "cluster" model.

This again consists of a crystalline and an amorphous phase, but postulates the existence of large ionic clusters of about 10 nm in diameter embedded in the latter[87]. The evidence which has been interpreted as supporting this model has been obtained[90,95-98] from wide and low-angle x-ray studies, electron microscopy and mechanical relaxation studies.

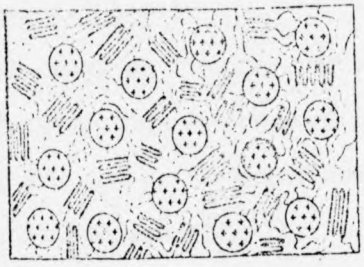

Model proposed by Longworth and Vaughan[87]

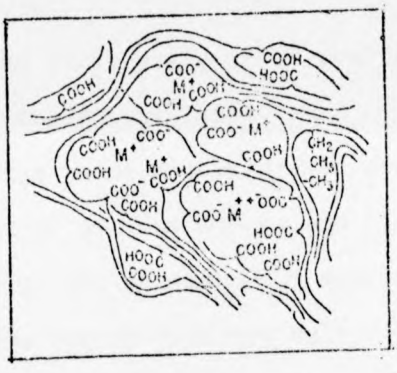

Model proposed by Bonotto and Bonner[81]

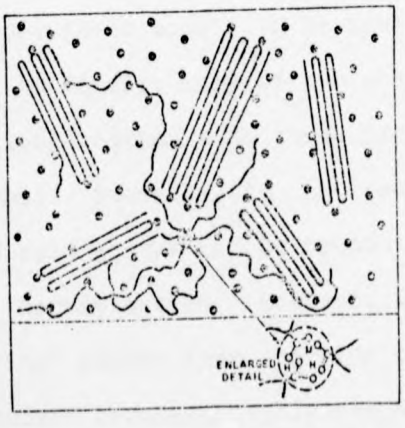

Model proposed by Marx, Caulfield and Copper[92]

Fig.4.36

(c) The "aggregate" model.

This model draws on the two previously mentioned in that aggregate distribution is assumed to be random, but that the aggregates are orders of magnitude smaller (0.5-1.0 nm) than that proposed for the "cluster" model. The aggregates, which contain both protons and metal ions, are distributed in the amorphous phase and can consist of from dimers to septemers, depending on the composition of the ionomer. The proposers of this model[92] use a detailed analysis of wide and small angle x-ray scattering and DSC studies to support their postulates.

Each of the three models are in accord on two points (i) aggregation of ions occurs and (ii) these aggregates reside exclusively within an amorphous matrix and are excluded from any crystalline region that may exist. Ionomers based on itaconic acid differ substantially from those derived from the polyethylene and polybutadiene copolymer systems on which these models are based. Firstly, crystallinity is absent and, for any of the above three models to be applicable, they must first be modified to consist only of two phases (ionic regions and amorphous regions) rather than three (ionic, amorphous and crystalline regions). Secondly, in the itaconate ionomers, up to 30% ionised acid groups can be present before they cease to become useful thermoplastics. However, if due allowance is made for a "dilution" effect from the side chains, a 30 mole % n-heptyl-based ionomer becomes roughly comparable with the commercially interesting 6% acrylic acid polyethylene-based ionomers.

4.4.6 General Discussion

This section of work was undertaken in an attempt to improve the properties of mechanically weak copolymers above Tg by neutralising them with mono- and divalent ions. Several attempts were made at neutralisation with the divalent calcium cation, but measurements of the degree of ionisation by IR techniques already reported[99] proved impossible due to overlapping of carbonyl and and carboxyl absorptions. The discussion is therefore restricted to the sodium and caesium salts of the poly(MBI + DBI) and poly(MHpI + DHpI) systems already described.

As noted in Chapter 2, segmental mobility depends to some extent on the nature of the interchain forces, which, in ionomers, will be influenced by the degree of ionisation. The experimental results of section 4.4.1 confirm these observations and show that in the systems studied here, as with others already reported, the electrostatic forces between the bound ions in the polymer chain and their counter ions reduce the segmental mobility and increase the value of Tg.

In an ionomer system it should, in principle, be possible to correlate the increase in the value of Tg with the degree of ionisation, i.e. to consider the ionomer as a conventional lightly cross-linked polymer[45,100]. It is not, however, possible to discuss such correlations here due to lack of data in the poly(MBI + DBI) systems, while the "double transition" nature of the poly(MHpI + DHpI) system makes it unsuitable for such considerations. In this latter system, however, one point of similarity with covalent cross-linking

is obvious (Figure 4.35) the tan δ peak for the main chain relaxation becomes significantly broader with increasing ionisation.

The main object, to increase the mechanical stability of the copolymers above Tg, has been realised. The elastic modulus in the rubbery region is stabilised by ionisation, the stability is directly related to the extent of ionisation, which can be usefully increased to 30 mole % in poly(MHpI + DHpI) and at least 9.5 mole % in poly(MBI + DBI). The reason for such enhanced stability must lie with an ionic cross-linking effect which is present even up to ∿420K.

The interpretation of the electromicrographs presented here is extremely difficult, especially without extensive additional evidence from x-ray studies. The dark areas on any micrograph are due, probably, to ionic group. Enhancement of definition when caesium ions are used is due to the higher electron density associated with this ion. No disruption of the random distribution of areas of high and low electron density is observed until the ion concentration reaches 30 mole % in the poly(MBI + DBI) system. At this point the ionic groups appear to commence aggregation, and at 55 mole %, large aggregated domains are clearly seen. The average dimensions of these are ∿2 nm in diameter. Unfortunately comparable caesium salt ionomers based on poly(MHpI + DHpI) were not studied due to lack of time. However, from the limited data, no evidence of aggregation is found up to 30 mole % content of MHpI in this system.

From the evidence presented here, there is no reason to suppose that there is ionic cluster formation in poly(n-alkyl itaconates)-based ionomers at low ion concentration. The most suitable model would seem to be the "aggregate" description. This would be in keeping with both the electron micrographs and the proportional change in mechanical modules with ionisation.

4.5 THERMAL DEGRADATION STUDIES

4.5.1 Interpretation of TVA traces

TVA thermograms are the recorded outputs of Pirani gauges mounted after cold traps of various temperatures through which the products of degradation may or may not pass, depending on their volatility (see figure 3.8 for diagram). If the response of a gauge following a trap at 273K is taken as the basis for comparison, then the behaviour of gauges in lines with lower trap temperatures has been found to take three forms[60].

(a) The trace is coincident with that of the 273K trap, i.e. the substance is not trapped out at all in this trap.

(b) The trace follows the baseline, i.e. the substance is fully condensed in this trap - and remains there.

(c) The trace rises to a plateau and remains there for some time. This is termed a "limiting rate effect" and is due to the substance being trapped, but also being volatile enough to distil slowly from the trap.

Products of degradation that are sufficiently involatile at the temperature of the water jacket at the

furnace exit will condense there, giving rise to the so-called[60] "cold ring fraction".

In the subsequent description, the TVA trace from a gauge following a 273K trap is called the "273K line", that following a 228K trap is called the "228K line" etc. The trap temperatures used in this work were 273K, 228K, 198K, 173K and 77K. The cold ring temperature was 285K.

4.5.2 Poly(di-n-alkyl itaconates)

Although the poly(di-n-alkyl itaconates) are unique, in that they possess two ester side chains per repeat unit, only a very limited study of their thermal stability has been reported[24]. The selected polymers, PDMI, PDBI, PDHpI and PDDI, were examined using TVA and TGA to assess the overall degradation pattern and the effect of varying side chain length.

PMMA. A useful starting point for a discussion of the thermal degradation of poly(di-n-alkyl itaconates) is the well-established polyacrylate system[60,101,102]. For that reason the TVA and TGA responses of a sample of atactic PMMA were obtained, using the same techniques and apparatus as were applied to the poly(n-alkyl itaconates). These are shown in figures 4.37 and 4.38, and indicate the polymer to be thermally stable up to ∿ 570K, after which weight loss commences and is accompanied by the evolution of volatile degradation products. The TVA thermogram shows two peaks for the 273K, 228K and 198K lines, both of these have been assigned to evolution of monomer, which is essentially the only degradation product. The 198K line, also due to monomer, exhibits a limiting rate effect. TVA response below ∿ 570K is simply due to absorbed solvents and water.

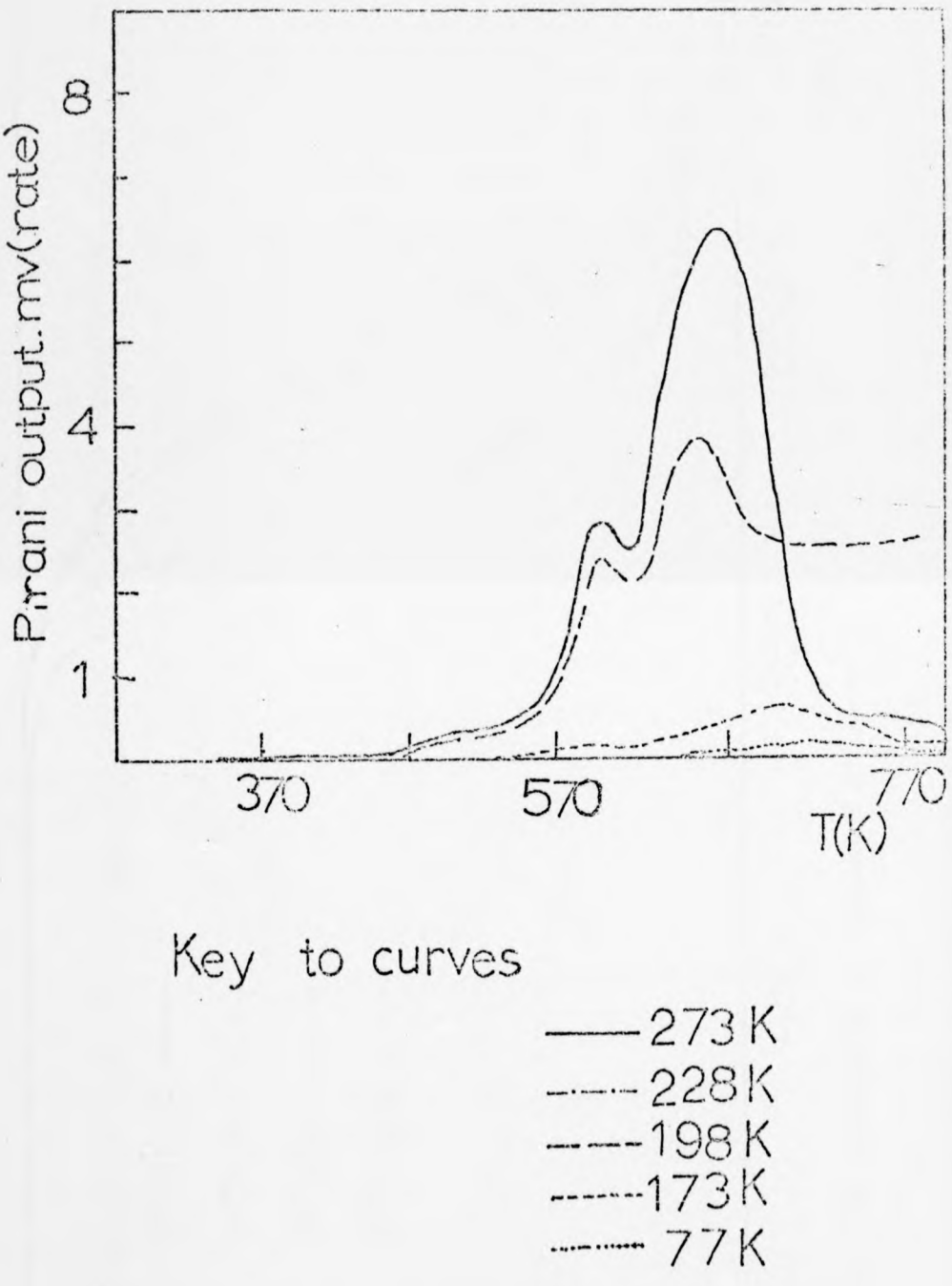

Fig.4.37 TVA thermogram for PMMA

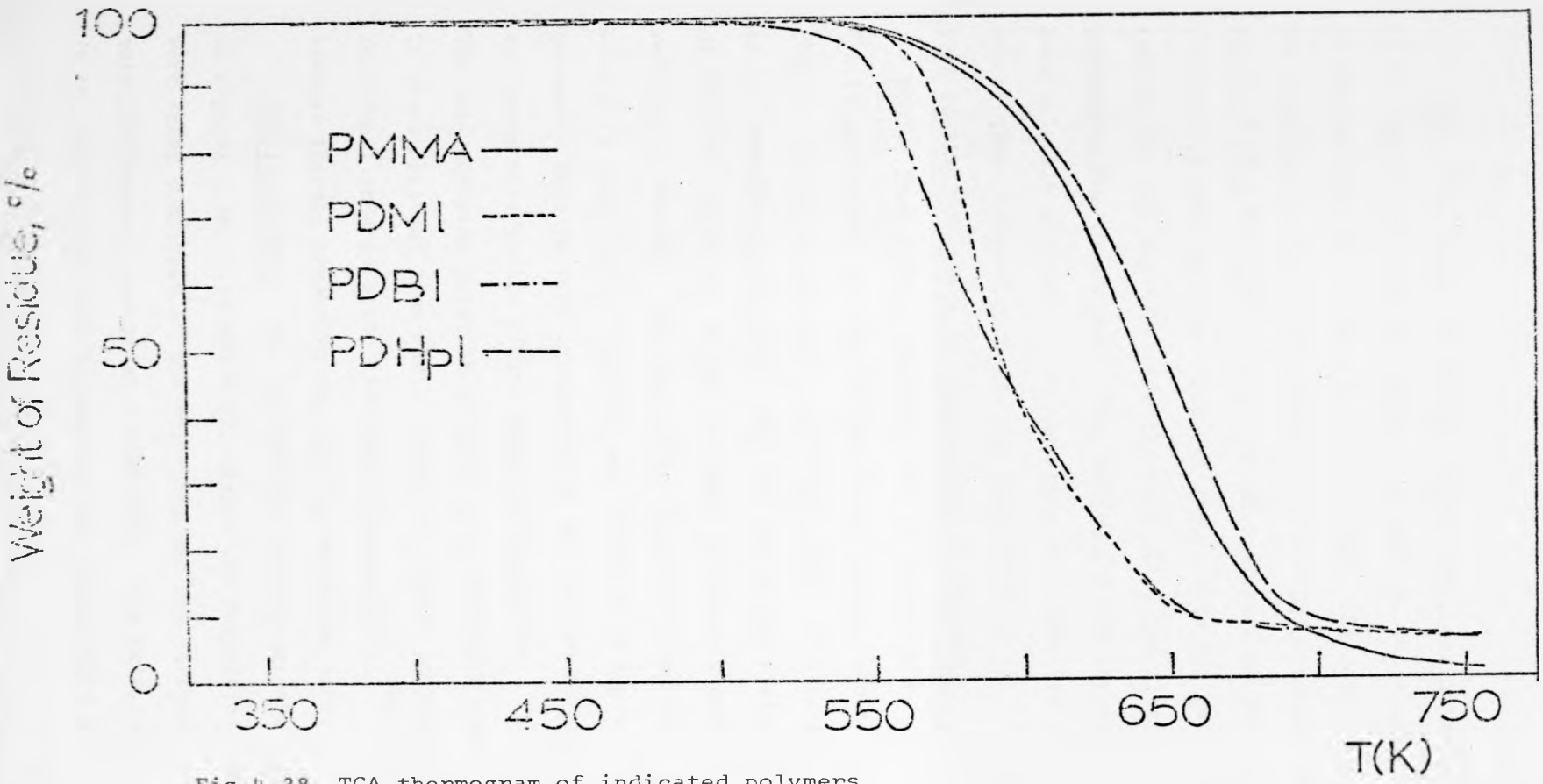

Fig.4.38 TGA thermogram of indicated polymers

PDMI. The onset of thermal degradation, as indicated by the TGA trace shown in figure 4.38 and the TVA trace shown in figure 4.39, is ∿ 550K, similar to PMMA. The majority of the volatile products from degradation of PDMI condensed in the cold ring fraction. These, on IR analysis, proved to be essentially 100% monomer. The TVA traces show two peaks (maxima at 583K and 630K) for the 273K line, the first being presumably due to monomer. The remaining lines are due to much more volatile products since they remain uncondensed at 77K and one of these, carbon dioxide, was identified by IR. The second peak of the 273K trace may also be due to monomer.

PDBI. The onset of degradation, as indicated by the TVA (figure 4.40) and TGA (figure 4.38) traces, shows that PDBI is significantly less stable than PDMI. The reason for this is not immediately obvious. The TVA traces are similar to those of PDMI but the first of the two peaks is greatly reduced in relative intensity. The reason for this was found when the cold ring fraction was analysed and found to be almost 100% monomer. This is very involatile at the cold ring temperature and leads only to low Pirani response thereafter. The second TVA peak contains volatile products of a different composition to those obtained from PDMI. Since the higher poly(n-alkyl acrylates) undergo ester side chain fragmentation[60,103], a similar thermal breakdown may also be occurring here.

PDHpI and PDDI. The TVA and TGA thermograms are shown in figures 4.38, 4.41 and 4.42. Again the respective monomers were found condensed in the cold ring and now virtually all the volatile products appear at ∿ 650K only. The relative increase in the second peak with increasing side chain would seem to

Fig.4.39 TVA thermogram for PDMI

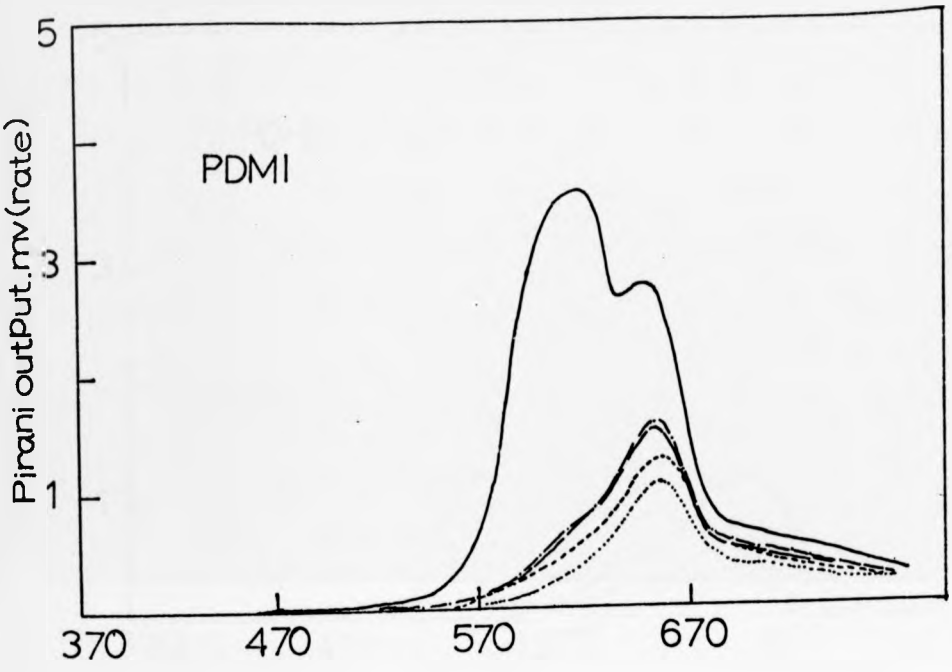

Fig.4.40 TVA thermogram for PDBI

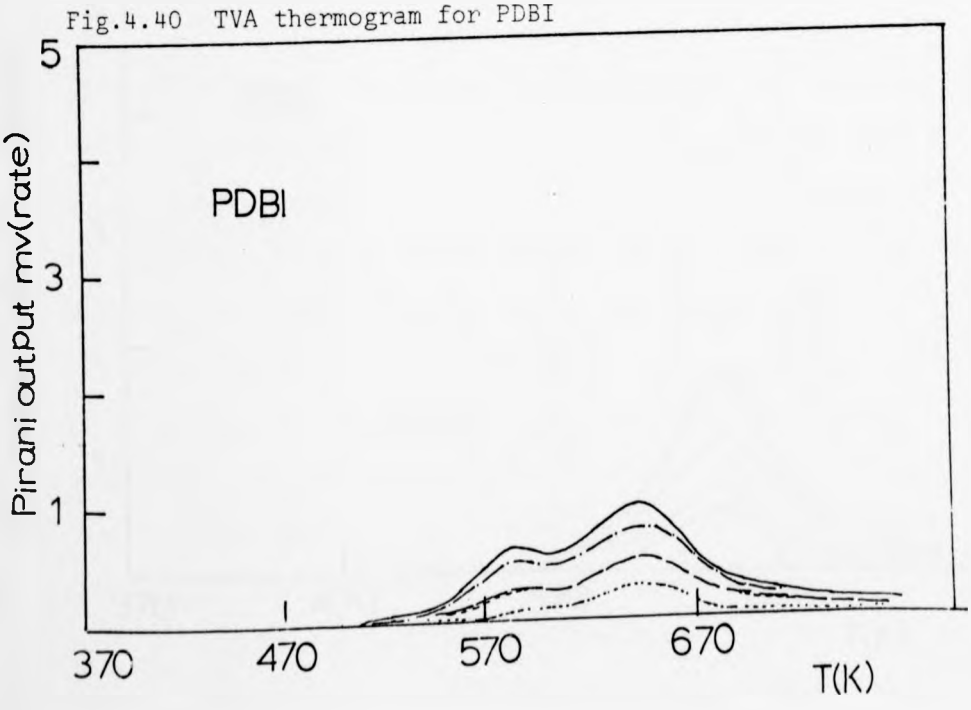

Fig.4.41 TVA thermogram for PDHpI

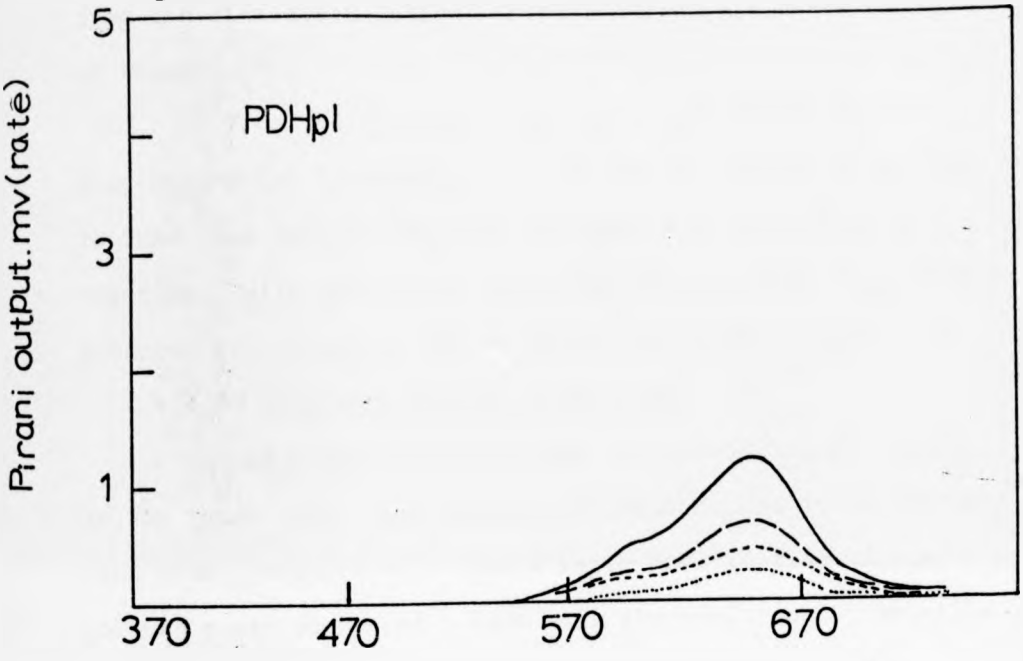

Fig.4.42 TVA thermogram for PDDI

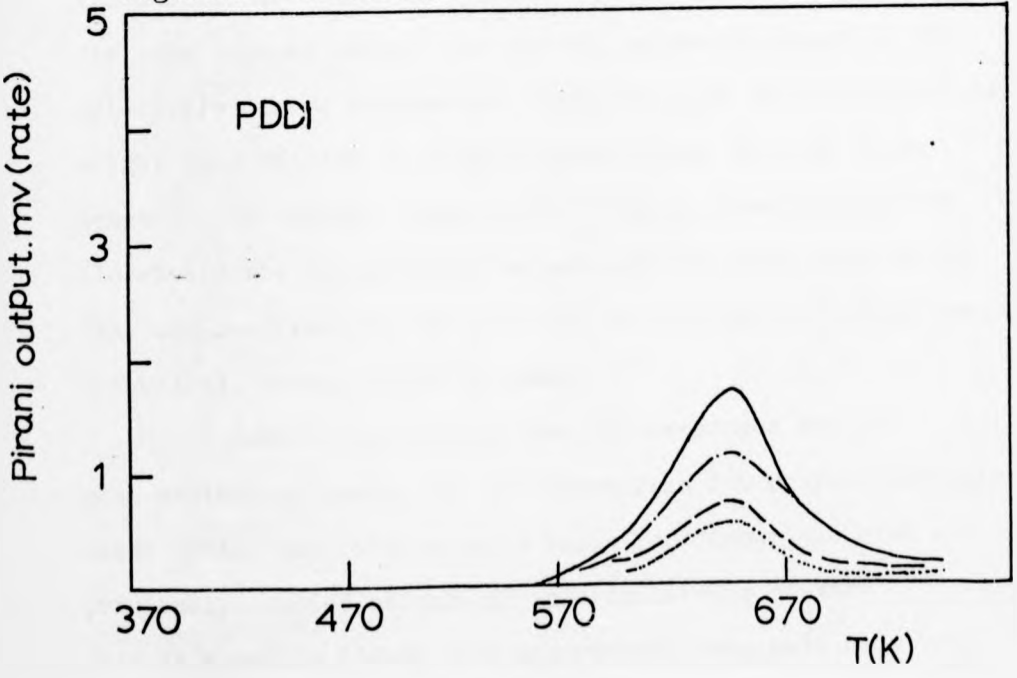

substantiate the postulate that it is due to fragments derived from the side chain. Again carbon dioxide was detected as one of these.

From the results above, it is concluded that the poly(di-n-alkyl itaconates) have a similar thermal stability to PMMA, and release monomer, presumably by an unzipping reaction. With increasing side chain length other degradation products are observed, one of which is carbon dioxide.

4.5.3 Poly(mono-n-alkyl itaconates)

The presence of an ester and carboxylic acid group in the repeat unit is a unique combination, and it has already been noted (section 4.2) that a major modification of the polymer chain occurs at ∿ 430K with the evolution of volatile products. The TGA thermograms of the poly(mono-n-alkyl itaconates) are shown in figures 4.43 and 4.44. These indicate that the initial weight loss for all polymers occurs in the relatively narrow temperature range 423-433K and that the total weight loss at 773K is roughly proportional to side chain length. The initial temperature of weight loss corresponds closely to the irreversible mechanical loss peak obtained by TBA, and confirms that this is due to a chemical, rather than a physical, change in the polymer.

Before establishing the TVA responses for the mono-n-alkyl polymers, the TVA thermogram for poly(methacrylic acid) (PMAA) was obtained as a basis for comparison with a previously studied carboxylic acid containing polymer[60,104]. This is shown in figure 4.45 and reveals two, well resolved, peaks, identical to those already published. The first of these is due to loss of water (at ∿ 500K) and the formation

Fig.4.43 TGA thermogram for poly(mono-n-alkyl itaconates)

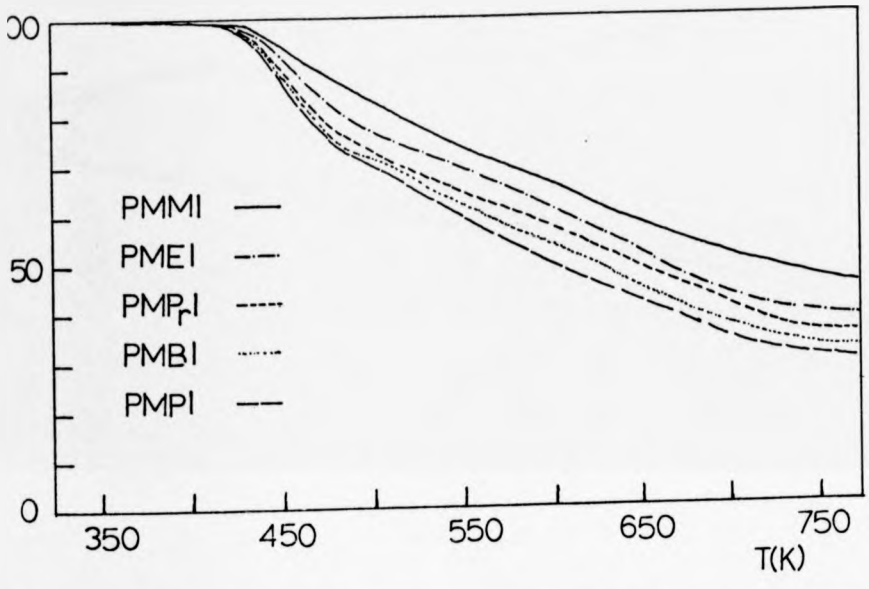

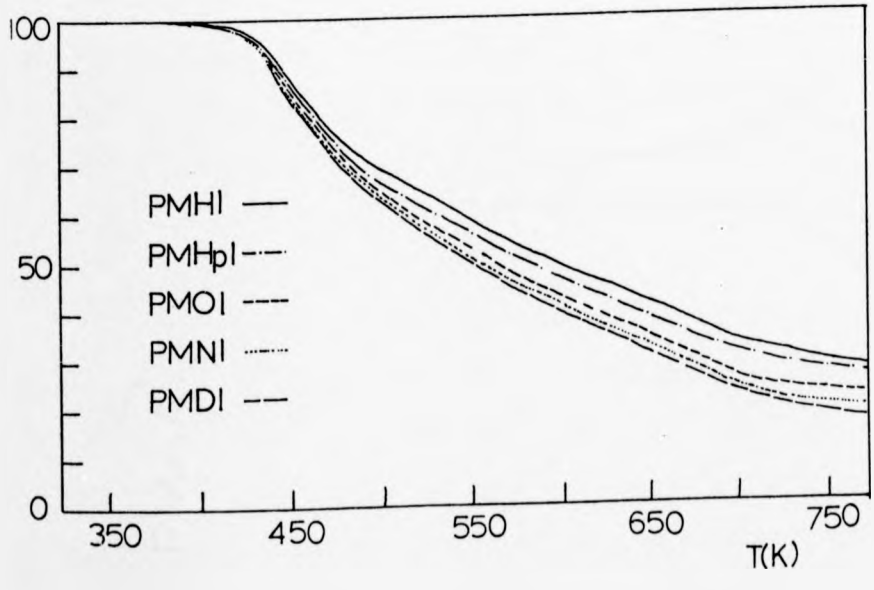

Fig.4.44 TGA thermogram for poly(mono-n-alkyl itaconates)

Fig.4.45 TVA thermogram for PMAA

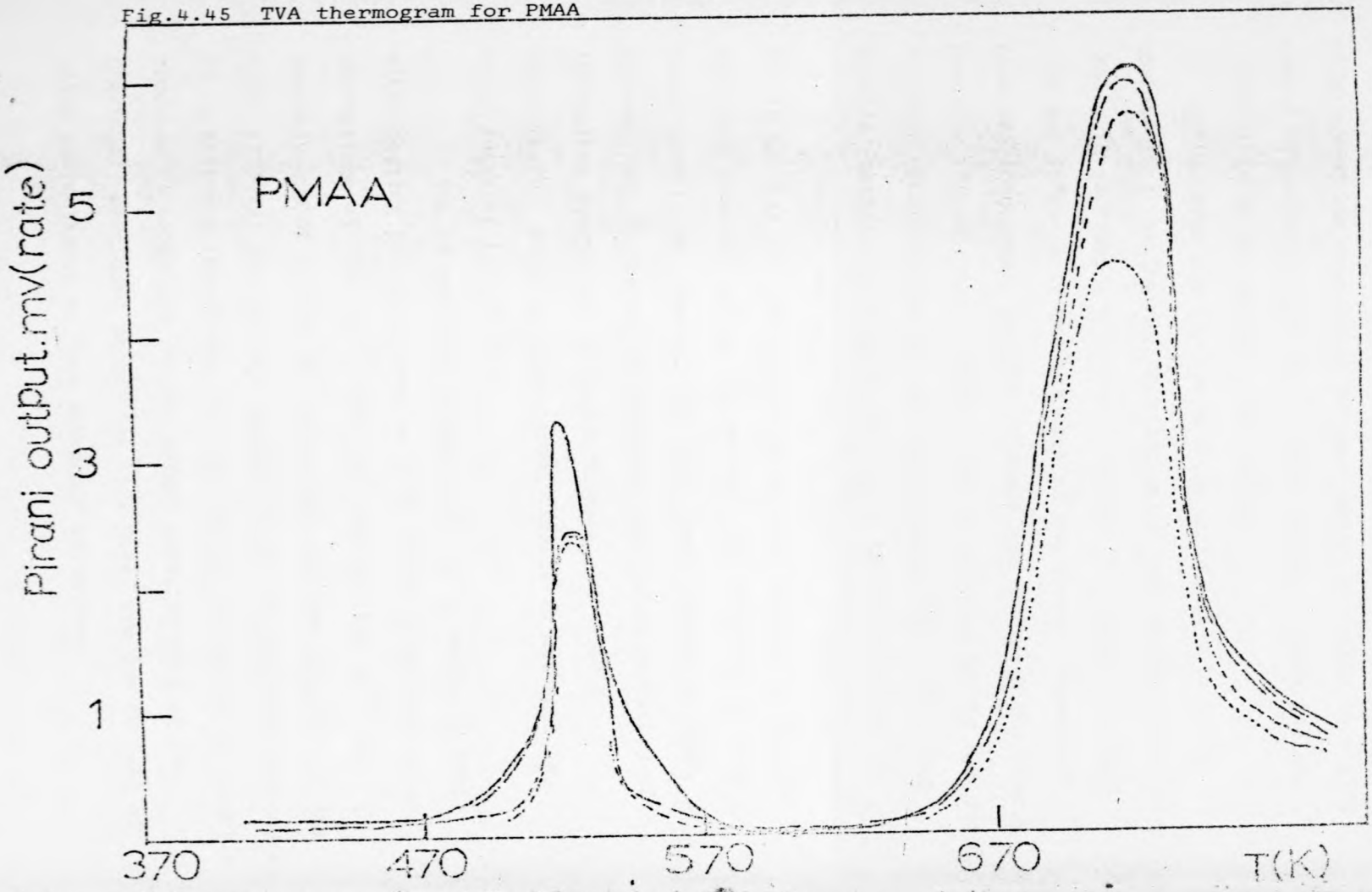

of an anhydride containing polymer which is stable to ∿ 673K, when a second evolution of volatiles occurs. These include carbon dioxide and monoxide and methane.

PMMI. From the TVA trace shown in figure 4.46 it is obvious that the thermal degradation is more complex than in PMAA. Three peaks are present, but not resolved, at ∿ 460K, 580K and 720K. Only the products of the lowest temperature peak are condensable at 173K, whereas non-condensable products occur in the two higher peaks. The IR spectrum of the collected volatile products show absorptions characteristic of carbon dioxide, methanol and small amounts of ketene (2160 cm^{-1}).

When a sample of PMMI is heated, in vacuo, at 453K for 15 minutes and the evolved gases are analysed by GLC and mass spectrometer, water and methanol are detected in roughly equal quantities. Repetition, with fresh samples of PMMI, at successively increased temperature, results in evolution of increasing quantities of carbon dioxide. At ∿ 500K, approximately twice as much carbon dioxide as methanol and water together is evolved.

The IR spectrum (figure 4.47) of a sample of PMMI, after heating for 15 minutes at 473K, shows three additional absorptions at 1780 cm^{-1}, 1805 cm^{-1} and at 1855 cm^{-1}, and possibly one at ∿ 1755 cm^{-1} as an ill-resolved shoulder on the ester carbonyl absorption, characteristic of anhydride structures. It is proposed therefore, that the initial evolution of volatile products (∿ 460K) and initial weight loss, as well as the previously mentioned mechanical loss peak, are due to loss of water and methanol to form anhydride structures.

The highest temperature TVA peak, at ∿ 720K, is similar to that observed in PMAA and is most likely caused by a comparable breakdown of the anhydride polymer. It is worth noting that in PMAA, methane is evolved (presumed to originate from the α-methyl groups)[60] but is absent in the volatile products from PMMI, which contains no methyl groups on the main chain.

The centre TVA peak of PMMI will be due, in part, to carbon dioxide which is being increasingly released up to 500K, other than this, the composition of the second peak is not known and no mechanism is proposed.

PMBI, PMHpI and PMDI. The TVA thermograms for these polymers are shown in figures 4.48 to 4.50 and are broadly similar to those of PMMI. When samples of each are heated at temperatures in the range 453K to 500K, GLC and mass spectral analysis of the volatile products reveal the presence of water, the corresponding alcohols and carbon dioxide. The relative amount of carbon dioxide, as for PMMI, increased with increasing temperature. The IR spectra of each polymer, after heating to 473K, again shows the same additional IR absorptions found for heated PMMI.

The first TVA peak of each of the above polymers shows decreasing content of volatile material as the side chain length increases. Also, as chain length increases, the two other TVA peaks move towards slightly higher temperatures. It seems obvious that a similar degradation pattern exists for all four poly(mono-n-alkyl itaconates) studied. Firstly, water and alcohol (which tends to remain in the cold ring for PMHpI and

Fig.4.46 TVA thermogram for PMMI

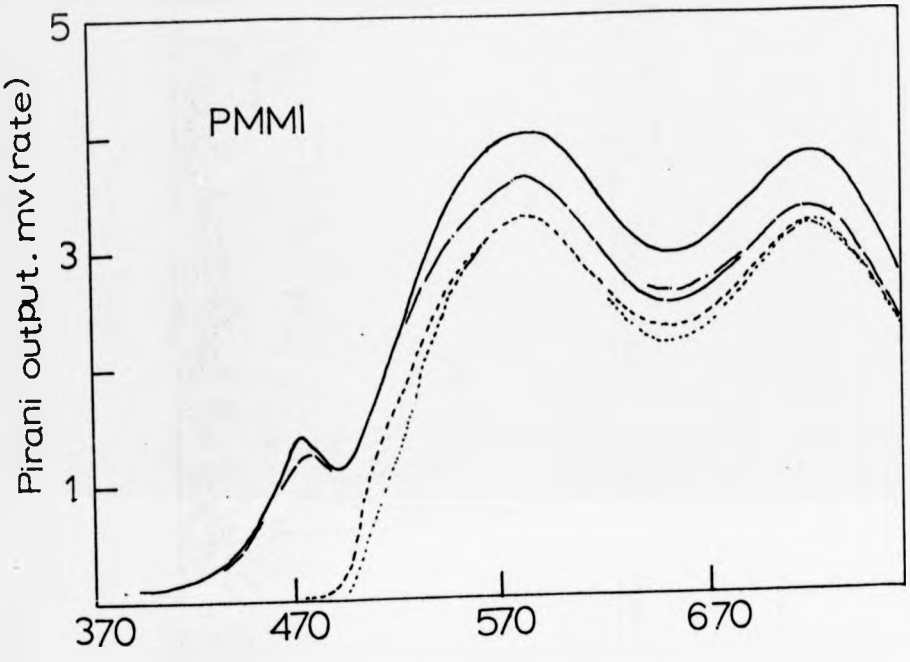

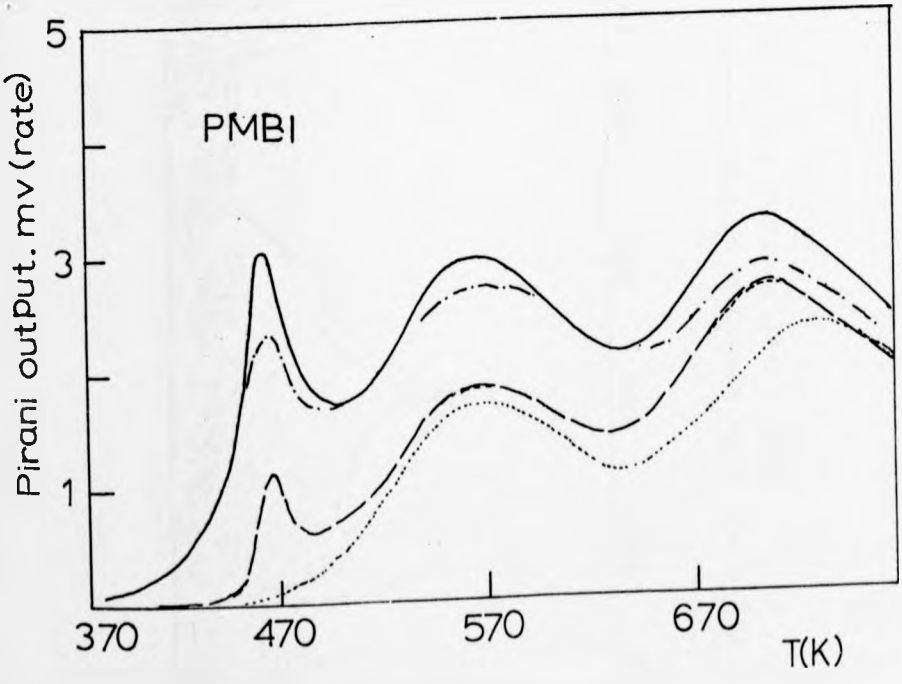

Fig.4.48 TVA thermogram for PMBI

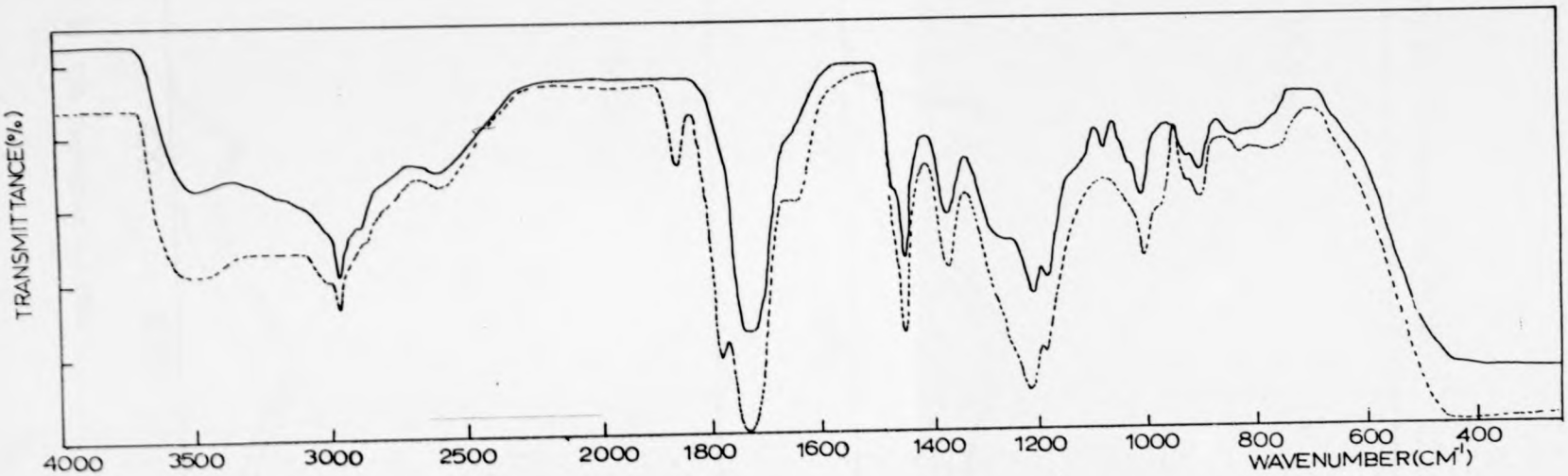

Fig.4.47 I.R. spectrum of PMMI(————)
PMMI after heating for 15 minutes (-----)

Fig.4.49 TVA thermograms for PMHpI

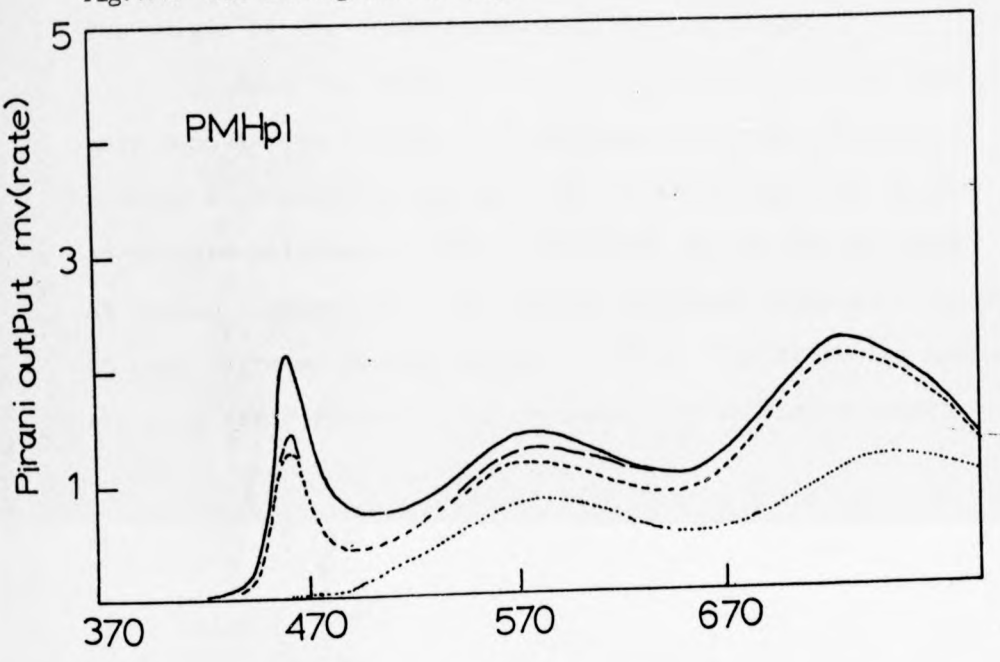

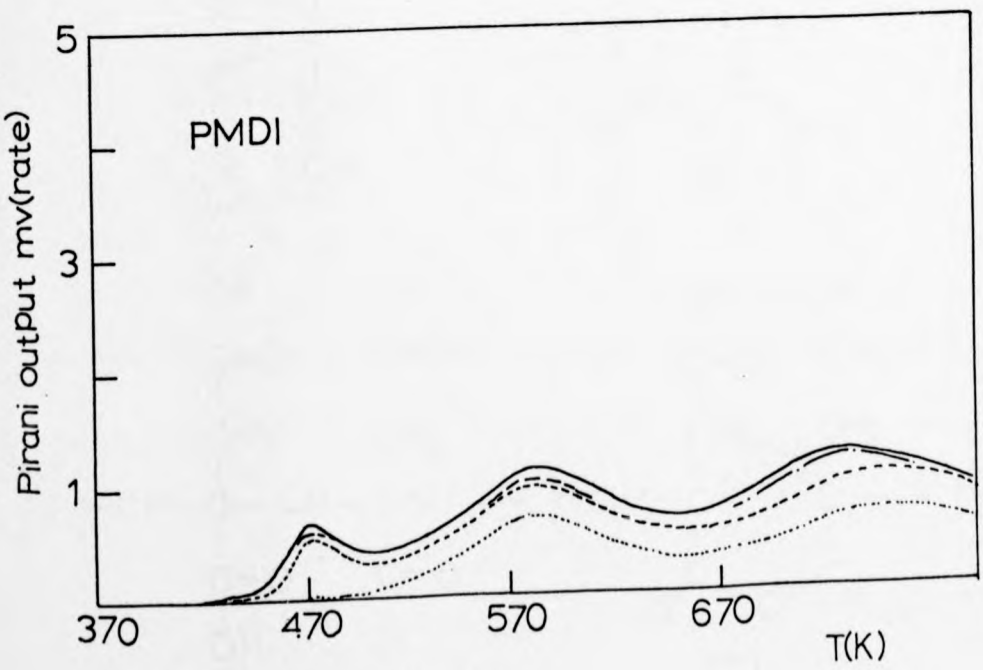

Fig.4.50 TVA thermogram for PMDI

PMDI) are evolved to give anhydride structures and eventually these break down at the temperatures of the highest TVA peak. The origin of the centre peak is still not known.

From the above results, it is concluded that the poly mono esters studied (and presumably all the others) undergo a dehydration and de-esterification reaction to give an anhydro-poly(mono-n-alkyl itaconate) on heating to ∿460K. At higher temperatures, the anhydro polymers degrade, at least in part, by a mechanism similar to PMAA. The following mechanisms are proposed for the initial formation of anhydro polymers.

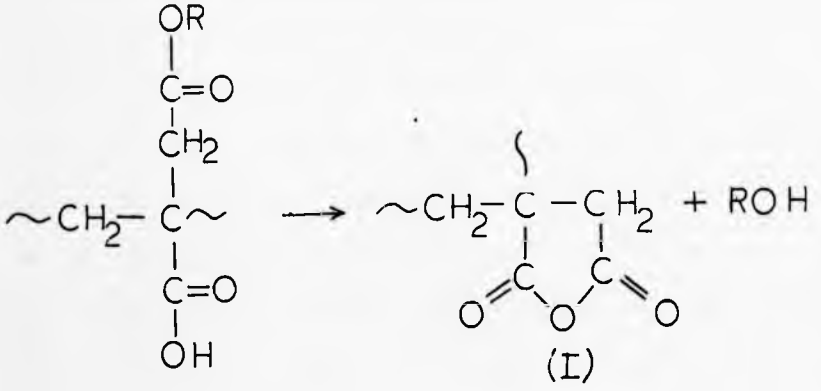

(I)

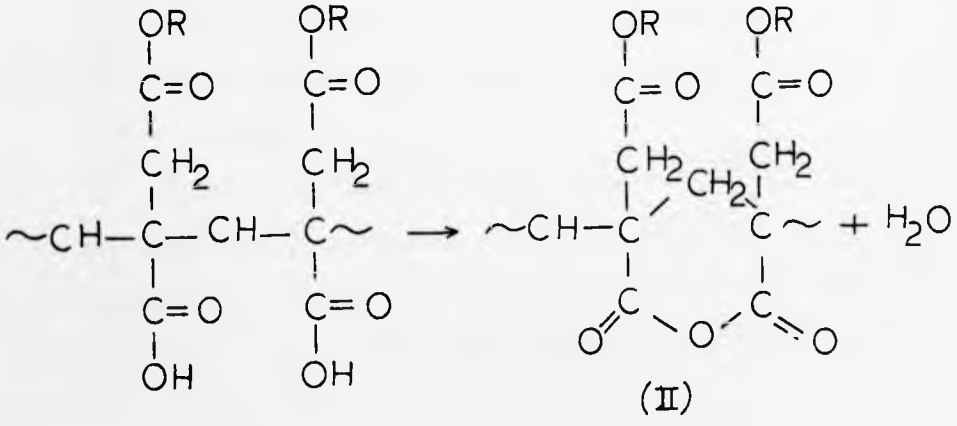

(II)

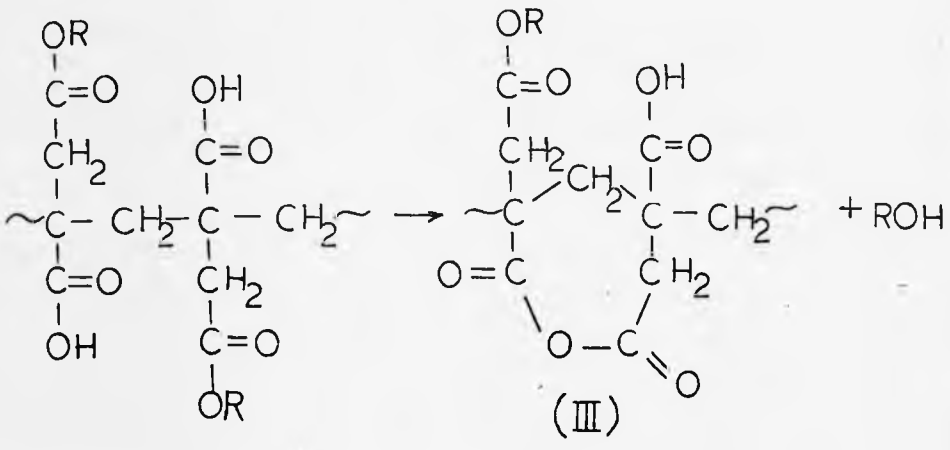

Structure (I) gives rings of a succinic anhydride type and would give rise to IR absorptions at 1855 cm^{-1} and 1780 cm^{-1}, corresponding to a strained five-membered ring. Structures (II) and (III) give relatively strain-free six and seven-membered rings respectively, and each would give rise to the absorptions at 1805 cm^{-1} and 1755 cm^{-1}. In addition, strain-free anhydride links between non-adjacent acid/ester groups, and acid/ester groups attached to different chains, could form giving cross links. Since the anhydro polymers are only soluble in reagents capable of hydrolysing anhydride units, it seems reasonable to suppose cross links are formed.

4.5.4 Polysalts

Very little work has been reported[105] on the thermal behaviour of polysalts (the metal salts of fully neutralised poly acids). These would be expected to show greater stability and a different degradation pattern when compared with the parent poly acid.

Sodium salt of PMMI. The TGA trace of PMMI as its 100% sodium salt are shown in figure 4.51 and show the latter to be only slightly more stable, the onset of weight loss being ∿ 450K as opposed to ∿ 423K. The TVA traces (figure 4.52) for the PMMI sodium salt reveal a degradation pattern which is much more complex than that of PMMI itself. The GLC analysis of the volatile products of degradation from a sample of PMMI sodium salt heated at ∿ 453K shows that very much more water than methanol is evolved. The infrared spectrum of the sodium salt of PMMI shows no change on heating up to 473K for one half hour. The evolution of water cannot, therefore, be a result of degradation of the polymer chain. It is likely that the poly salt contains large amounts of absorbed water, associated with the ionic groups, and that its release accounts for the major part of the first TVA peak, and the initial weight loss.

At very high temperatures (∿ 750K) the TVA indicates fragmentation to very volatile products. No mechanism is proposed for this, and for the intermediate peaks, from the limited study undertaken here.

PMBI, PMHpI and PMDI sodium salts. The TVA and TGA responses of these polysalts are shown in figures 4.51, and 4.53-4.55. The TGA curves and GLC analyses show that the salts all lose large amounts of water initially as in the case of PMMI. However the TVA traces indicate less volatile product response around 473K. Presumably the increasing hydrocarbon content of the polymers is less conducive to absorption of water. The higher temperature TVA responses become increasingly complex as chain length increases; no attempt is made to rationalise these.

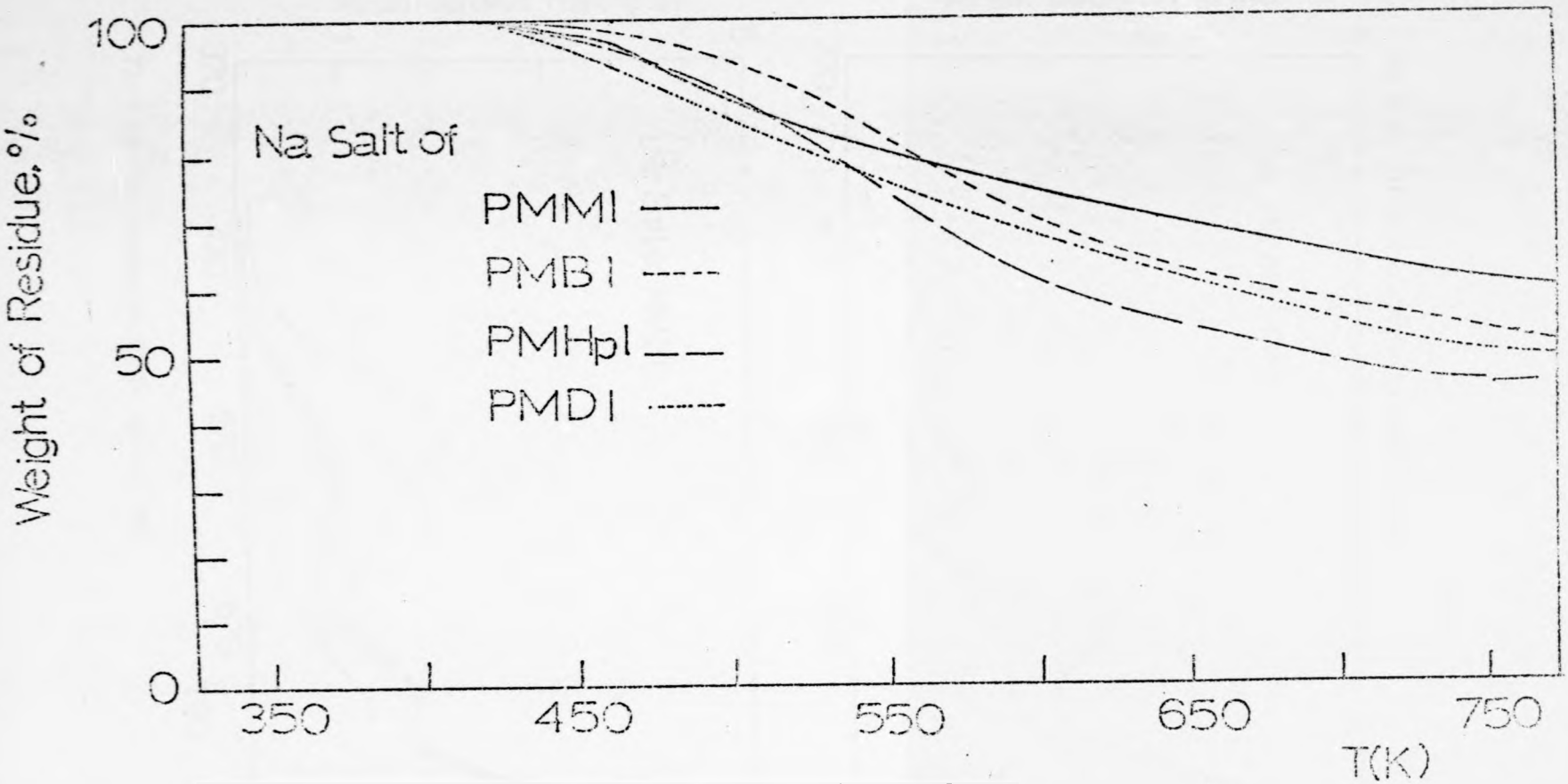

Fig.4.51 TGA thermogram for the Na salts of the indicated polymers

Fig.4.52 TVA thermogram for Na salt of PMMI

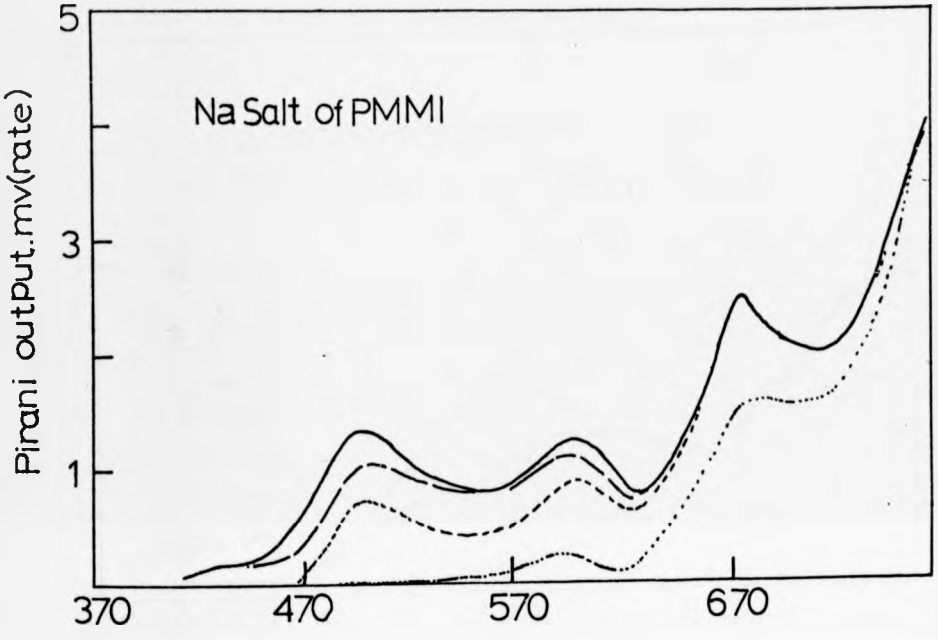

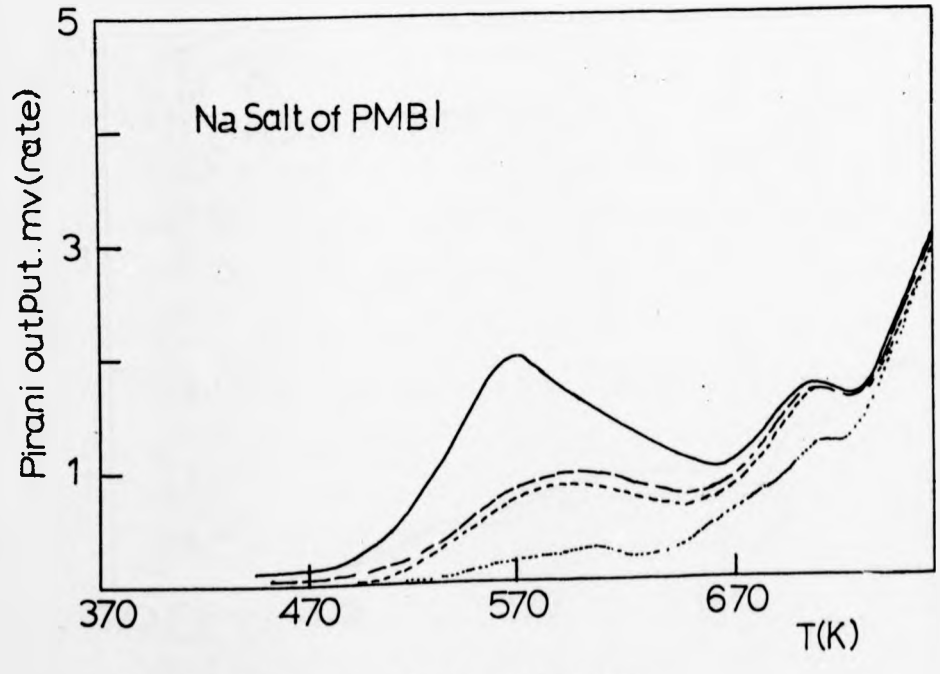

Fig.4.53 TVA thermogram for Na salt of PMBI

Fig.4.54 TVA thermogram for Na salt of PMHpI

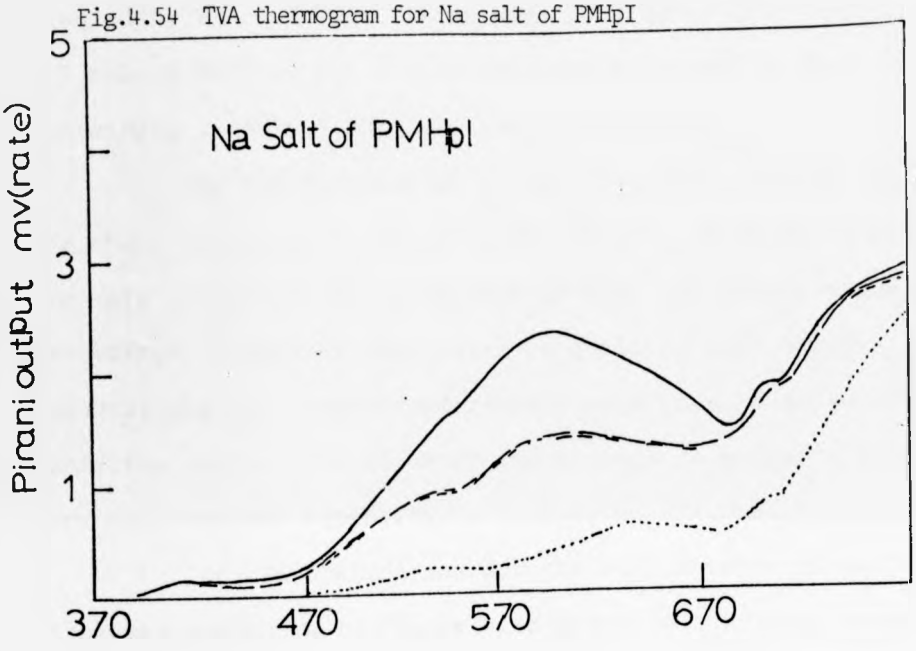

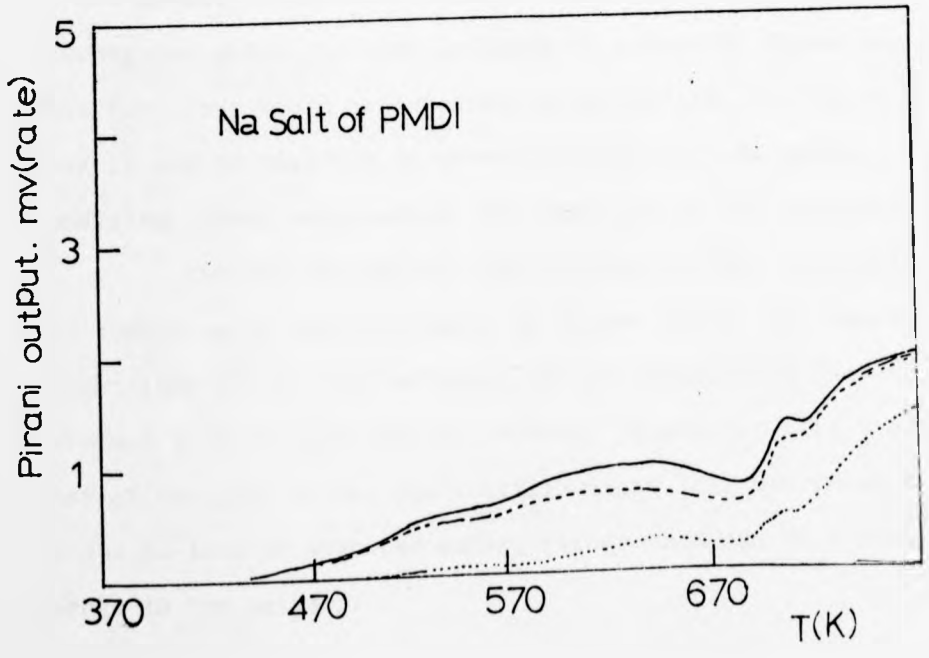

Fig.4.55 TVA thermogram for Na salt of PMDI

4.5.5 Ionomers

Two ionomers and their parent copolymers were studied by TVA and TGA. These were poly(MBI + DBI) containing 9.5 mole % MBI and its sodium salt and poly(MHpI + DHpI) containing 16 mole % MHpI and its sodium salt.

The TVA thermograms of the unionised, parent copolymers are shown in figures 4.56 and 4.57. These, as might be expected, are very similar to the responses of PDBI and PDHpI, since the percentage content of mono ester is small in both cases. However, the low temperature response assigned to anhydride formation due to loss of water and alcohol is evident, but at very much reduced intensity.

The TVA thermograms for the sodium salts of each copolymer are shown in figure 4.58 and 4.59. Notably absent is the lowest temperature peak of the parent copolymer TVA thermograms which has been assigned to anhydride formation. This behaviour would be expected on ionisation, if indeed the peak is due to reaction of parent carboxylic acid group. The remaining higher temperature, TVA response is not analysed here.

The TGA thermograms for poly(MBI + DBI) copolymer and sodium salts are also shown in figure 4.60. The onset of weight loss is not much affected by ionisation, but the eventual total weight loss is reduced. However, as in the case of the poly salts, the initial weight loss was shown to be due to loss of absorbed water, rather than due to a structural change in the polymer.

Fig.4.56 TVA thermogram for poly(MBI + DBI)
9.5 90.5

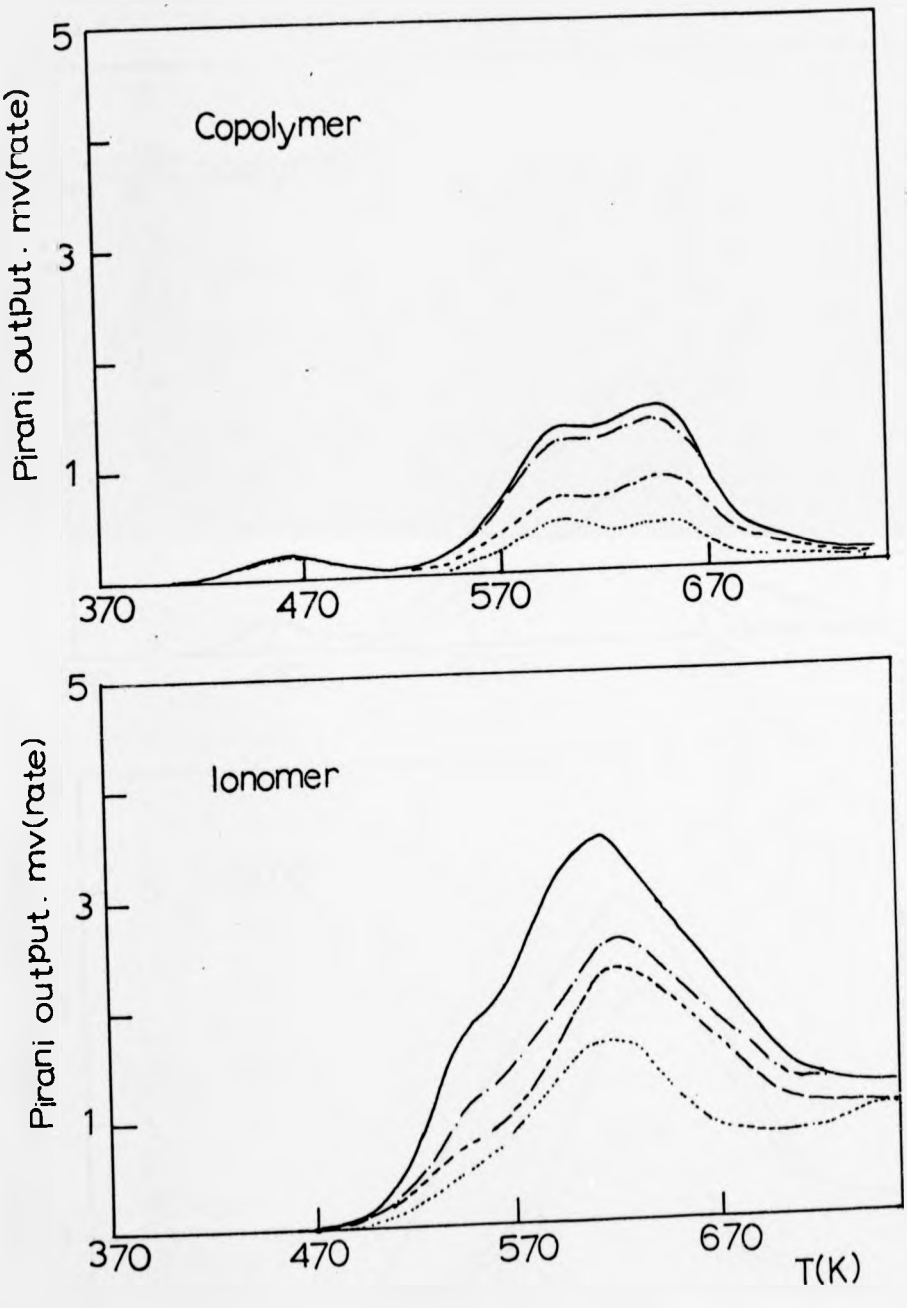

Fig.4.58 TVA thermogram for the Na salt of poly(MBI + DBI)
9.5 90.5

Fig.4.57 TVA thermogram for poly(MHpI$_{16}$ + DHpI$_{84}$)

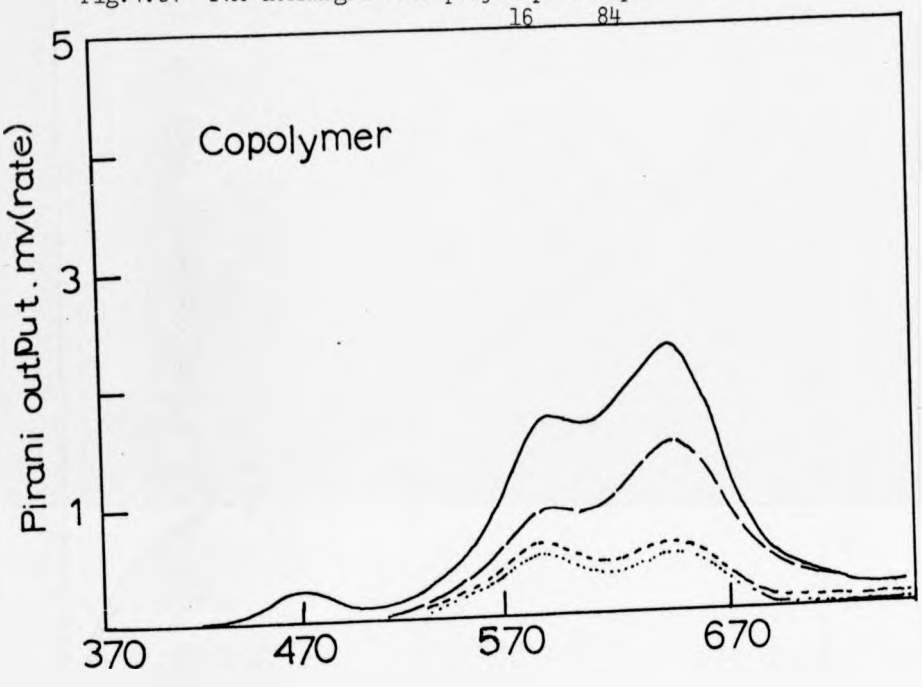

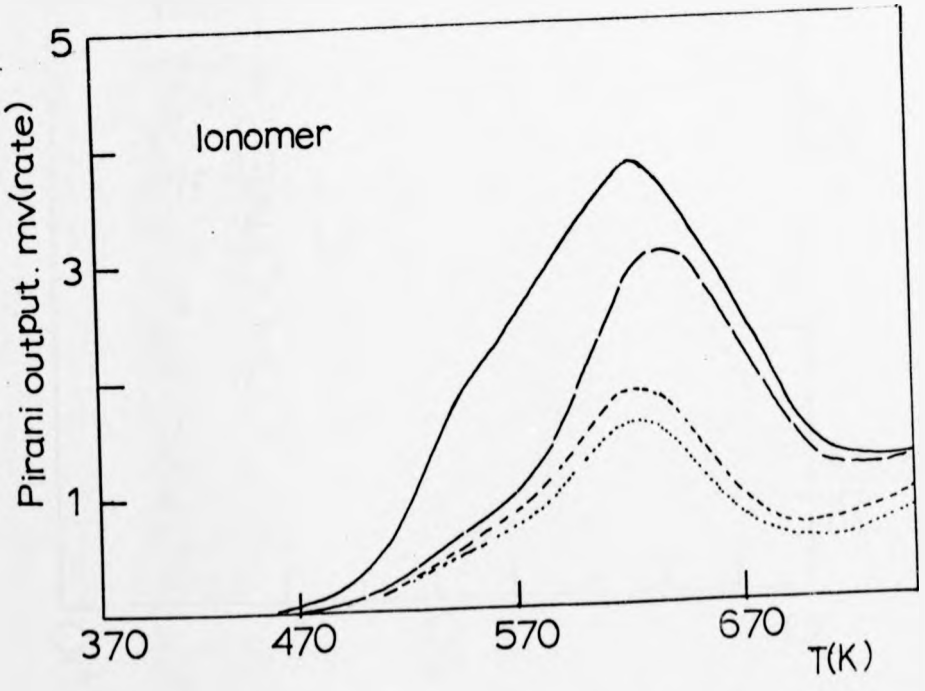

Fig.4.59 TVA thermogram for the Na salt of poly(MHpI$_{16}$ + DHpI$_{84}$)

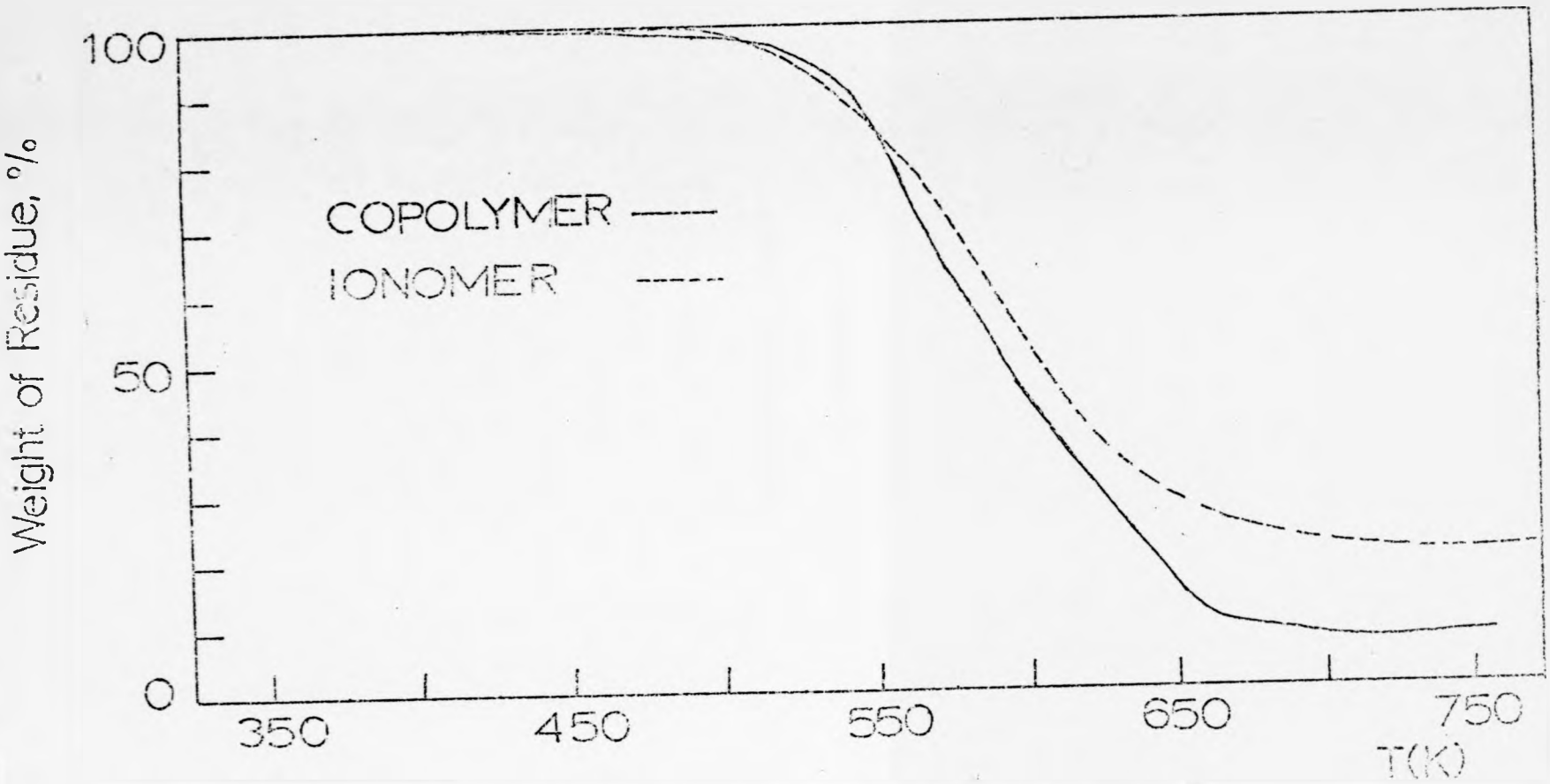

Fig.4.60 TGA thermogram for poly(MBI$_{9.5}$ + DBI$_{90.5}$) and its Na salt ionomer

CHAPTER 5

SUMMARY AND CONCLUSIONS

Polymers based on esters of itaconic acid have received relatively little attention in the past. The area merits study, firstly because the fundamental monomer, itaconic acid, is not an oil-based product, but is obtained by a fermentation process, and secondly, the esters are structurally similar to the poly(alkyl methacrylates). In this thesis the results of a relatively broad study of the physical properties of polymers based on itaconic acid have been reported. As an inevitable result of such an approach, several areas have not received the detailed investigation they undoubtedly warrant.

It has been shown that both mono- and di-n-alkyl esters of itaconic acid can be readily polymerised and copolymerised to high molecular weight products, although the former require the adoption of standard emulsion techniques in order to avoid thermal modification of the polymer chain. Refractive index increments (dn/dc) have been established for all the poly(monoesters) in several solvents suitable for light scattering molecular weight determination. Since the chain propagation is by a radical mechanism, and since relatively high polymerisation temperatures were used, it has to be assumed that the polymers have a random (atactic) structure. The study of tacticity in the lower poly(di-n-alkyl itaconates) could possibly be undertaken using N.M.R. techniques, similar to those applied to PMMA.

Poly(di-n-alkyl itaconates) vary from brittle solids

to relatively mobile polymeric liquids at room temperature, depending on the length of the n-alkyl side chains. Glass transition temperatures for each member of the series from PDMI to PDDoI have been established and these show a smooth decrease from 373K(PDMI) to 250K(PDHpI), followed by a slight increase to ∿260K (PDDI). When more than six carbon atoms are present in the side chain, it is necessary to consider the polymer as a graft copolymer (containing two essentially separate regions) in order to interpret the observed thermo-mechanical behaviour. Two transitions are present, one due to the onset of molecular motion in the side chain region, and a second (at a higher temperature) due to cooperative motion of the main polymer backbone. The second transition may be considered to be the true glass transition. Evidence of crystallinity in the side chain regions was observed in PDDoI and (to a lesser extent) in PDuDI.

In addition to those mentioned in the previous paragraph, two additional transitions are observable in the poly(di-n-alkyl itaconate) series. In all polymers with four or more carbon atoms in the side chain a relaxation can be detected at ∿100K and this has been assigned to crankshaft motion of the methylene segments of the side chain. A broad transition, centred at ∿260K, and thought to originate from hindered rotation of the ester linkages, can also be observed in PDMI. In the remaining polymers, this transition, if present, is obscured by the glass transition.

Copolymers of two di-n-alkyl esters were prepared and reactivity ratios established. When the thermomechanical properties of these copolymers were examined, they were found to display a predictable gradation from one homopolymer to the other. Nevertheless, attempts to describe the variation of the glass transition with copolymer composition, using the Gordon-Taylor approach, were not completely successful. Further study of the theoretical aspects of glass transitions in itaconate copolymers would require expansion coefficient data for the homo polymers. When copolymers were made from comonomers with large differences in ester side chain length, evidence of block formation was observed from the thermomechanical spectra. However no attempt at sequence distribution analysis was undertaken and the question whether or not significant blocks are indeed present in these copolymers remains unresolved.

The thermal stability of di-n-alkyl itaconate polymers was studied by both TGA and TVA. The onset of thermal breakdown was found to be typical of that for vinyl polymers, and almost identical to that for poly(n-alkyl acrylates). The mode of degradation is most likely by an unzipping reaction (depolymerisation) to give monomer. However, a detailed analysis of the TVA traces obtained was not made. Thermal stability and degradation is a sufficiently complex subject which warrants a complete study on its own.

The poly(mono-n-alkyl itaconates) are significantly different from the diester polymers. All are brittle solids at room temperature. The introduction of a pendant carboxyl

group into the repeat unit was found to give polymers which can undergo an irreversible, thermally induced, structural change at ∿430K. This involves the loss of water and alcohol and the formation of anhydride structures between two carboxyl groups and/or between a carboxyl and an ester group giving a modified polymer backbone and crosslinks between adjacent polymer chains. This change was observed by thermochemical techniques, by IR spectroscopy, by TVA and by TGA. After the formation of anhydride structures, the thermal stability is relatively poor. The exact nature of the thermal breakdown was not examined in detail.

Several copolymers of a di- and a mono-n-alkyl ester were made and their thermomechanical behaviour investigated. Again a fairly predictable gradation in properties was observed. Estimates of the glass transition temperature of PMBI and PMHpI were made by extrapolation of copolymer Tg data. They were found to lie at temperatures well above the point at which anhydride formation occurs. Only in the cases of PMDI and PMNI was the glass transition directly observable.

The two copolymer systems, poly(MBI + DBI) and poly(MHpI + DHpI), were chosen as the precursors of sodium and caesium ionomers. These were prepared by neutralising selected amounts of free carboxyl groups (on the mono-ester repeat units) in the copolymers with sodium or caesium hydroxides. The effect of introducing ionic groups on the thermomechanical behaviour was studied by both TVA and RV. It was found that mechanical stability above the glass

transition was significantly improved and that tough, leathery thermoplastics could be obtained. It would appear that further preparations and studies of ionomers, with side chain lengths in the five to eight carbon region, could lead to viable thermoplastics that are mechanically stable in the temperature range 270-400K. Investigation of neutralisation with divalent cations would also be a worthwhile extension of this work.

Morphological studies of the ionomers were undertaken using the electron microscope. Except at relatively high ion concentration ($\sim$ 30%), no evidence for aggregation of ionic groups was observed. The ionomers apparently adopt an amorphous structure with the ionic groups distributed randomly. Confirmation of this conclusion would require additional studies using low angle x-ray diffraction which should be able to detect the presence of ionic aggregates, if present. In this study, ionomers with relatively long side groups were used. It would be possible to use the itaconate polymers as a basis for an investigation of the effect of side chain length on ionomer properties. Indeed further study of ionomers based on itaconic acid would seem extremely worthwhile, since they appear capable of providing plastics with commercially interesting properties.

In general, therefore, this study has shown that itaconic acid based polymers and copolymers are an interesting group of polymers whose properties resemble closely those of the polyacrylates. They have additional advantages in that their polyfunctionality could be commercially desirable

(good dyeability) and that the basic unit is non-oil derived. They also could form the basis of a family of ionomers, a class of material which is attracting increasing attention, both as a subject for academic study and for commercial application.

REFERENCES

1. Baup, S., Ann., 1837, 19, 29.
2. Stobbe, H. and Lippold, A., J.Prkt.Cham., 1914, 95, 336.
3. Kinoshita, K., Acta Phytochim.Japan, 1931, 5, 272.
4. Calam, C.T., Clutterbuck, P.W., Oxford, A.E. and Raistrick, H. Biochem.J., 1939, 33, 1488.
5. U.S. Patent No.2,385,283 Sept., 1945.
6. U.S. Patent No.2,462,981 March, 1949.
7. U.S. Patent No.2,448,831 Sept., 1948.
8. Scheldknecht, C.E., page 308, "Vinyl and Related Polymers", John Wiley and Sons, New York, 1952.
9. Marvel, C.S. and Shepherd, T.H., J.Org.Chem., 1959, 24, 599.
10. Tate, B.E., Adv.Polym.Sci., 1967, 5, 214.
11. Nagai, S. and Yoshida, I., Kobunshi Kagaku, 1960, 17, 748.
12. U.S. Patent No.2,790,736 (1957).
13. U.S. Patent No.31,161,532 (1964).
14. Knuth, B., Ind.Eng.Chem., 1955, 47, 1572.
15. Pfizer Chemicals, Pfizer Ltd., Kent, Product Information Sheets No. 403, 404.
16. Swarts, S., Ball.acad.royal Belg.(2), 1873, 36, 64.
17. Tate, B.E., "The polymerisation of itaconic acid and its ester", published by Pfizer Europe Chemicals.
18. Nagai, S., Yoshida, I. and Uno, T., Chem.High Polym.Japan, 1960, 17, 117.
19. Nagai, S. and Yoshida, I., Chem.High Polym.Japan, 1958, 15, 550.
20. Nagai, S. and Yoshida, I., Chem.High Polym.Japan, 1960, 17, 79.
21. Pfizer Chemicals, Pfizer Ltd., Kent, Product Information Sheet No. 402.
22. Braun, D., Kolloid.Z., 1963, 188, 1.
23. Nagai, S., Bull Chem.Soc.Japan, 1963, 36, 1459.

24. Boudevska, H., Bozhkova, N. and Panamsky, I., Die makromolekulare chemie, 1973, 28, 121.

25. Tate, B.E., Die makromolekulare chemie, 1967, 109, 176.

26. Velickovic, J., Jovanovic, D., Vukjilovic, T., Die makromolekulare chemie, 1969, 129, 203.

27. Velickovic, J. and Vasovic, S., Die makromolekulare chemie, 1972, 153, 207.

28. Velickovic, J., Coseva, S. and Fort, J., Europ.Polym.J., 1975, 11, 377.

29. Bekiturov, Y.A., Bimendina, L.A., Rogonov, V.V. and Rafikov, S.R., Vysokmol Soyed, 1972, A14, No.2 343.

30. Nagai, S. and Fujimara, F., Polym.Letters, 1969, 7, 177.

31. Yokota, K., Hirabayashi, T., and Takashima, T., Die makromolekulare chemie, 1975, 176, 1197.

32. Henshall, S.A.E., Ph.D. Thesis (1974), Dept. of Chemistry, University of Stirling.

33. Cowie, J.M.G., McEwen, I.J. and Velickovic, J., Polymer, 1975, 16, 869.

34. Buderska, H. and Platchokova, S., Die makromolekulare chemie, 1973, 174, 231.

35. Kargin, V.A., Kitaigorodskii, A.I. and G. L. Slonanskii, Kolloid Z., 1957, 19, 131.

36. Volkerstin, M.V., Sov.phys.Doklody, 1959, 4, 351.

37. Cowie, J.M.G., "Polymers: Chemistry and Physics of Modern Materials", Intertext, England (1973).

38. McCrum, M.G., Read, B.E. and Williams, "Anelastic and Dielectric Effects in Polymeric Solids", John Wiley & Sons, London (1967).

39. Cowie, J.M.G., Europ.Polym.J., 1975, 11, 297.

40. Heijboer, J., Kolloid Z., 1960, 171, 7.

41. Wood, L.A., J.Polym.Sci., 1958, 28, 319.

42. Fox, T.G., Bull Ann.Phys.Soc., 1956, 1, 123.

43. Gordon, M. and Taylor, J.S., J.Appl.Chem., 1952, 2, 493.

44. Di Marzio, E.A. and Gibbs, J.A., J.Polym.Sci., 1959, 40, 121.

45. "Ionic Polymers", Holliday L., Ed., Applied Science Publishers, London (1975).

46. Vogel, A.I., Practical Organic Chemistry, 3rd ed., Longmans Green & Co., London, 1956, page 381.

47. Baker, B.R., Schaub, R.E. and Williams, J.H., J.Org.Chem., 1952, 24, 116.

48. Collins, E.A., Bares, J. and Bellmeyer, J.R., "Experiments in Polymer Science", John Wiley & Sons, USA, (1973).

49. Lewis, A.F. and Gillham, J.K., J.Appl.Polym.Sci., 1962, 6, 422.

50. Gillham, J.K. and Lewis, A.F., Nature, 1962, 195, 1199.

51. Gillham, J.K., Macromolecular Sci., 1972, 83, 225.

52. Gillham, J.K., in "Thermal Characterization Technique", ed. by Slade, P.E. and Jenkins, L.T., Marcel Dekker Inc., New York, (1970).

53. Gillham, J.K., Review Paper, Alche Journal, Nov. 1973.

54. Wunderlich, B., Physical Method of Chemistry, Vol.1, Chap.VIII, of a Weissberger ed. Technique of Chemistry Part 5, Interscience Div., John Wiley & Sons, New York, (1971).

55. Baxter, R.A., page 65, in "Thermal Analysis", eds. Schwenker, R.F. and Garn, P.D., Academic Press, New York, (1969).

56. McNeill, I.C., J.Polym.Sci., 1966, A4, 2479.

57. McNeill, I.C. and Neil, D., page 353, in "Thermal Analysis", eds. Schwenker, R.F. and Garn, P.D., Academic Press, New York, (1969).

58. McNeill, I.C., page 417, in "Thermal Analysis", eds. Schwenker, R.F. and Garn, P.D., Academic Press, New York, (1969).

59. McGuchin, R. and McNeill, I.C., Europ.Polym.J., 1968, 4, 115.

60. McNeill, I.C., Europ.Polym.J., 1970, 6, 373.

61. Rogers, S.S. and Mandelkern, L., J.Phys.Chem., 1957, 61, 985.

62. Alexandrov, A.P. and Lazurkin, J.S., Acta Phys.Chem., USSR, 1940, 12, 647.

63. McLoughlin, J.R. and Tobolsky, A.V., J.Colloid Sci., 1952, 7, 555.

64. Ishida, Y. and Yamafuji, K., Kolloid Z., 1961, 117, 97.

65. Heijboer, J., in "Physics of Non Crystalline Solids", North Holland, Amsterdam (1965), page 231.

66. Schatzki, T.F., J.Polym.Sci., 1962, 57, 496.

67. Schatzki, T.F., Polym.Preprint, 1965, 6, 646.

68. Sharples, A., "Introduction to Polymer Crystallization", Edward Arnold Ltd., London (1966).

69. Kurath, F., Yin, T.P., Berge, J.W. and Ferry, J.D., J.Colloid Sci., 1969, 14, 147.

70. Jordan Jr., E.F., Riser, G.R., Parker, W.F. and Wrigley, A.N., J.Polym.Sci. A-2, 1966, 4, 975.

71. Jordan Jr., E.F., Feldeisen, D.F. and Wrigley, A.N., J.Polym.Sci. A-1, 1971, 9, 1835.

72. Jordan Jr., E.F., Riser, G.R., Artymyshyn, B., Pensabene, J.W. and Wrigley, A.N., J.Polym.Sci. A-2, 1972, 10, 1657.

73. Broadhurst, M.G., J.Res.Nat.Bur.Stand., 1962, 66A, 241.

74. Johnston, N.W., Macromolecules, 1973, 6, 453.

75. Comyn, J. and Fernandez, R.A., Europ.Polym.J., 1975, 11, 149.

76. Rees, R.W., Mod.Plastics, 1964, 42, 1.

77. Rees, R.W. and D. Vaughan, D.J., Polymer Preprints, 1965, 6, 296.

78. Bonotto, S. and Purcell, C.L., Mod.Plastics, 1965, 42, 7.

79. Otocka, E.P., J.Macromol Sci.Revs.Macromol.Chem., 1971, C5(2), 275.

80. MacKnight, W.J., McKenna, L.W. and Read, B.E., J.Appl.Phys., 1967, 38, 4208.

81. Bonotto, E.F. and Bonner, E.F., Polymer Preprints, 1968, 9, 537.

82. Eisenberg, A. and Narratil, M., Macromolecules, 1973, 6, 604.

83. MacKnight, W.J., Taggart, W.P. and Stein, R.S., J.Polym.Sci. Symposium No. 45, 1974, 113.

84. Rafikov, S.R., Monakor, Y.B., Ionova, I.A., Gladyshev, G.P., Andrusenko, A.A., Ponomarev, O.A., Vorob'eva, A.I., Berg, A.A., Antonova, L.F., Ablyakimov, E.I., Sisin, M.F. and Smorodin, A.A., Vysokomol soyed, 1974, A15, No.9, 1973.

85. Yeo, S.C. and Eisenberg, A., Polymer Preprints, 1975, 16, 104.

86. Otocka, E.P. and Kwei, T.K., Macromolecules, 1968, 1, 243.

87. Longworth, R. and Vaughan, D.J., Nature, 1968, 218, 85.

88. Marx, C.L. and Cooper, S.L., J.Macromol Sci.Phys., 1974, B9(1), 19.

89. Marx, C.L., Koutsky, J.A. and Cooper, S.C., J.Polym.Sci., 1971, C9, 167.

90. Eisenberg, A., J.Polym.Sci. Symposium No.45, 1974, 49.

91. Eisenberg, A., Macromolecules, 1970, 3, 147.

92. Marx, C.L., Caulfield, D.F. and Cooper, S.C., Polymer Preprint, 1973, 14, 890.

93. Otocka, E.P. and Davis, D.D., Macromolecules, 1969, 2, 437.

94. Roe, R.J., Polymer Preprints, 1970, 12, 730.

95. Wilson, F.C., Longworth, R. and Vaughan, D.J., Polymer Preprint, 1968, 9, 505.

96. Phillips, R.J., J.Polym.Sci. (Polymer Letters), 1972, C10, 443.

97. MacKnight, W.J., Kajiyama, T. and McKenna, L.W., Polym.Eng.Sci. 1967, 8, 267.

98. Kajiyama, T., Oda, T., Stein, R.S. and MacKnight, W.J., Macromolecules, 1971, 4, 198.

99. MacKnight, W.J., McKenna, L.W., Read, B.E. and Stein, R.S., J.Phys.Chem., 1968, 72, No.4, 1122.

100. Williams, H.L., in "Polymer Engineering", Elsevier Publications Company, New York, 1975.

101. McNeill, I.C. and Neil, D., Europ.Polym.J., 1970, 6, 143.

102. McNeill, I.C. and Neil, D., Europ.Polym.J., 1970, 6, 569.

103. Grassie, N. and Grant, D., Polymer, 1960, 1, 445.

104. Grassie, N. and Grant, D., Polymer, 1960, 1, 125.

105. Zulifqar, M., Ph.D. Thesis, Oct. 1975, Dept. of Chemistry, University of Glasgow.

APPENDIX

Reactivity Ratio Data for Poly(MBI + DBI)

H	h	H^2/h	H(1-h)/h
5.207	3.501	7.744	- 3.7197
3.903	3.060	4.98	- 2.626
3.035	2.669	3.45	- 1.898
1.952	1.541	2.47	- 0.615
1.301	1.323	1.28	- 0.318
0.867	0.840	0.90	0.165
0.558	0.547	0.57	0.463
0.145	0.157	0.133	0.775

Reactivity Ratio Data for Poly(MHpI + DHpI)

H	h	H^2/h	H(1-h)/h
2.145	3.223	1.428	- 1.48
1.430	2.284	0.895	- 0.804
0.953	1.748	0.520	- 0.449
0.678	1.268	0.363	- 0.1433
0.360	0.567	0.229	0.275
0.159	0.243	0.1039	0.495

Reactivity Ratio Data for Poly(MBI + DMI)

H	h	H^2/h	H(1-h)/h
3.355	3.253	3.684	- 2.323
1.867	1.867	1.867	- 0.867
1.258	1.139	1.389	- 0.1539
0.839	0.806	0.873	+ 0.202
0.559	0.559	0.559	0.441
0.210	0.265	0.166	0.582

Reactivity Ratio Data for Poly(DMI + DHpI)

H	h	H^2/h	H(1-h)/h
5.502	10.099	2.755	- 4.957
2.059	2.413	1.757	- 1.206
0.885	1.160	0.675	- 0.122
0.516	0.592	0.450	0.357
0.229	0.282	0.186	0.583
0.108	0.095	0.123	1.029

Reactivity Ratio Data for Poly(DMI + DDI)

H	h	H^2/h	H(1-h)/h
12.957	24.710	6.805	- 12.44
5.189	7.750	3.474	- 4.586
1.297	1.890	0.930	- 0.581
0.779	1.229	0.494	- 0.145
0.519	0.867	0.311	0.793
0.259	0.338	0.199	0.508

Calculation of Gordon-Taylor constant (K) in Poly(DMI + DHpI) system.

mole fraction DMI w_1	mole fraction DHpI w_2	Tg/k	$(Tg-Tg_1)$	$Tg-Tg_2$	$K = \frac{w_1(Tg-T_1)}{w_2(Tg-T_2)}$
0.035	0.965	252	- 121	2	2.19
0.098	0.902	261	- 112	11	1.11
0.186	0.814	276	- 97	26	0.85
0.310	0.690	291	- 82	41	0.89
0.402	0.518	316	- 57	66	0.83
0.000	0.200	344	- 29	94	1.23

Tg = glass transition of copolymer

Tg_1 = " " of PDMI

Tg_2 = " " of PDHpI

Calculation of Gordon-Taylor constant (K) in Poly(DMI + DDI) system.

mole fraction DMI w_1	mole fraction DDI w_2	Tg/K	$(Tg-Tg_1)$	$Tg-Tg_2$	$K = \frac{w_1(Tg-Tg_1)}{w_2(Tg-Tg_2)}$
0.0904	0.91	263	- 110	8	1.37
0.166	0.834	269	- 104	14	1.48
0.230	0.770	280	- 93	25	1.11
0.332	0.668	290	- 83	35	1.18
0.665	0.335	340	- 33	85	0.77
0.832	0.168	357	- 16	102	0.776

Tg = glass transition of copolymer

Tg_1 = " " of PDMI

Tg_2 = " " of PDDI

D 19157 7

END